Distribution Agreement

In presenting this thesis or dissertation as a partial fulfillment of the requirements for an advanced degree from Emory University, I hereby grant to Emory University and its agents the non-exclusive license to archive, make accessible and display my thesis or dissertation in whole or in part in all forms of media, now or hereafter known, including display on the world wide web. I understand that I may select some access restrictions as part of the online submission of this thesis or dissertation. I retain all ownership rights to the copyright of the thesis or dissertation. I also retain the right to use in future works (such as articles or books) all or part of this thesis or dissertation.

Signature:

Candice A. Elam

_____ _____

Student's Name Date

Regulation of ciliary motility by phosphorylation: an axonemal PP2A B-subunit is required for PP2A localization and ciliary motility

By
Candice A. Elam
Doctor of Philosophy

Graduate division of Biological and Biomedical Science
Biochemistry, Cell and Developmental Biology

_____
Winfield S. Sale, Ph.D.
Advisor

_____

Tamara Caspary, Ph.D.
Committee Member

_____

Victor Faundez, M.D, Ph.D.
Committee Member

_____

John Hepler, Ph.D.
Committee Member

_____

David Pallas, Ph.D.
Committee Member

_____

Maureen Powers, Ph.D.
Committee Member

Accepted:

_____
Lisa A. Tedesco, Ph.D.
Dean of the Graduate School

_____
Date

Regulation of ciliary motility by phosphorylation: an axonemal PP2A B-subunit is required for PP2A localization and ciliary motility

By

Candice A. Elam
M.S. University of Maryland, Baltimore County, 2002
B.S. University of Maryland, Eastern Shore 2000

Advisor: Winfield S. Sale, Ph.D.

An abstract of
a dissertation submitted to the Faculty of the Graduate School of Emory University in partial fulfillment of the requirements for the degree of
Doctor of Philosophy
in Biochemistry, Cell and Developmental Biology

2011

Abstract

Regulation of ciliary motility by phosphorylation: an axonemal PP2A B-subunit is required for PP2A localization and ciliary motility

By

Candice A. Elam

The overall goal of this work is to determine the mechanisms that regulate dynein motors involved in ciliary/flagellar motility. Cilia are highly conserved organelles that play essential motile and sensory roles required for normal development and function of most organs in the adult; cilia are found on nearly every differentiated cell where they play vital motility and cell signaling functions: failure in assembly or function can result in a wide range of developmental disorders or diseases called "ciliopathies". Ciliary/flagellar motility is regulated by conserved kinases and phosphatases that are localized in the axoneme. I focused on the heterotrimeric phosphatase PP2A, and tested the hypothesis that the axoneme contains a specialized B-type subunit required for targeting the PP2A C-(catalytic) and A-(scaffold) subunits. I identified an axonemal PP2A B-subunit (PR55 B subfamily). The *Chlamydomonas* PP2A B-subunit gene maps to LG1 at the PF4 locus. The *pf4* cells display a slow swimming phenotype and are defective in phototaxis. This motility phenotype is similar to the phenotype of I1 dynein mutants. However, I1 dynein is fully assembled in *pf4* axonemes. The B-subunit gene is mutated in *pf4*, and immunoblots confirmed that the B-subunit is absent in *pf4* cells. The PP2A C-subunit, while expressed in *pf4* cells, fails to assemble in the axoneme. Two independent, UV-induced *pf4* intragenic revertants (*pf4rV5*, *pf4rV11*) were recovered from a genetic screen for suppressors. Both revertants contain a seven-base pair insertion which alters several amino acids in the fifth WD-repeat of the B-subunit protein. The reading frame is restored and the new B-subunit is expressed in both revertants. Notably, PP2A is assembled in the revertant axonemes, phototaxis is restored and swimming is partially restored. The revertant cells confirm that the *pf4* phenotype is a consequence of the mutation in the PP2A B-subunit, and, consistent with my hypothesis, the results reveal that the PP2A B-subunit is required for assembly of the PP2A holoenzyme in the axoneme. The results reveal that PP2A is required for normal motility.

Regulation of ciliary motility by phosphorylation: an axonemal PP2A B-subunit is required for PP2A localization and ciliary motility

By

Candice A. Elam
M.S. University of Maryland, Baltimore County, 2002
B.S. University of Maryland, Eastern Shore 2000

Advisor: Winfield S. Sale, Ph.D.

A dissertation submitted to the Faculty of the Graduate School of Emory University in partial fulfillment of the requirements for the degree of
Doctor of Philosophy
in Biochemistry, Cell and Developmental Biology

2011

Acknowledgements:

First, I would like to thank God for allowing me to achieve such an important goal. I find that many people are afraid to express their religious beliefs, but I don't think I could have made it through without my faith. Second, I would like to thank my parents for everything that they have done for me. They are truly genuinely good people, and I am truly blessed to have them in my life. I would also like to thank the many members of my family, throughout the years they have shown me a tremendous amount of love even though I can't see them quite as often as I used to.

To the members of the Sale lab: Laura, Maureen, Lea, Rasagnya, Jennifer, Amadu and Ryosuke and Avanti (honorary member). You all have been great to me. I truly have learned a ton from each one of you. I am going to miss each and every one of you so much. I wish that I didn't have to go. I wish all of you continued success, and happiness in all that you undertake.

To Dr. Sale: where would I be without you? I really appreciate your mentoring. Mostly, I appreciate you for treating me not like a data machine, but like a human being. You are truly irreplaceable, and I also wish you continued success in your life. Dr. L'Hernault is going to have some pretty big shoes to fill.

There are countless others that I could name, but I hope that they aren't unhappy that I didn't mention them by name. If you think this refers to you, then I hope you know that I appreciate you, and know that you have played a significant role in shaping my life. Finally, I am dedicating this thesis to my brother, James David Elam, Jr. and my friend Mrs. Carrie L. Jackson. I pray that your souls are at peace in heaven.

Table of contents:

List of Figures and Tables:

List of abbreviations:

AKAP - A-kinase anchoring protein

BAC - Bacterial artificial chromosome

BBS- Bardet-biedl syndrome

CK1-7- N-(2-aminoethyl)-5-chloroisoquinoline-8-sulfonamide

CP – Central pair

CSC – Calmodulin and spoke associated complex

DMSO – Dimethyl sulfoxide

DRB - 5,6-dichloro-1-beta-D-ribofuranosylbenzimidazole

DRC- Dynein regulatory complex

EDTA - Ethylenediaminetetraacetic acid

EGTA- Ethylene glycol tetraacetic acid

HC – Heavy chain

IC – Intermediate chain

IDA- Inner dynein arm

IFT – Intraflagellar transport

IPTG- Isopropyl β-D-1-thiogalactopyranoside

LC – Light chain

MC- Microcystin-LR

ODA – Outer dynein arm

ODA-DC – Outer dynein arm – docking complx

PCD - Primary ciliary dyskinesia

PKA - Protein kinase A

PKD- Polycystic kidney disease

PKI- Protein kinase inhibitor

PMSF- Phenyl-methane-sulphonyl-fluoride

PVDF- Polyvinylidene Fluoride

RS – Radial spoke

Overview and Significance:

The overall focus of this thesis is to understand how ciliary/flagellar motility is regulated using the biflagellate, green alga, *Chlamydomonas reinhardtii* as a model system (Fig. 1). As, discussed, *Chlamydomonas* is the most powerful model genetic organism for study of genes and mechanisms common to all cilia including ciliated cells in humans. We are particularly interested in defining a ciliary signaling pathway that ultimately controls dynein motor activity by phosphorylation. Specifically, I explore the role of the phosphatase, PP2A, in regulating an axonemal molecular motor dynein called I1 (Fig. 2). The foundation for studying ciliary regulation stems from the inherent interest in this conserved organelle and interest in regulation of the dynein motors that drive motility required for several cell functions. In addition, current data shows that cilia are present on every cell during vertebrate development and in the adult where they play vital roles in motility and cell signaling. Indeed, disruption of assembly or function of cilia can result in a failure in body symmetry, polycystic kidney disease, blindness, obesity, hydrocephaly and fertility (Nigg and Raff, 2009; Gerdes et al., 2009;Sharma et al, 2008;Pazour and Rosenbaum, 2002; Ong and Wheatley, 2003; Scholey, 2003; Snell et al., 2004; Pazour, 2004). Since the 9+2 axonemal microtubule arrangement of cilia/flagella is highly conserved in all eukaryotic organisms, using *Chlamydomonas* as a model system has proven to be most beneficial for understanding ciliary/flagellar assembly and regulation (Fig. 3. Axoneme). For example, conserved genes that are required for assembly of all cilia, originally discovered in *Chlamydomonas*, have led to a revolution in our understanding of cilia in humans, and mutations in these genes can

result in a very wide range of diseases called "ciliopathies" (Gerdes et al., 2010; Berbarie et al., 2009; Goetz and Anderson, 2010).

In *Chlamydomonas,* cilia serve as the machinery that regulates the cell's motility and behavior such as phototaxis. As defined below, and in figure 3, together, the central pair apparatus, radial spokes and I1 dynein of the axoneme define a network of conserved structures and enzymes – the "CP/RS/I1 regulatory mechanism"- important for regulating normal ciliary motility (reviewed in Wirschell et al., 2007, Elam et al., 2009). Within the cilium there is a network of structural and motor proteins that are regulated by post-translational modifications; one of these proteins is I1 dynein (Fig. 4.;Smith and Sale, 1992; Habermacher and Sale, 1997; King and Dutcher; 1997). I1 dynein is a tripartite structure located at the proximal end of a group of proteins that repeat every 96 nm along the axoneme (Fig. 5.; Porter and Sale, 2000; Wirschell et al., 2007). From previously published data from our lab and from others, we have found that I1 dynein controls the size and shape of the flagellar bend and is regulated by kinases and phosphatases that are anchored within the axoneme (Brokaw and Kamiya, 1987; Bayly et al., 2010; Yang et al., 2000; Yang and Sale, 2000; Gaillard et al., 2001 and 2006; Hendrickson et al., 2004; Gokhale et al., 2009). In particular, phosphorylation of the intermediate chain, IC138, of I1 dynein inhibits its activity leading to altered flagellar motility and an inability to undergo phototaxis (King and Dutcher, 1997; Okita et al., 2005; Bower et al; 2009; Wirschell et al., 1996). In turn, phosphatase activity is crucial in the restoration of I1 dynein activity (Habermacher and Sale, 1996). Current and published data from our lab has shown that protein phosphatase 2A (PP2A) is a component of the ciliary axoneme and plays a critical role in the regulation of I1 dynein

(Yang et al., 2000). As defined in detail below and illustrated in Figure. 6, the phosphatase PP2A is composed of three subunits: the regulatory B-subunit, the scaffolding A-subunit, and the catalytic C-subunit (reviewed in Shi, 2009a). Together these subunits are thought to be responsible for phosphatase activity in the axoneme, "CP/RS/I1 phospho-regulatory" pathway, and regulation of flagellar motility.

The goal of this thesis is to address two main questions: What is the role of the phosphatase PP2A in the regulation of flagellar motility? How does PP2A become targeted to the ciliary axoneme? With regard to targeting PP2A in the axoneme, I tested the hypothesis that a special, axonemal PP2A B-subunit targets the PP2A holoenzyme. This hypothesis is based on the general idea that B-subunits function, in part, to localize PP2A in the cell (reviewed in Shi, 2009; Virshup and Shenolikor, 2009; Mumby, 2007). The model is also founded on how kinases and dynein motors become targeted in the axoneme. Currently, two molecular mechanisms for targeting of kinases and motorsinclude: (1) radial spoke 3 (RSP3) is an AKAP responsible for targeting PKA within the axoneme and, (2) the identification of the outer dynein arm docking complex (ODA-DC) consisting of three proteins that localize the outer dynein arms (Gaillard et al., 2001; Takada et al., 2002; Takada and Kamiya, 1994; Koutoulis et al., 1997; Casey et al., 2003). Here I expand upon the theme that specificity of kinase or phosphatase activity requires precise localization relative to phospho-protein substrates.

As indicated above, in this thesis I tested the hypothesis that PP2A is localized and anchored by a special B-type subunit in cilia. I identified a candidate B-subunit and showed that it localizes to the cilium. We identified a flagellar mutant, *pf4*, which is a functional null mutant for the axonemal PP2A B-subunit (Elam et al., submitted). We

showed that in the absence of B-subunit expression, the entire PP2A holoenzyme fails to target to the axoneme. Additionally, *pf4* mutant cells had a reduced swimming velocity phenotype and failed to undergo phototaxis. Two *pf4* intragenic revertants were recovered in a genetic screen that expressed a functional B-subunit protein. These revertant cells restore PP2A to the axoneme, partial recovery of swimming velocity and full restoration of phototaxis. The *pf4* revertants provide strong proof that the gene responsible for the *pf4* phenotype is the B-subunit gene. These results have revealed new principles for control of ciliary motility by the axonemal phosphatase PP2A, and provided further evidence showing that the PP2A B-subunits regulate PP2A by localization, restricting access to only a subset of substrates. In fact, these studies provide outstanding proof that one of the roles of the PP2A B-subunit is to precisely localize PP2A in the cell (reviewed in Shi et al., 2009) Moreover, *pf4*, and the *pf4* revertants, demonstrate that PP2A is required for normal ciliary motility, and that the mechanisms likely include regulation of I1 dynein through control of phosphorylation of the regulatory intermediate chain, IC138.

Fig. 1

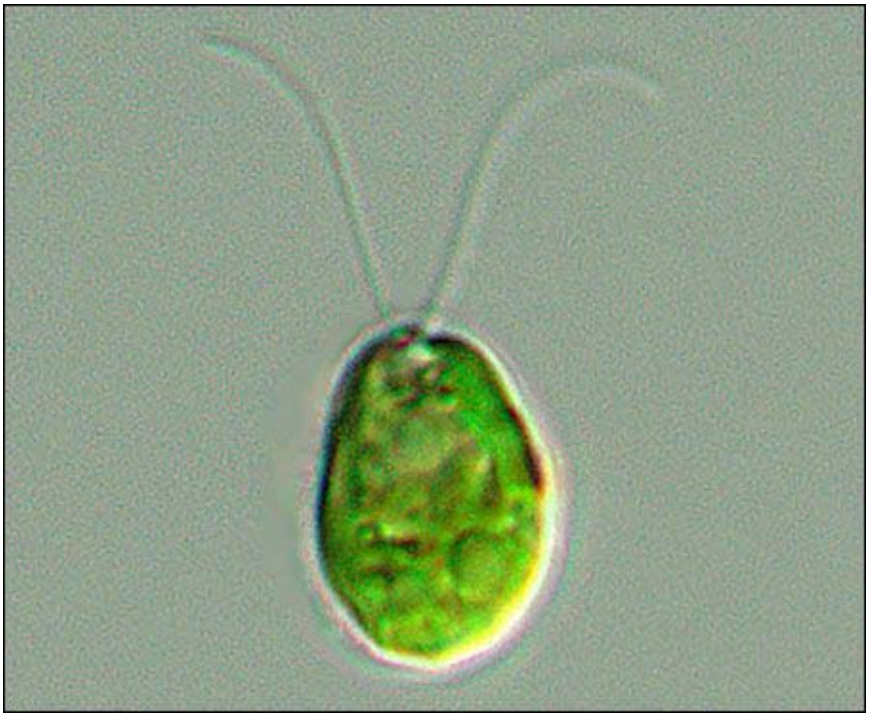

Fig. 1: Differential interference contrast image of *Chlamydomonas reinhardtii*. *Chlamydomonas* is a unicellular, biflagellate, green alga. Wild-type cells are typically 10µm in length and 3µm in width. Flagella of wild-type cells are usually 10-12 µm in length. *Chlamydomonas* cells typically exist as haploids and they possess three autonomous genomes of the nucleus, mitochondria and chloroplast. Photo taken by Brian Prasecki.

Fig. 2.

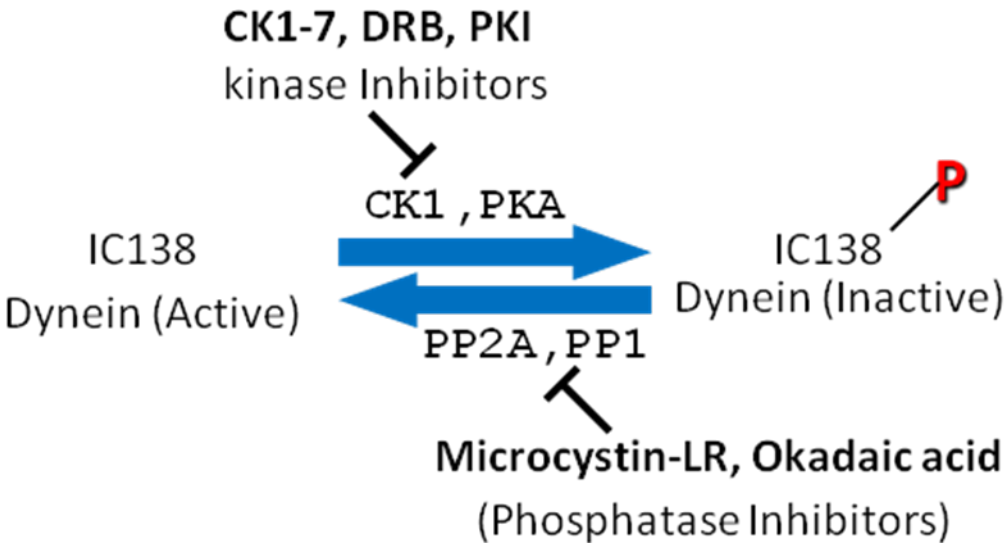
CK1-7, DRB, PKI
kinase Inhibitors
CK1 , PKA
IC138
Dynein (Active)
P
IC138
Dynein (Inactive)
PP2A , PP1
Microcystin-LR, Okadaic acid
(Phosphatase Inhibitors)

Fig. 2: Model for I1 dynein regulation. Previous experimental evidence, using the *Chlamydomonas* model system, has demonstrated that the key regulatory phospho-protein in I1 is the intermediate chain IC138. This pathway was revealed in paralyzed flagellar mutants where the kinases are apparently misregulated leading to a global phosphorylation of IC138. IC138 when phosphorylated by axonemal kinases CK1 or PKA, results in inhibition of dynein activity as revealed by a decrease in microtubule sliding velocity observed in motility assays. This inhibition can be relieved by specific kinase inhibitors. Furthermore, in wild-type axonemes, radial spokes regulate axonemal kinase activity, thus allowing normal ciliary waveform and movement. IC138 can be dephosphorylated by an axonemal phosphatase PP2A, resulting in activation of dyneins and therefore increases microtubule sliding velocity.

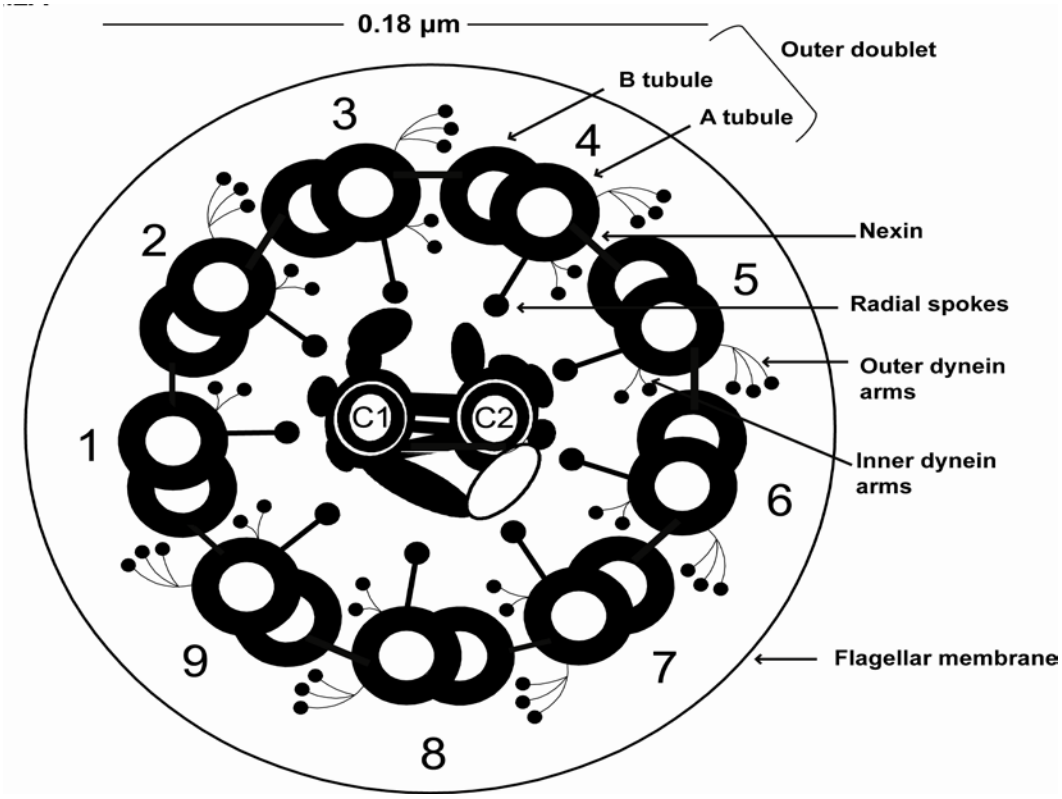
0.18 µm
Outer doublet
B tubule
A tubule
Nexin
Radial spokes
Outer dynein arms
Inner dynein arms
Flagellar membrane
1
2
3
4
5
6
7
8
9
C1
C2

Fig. 3: Cross section of the ciliary/ flagellar axoneme. The axoneme has a conserved 9+2 arrangement, which refers to the nine outer doublet microtubules and the two central pair microtubules. The radial spokes are attached to the outer doublet microtubules and project toward the central pair apparatus. The outer doublet microtubules consist of a complete A microtubule and an incomplete B tubule. Each microtubule doublet is connected to its neighbor by the protein nexin/DRC. The inner and outer dynein arms are located on the A tubule of the doublet, and transiently interact with the B-tubule of the adjacent doublet during microtubule sliding.

Fig. 4.

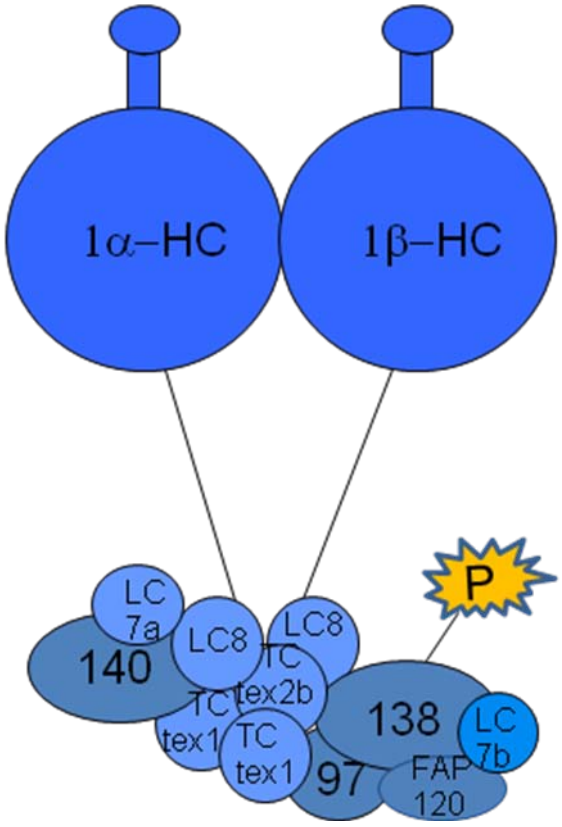
1α–HC
1β–HC
P
LC
7a
140
LC8
LC8
TC
tex2b
TC
tex1
TC
tex1
138
LC
7b
97
FAP
120

Fig. 4: Model for I1 dynein. I1 dynein is located at the proximal end of the 96nm repeat (Fig. 5). It is a tripartite structure consisting of two heavy chains,1α and 1β; three intermediate chains, 97, 138, 140, an intermediate light chain, FAP 120, and several light chains including,LC7a, LC7b, LC8, Tctex1, and Tctex2. The intermediated chain IC138 is associated with IC97, FAP120 and LC7b forming the IC138 complex . IC138 is a phospho-

Fig. 5.

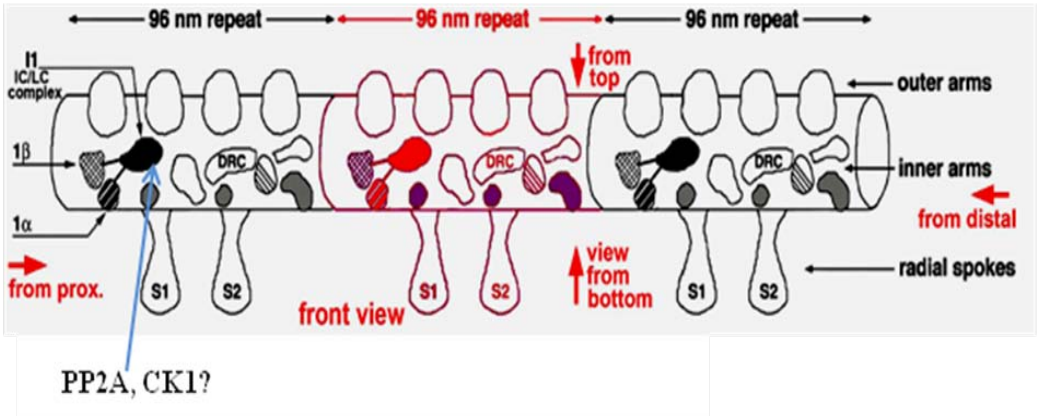
96 nm repeat
96 nm repeat
96 nm repeat
I1
IC/LC
complex
1β
1α
DRC
DRC
DRC
from
top
outer arms
inner arms
from distal
radial spokes
from prox.
S1
S2
front view
S1
S2
view
from
bottom
S1
S2
PP2A, CK1?

Fig. 5: The axonemal "96nm repeat". All dyneins and regulatory subunits (radial spokes, DRC) repeat at 96 nm intervals along each doublet microtubule. Three repeats are shown. I1 dynein is located toward the proximal end of the 96nm repeat, The kinase, CK1, and the phosphatases, PP2A are thought to be anchored in the axoneme in position to regulate IC138 in I1 dynein (blue arrow). The single-headed inner arm dyneins a, b, c, d, e, g are dispersed along the tubule within the 96nm repeat. Other components of the repeat include the outer dynein arms which repeat every 24nm, two radial spoke complexes and the nexin/dynein regulatory complex (DRC). Adapted from: Heuser et al., 2009, Porter and Sale, 2000.

Fig. 6.

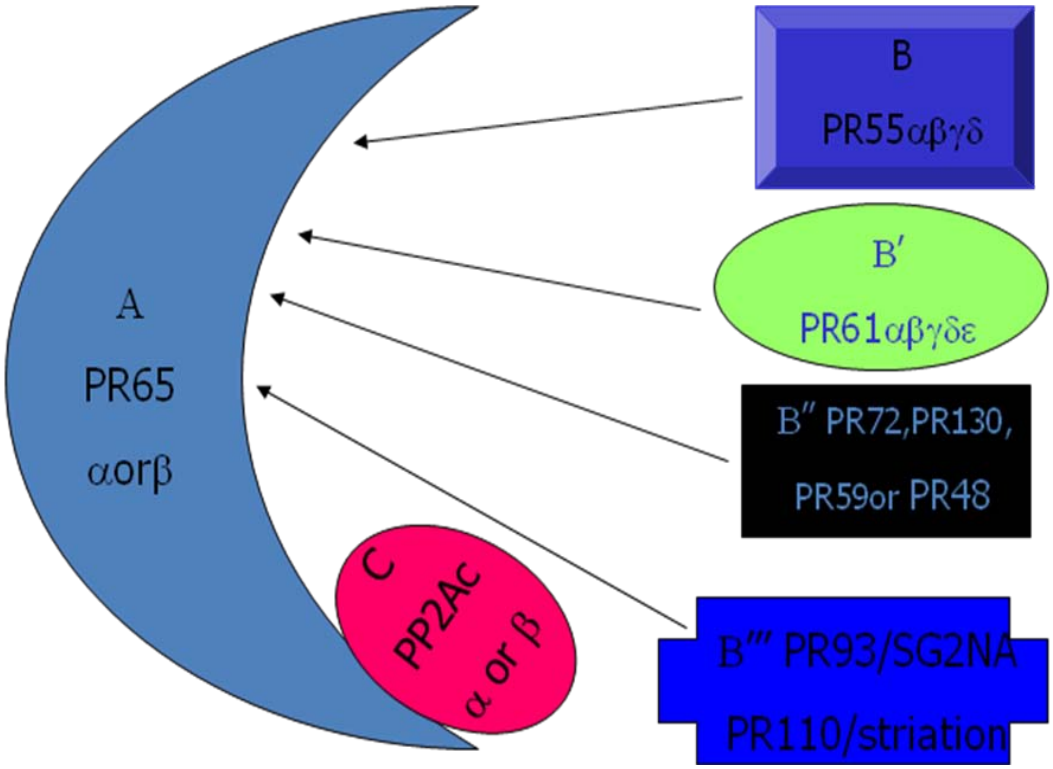
A
PR65
αorβ
B
PR55αβγδ
B′
PR61αβγδε
B″ PR72,PR130,
PR59or PR48
C
PP2Ac
α or β
B‴ PR93/SG2NA
PR110/striation

Fig. 6. Model of the PP2A heterotrimer. The A and C subunits are usually found bound together as a heterodimer in the cell. This heterodimer forms the heterotrimeric holoenzyme by the B-subunit binding to the A-subunit. Any one isoform of the different B-subunit families may bind to the A-subunit at one time to confer, substrate specificity for the phosphatase. Fig. adapted from Janssens et al., 2005.

Chapter 1: Introduction

Prelude:

In this introduction I will review relevant features of ciliary structure and function that provide part of the foundation for my study of the phosphatase PP2A and its role in cilia. This includes review of the structure of the 9+2 ciliary axoneme, evidence that one of the motors, I1 dynein, is regulated by phosphorylation and that a key enzyme, the phosphatase PP2A, may be an important component of regulation and is physically localized in the axoneme. I will review the PP2A family of phosphatases and finish by defining the hypothesis that the otherwise ubiquitous PP2A holoenzyme is targeted and anchored in the axoneme by an axonemal PP2A B- subunit. This is an important idea, providing a basis for specificity of phosphatase activity. In Chapter 2, I will provide additional background on the identification of PP2A in the axoneme. In this thesis, I will demonstrate that PP2A is required for normal ciliary movement.

I. An overview of Cilia and Flagella

Cilia and flagella (the terms are interchangeable) are antenna-like organelles that protrude from the cellular surface and play both motile and signaling roles (Scholey, 2000; Satir and Christensen, 2007; Satir et al., 2010). These highly conserved organelles contain a microtubule based structure called the axoneme, which is enclosed within a ciliary membrane that is continuous with the plasma membrane of cell body. The ciliary membrane contains specialized membrane receptors and channels that transmit signals from the environment back to the cell body for the regulation of both the sensory and

motility functions of the cilium (reviewed in Rohalgi and Snell, 2010; Emmer et al., 2010; Nachury et al., 2010). Interestingly, new evidence indicate that ciliary membrane proteins are transported by a special targeting machinery that includes the "BBsome" (Nachury et al., 2007; Jin et al., 2010,) and that ciliary membrane proteins are segregated by barriers located at the "transition zone" (Fig. 1.1; Craige et al., 2010; Hu et al; 2010).

There are two different types of cilia/flagella: primary/non-motile cilia and motile cilia. Once it was thought that primary cilia were vestigial organelles, and were a non-essential component of the cell (Satir et al., 2010). Now we know that virtually every differentiated cell in the human body has a cilium and when these organelles are absent or non-functional, it can lead to various types of diseases and syndromes referred to as "ciliopathies" (reviewed in Gerder et al., 2010; Goetz and Anderson, 2010; Berbari et al., 2009). Recent data has revealed that primary/non-motile cilia have sensory and signaling functions in many sensory-neuronal cells, (e.g. photoreceptor cells and olfactory cells (Bloodgood, 2010; McEwen et al., 2008; Insinna and Besharse, 2008) as well as chemo- and mechano-sensory transduction in unexpected organs (e.g. the kidney, endothelial cells of the vascular system). The cilium is also important for cell growth and may be vital to understanding certain cancers (Quarmby and Parker, 2005; Wong and Reiter, 2008; Seely and Nachury, 2009; Michaud et al., 2006).

Motile cilia allow the cell to elicit a physical response movement to the ever changing environmental cues around them. The most recognizable cilium is that of the sperm tail, which when defective can result in male infertility (Leigh et al., 2009a, 2009b; Zariwala et al., 2007). Other motile cilia include those found in the epithelia of brain ventricles, the oviducts, the respiratory airway and the nodal cells of early embryos.

These cilia are responsible for moving cerebral spinal fluid, facilitating and protecting egg passage from the oviduct to the uterus, moving mucus out of the lungs and establishing left-right asymmetry in early embryos, respectively (Wallingford, 2010; Basu and Brueckner, 2008,2009; Satir and Christensen, 2007). Defects in these types of cilia can lead to an immotile cilia phenotype referred to as primary ciliary dyskinesia (PCD) (Standard et al., 2010; Leigh et al; 2009). Common symptoms of PCD patients include: chronic sinusitis, bronchiectasis, neonatal respiratory distress, male infertility and situs inversus, a reversal of left-right asymmetry. Much of the work done to identify defects in cilia has been achieved using the green alga, *Chlamydomonas reinhardtii*, as a model system (Snell et al., 2004). The effective use of *Chlamydomonas* as a tool for the identification of ciliary defects in vertebrates was shown when the *Chlamydomonas* IFT88 gene was identified as an ortholog of the polaris/Tg737 gene found in mice (Pazour et al., 1998). Mice with defects in the Tg737 gene were shown to have kidney and liver defects similar to humans that had autosomal recessive polycystic kidney disease (Moyer et al., 1994). The function of the Tg737 disease remained unknown until Pazour et al showed that defects in the IFT88 gene lead to abnormally short or missing cilia (Pazour et al.,1998; 2000). This was a phenotype similar to the short flagellar phenotype in the Tg737 mutant mice. This was one of the first of many examples demonstrating the high conservation of ciliary genes in *Chlamydomonas* and its effective use in the study of vertebrate ciliary defects. In this case, *Chlamydomonas* defined the genes and mechanisms of IFT (intraflagellar transport), a conserved machinery required for assembly of all cilia (Pedersen and Rosenbaum, 2008; Rosenbaum and Witman, 2002). Other new and outstanding examples include study of hydin in *Chlamydomonas*

and the mouse (Lecktreck et al., 2007; 2008), and study of CEP290 (Craige et al., 2010). The other general major advances leading to our current understanding of cilia was the discovery of cilia at the embryonic node and its role in left-right patterning in the vertebrates (reviewed in Hirokawa et al., 2006; Basu and Brueckner, 2008).

II. Experimental model system

The model system *Chlamydomonas reinhardtii* is a eukaryotic, unicellular, biflagellate, green alga (Fig. 1.; The Chlamydomonas Sourcebook, Second Edition). *Chlamydomonas reinhardtii* is the most common species of *Chlamydomonas* used in the laboratory as a model organism. It is one of few organisms to have the mitochondrial, nuclear, and chloroplast genomes represented in one single cell (Grossman et al., 2003; Merchant et al., 2007). *Chlamydomonas* is normally haploid, and has two mating types, "+" and "-" that, when differentiated, can mate, undergo zygote formation and meiosis (Fig.1.2). Meiotic progeny allow genetic mapping by tetrad analysis in mapping strains (Dutcher, 1995). Thus, like yeast and other haploid organisms, *Chlamydomonas* is amenable to efficient genetic analysis and mapping of genes by relatively simple approaches and use of both genetic and physical markers in the genome. The cells can also be transformed by exogenous DNA (Kindle et al., 1989; Kindle, 1990; Dunahay, 1993; Tam and Lefebvre, 1993) and stable diploid cells can be isolated by taking advantage of useful auxotrophic mutations for selection (Ebersold, 1967, Nelson et al., 1994).

To date, *Chlamydomonas* is the only organism that allows for transformation of the nuclear, chloroplast and mitochondrial genome (The Chlamydomonas Sourcebook,

Second Edition). The nuclear genome has been sequenced and a well annotated genomic database has been produced and maintained, founded on a nearly complete sequence analysis (http://genome.jgi-psf.org/Chlre4/Chlre4.home.html). Additionally, BAC, cDNA and nuclear genomic libraries, and mutant maps, are available in a very useful public database (http://www.chlamy.org/chlamydb.html). The database includes descriptions of mutant strains and reagents important for *Chlamydomonas* research. Using these molecular tools, we can often directly map and clone genes starting with protein or genomic sequence or identify mutants corresponding to a particular region in a chromosome using a positional mapping approach (see below). In addition, genomic analysis comparing the *Chlamydomonas* genome to other ciliated and non-ciliated organisms has been a very effective approach revealing a link between cilia and human diseases such as BBS (Bardet-Biedel Syndrome, Li et al., 2004)

The *Chlamydomonas* flagellar proteome is another useful database and tool available for characterization of the eukaryotic cilium (Pazour et al., 2005; http://labs.umassmed.edu/chlamyfp/index.php). The proteome was produced by a large scale mass-spectrophotomertric analysis of all the proteins contained within the *Chlamydomonas* flagellum**.** Key advantages included the ability to isolate pure fractions of cilia and, of course, the completed genome. The peptides in this database were identified from isolated flagellar fractions including: tergitol-insoluble (membrane and axonemes), nonidet soluble (Membrane +Matrix), KCl (from nonidet demembranated axonemes), and axonemal (axonemal proteins remaining after KCl extraction) (Fig. 1.3). Of the proteins identified 360 were identified with high confidence and 292 with moderate confidence. Ensuring confidence in the analysis, 97 of the 101

previously known flagellar proteins were identified with high confidence. This is a well maintained publically available and annotated database that facilitates identification of conserved proteins unique found in the eukaryotic cilium.

The *Chlamydomonas* cells are approximately 10µm in diameter with two flagella that are approximately 10-12µm long (Fig. 1). The cells swim with a breast-stroke type fashion with their two flagella beating in an asymmetric ciliary-like pattern or can reverse and produce symmetrical, flagellar-like bend patterns (Bayly et al., 2011; Brokaw and Luck, 1983; Brokaw and Kamiya, 1987). This ciliary waveform can be altered in response to light in a process called phototaxis, a ciliary activity precisely regulated in the cell for turning toward or away from light (Witman, 1993). The flagella of *Chlamydomonas* are not required for cell viability. Therefore, this allows us the opportunity to screen for mutants defective in assembly or normal flagellar functions such as decreased swimming velocity, improper waveform (Kamiya et al., 1991), abnormal beat frequency (Kamiya, 2002), or an inability to undergo normal phototaxis (Pazour et al., 1995; King and Dutcher, 1997). In fact, use of phototaxis as a screen has been a productive and powerful approach for defining of conserved ciliary proteins important for regulation (King and Dutcher, 1997; Okita et al., 2005). One of the most important features of *Chlamydomonas* is the fact that unlike vertebrate cells, large quantities of flagella can be isolated and easily separated from their cell bodies. As a result, we can isolate large amounts of protein to be used in biochemical assays. Due to the shared conservation of ciliary structures and pathways between *Chlamydomonas* and humans, a number of ciliary defects identified first in *Chlamydomonas* have been associated with human disease models. Equally important for discovery of conserved

genes, *Chlamydomonas* offers exceptional experimental advantages. Thus, it is one of the most powerful model genetic organisms that offer convenient biochemistry, *in vitro* functional studies, molecular approaches, a collection of motility mutants and structural analysis, all in one cell.

III. The Axoneme

Removal of the flagellar membrane exposes the highly conserved microtubule based structure called the axoneme (Figs.3 and5). The axoneme is a highly ordered structure whose proper function is determined by precise positioning of proteins within and along the microtubule of the "9+2" the axoneme (Fig. 5). The ciliary axoneme originates from the basal body, which provides a template for microtubule growth and is required for assembly of all cilia (Dutcher, 2003; Hiraki *et al.*, 2007; Nakazawa *et al.*, 2007; Marshall, 2008a). The basal body is a barrel shaped structure derived from the centriole and composed of 9 triplet microtubules; the A tubule is attached to an incomplete B tubule that is in turn attached to an incomplete C tubule (Fig. 1.1). A and B tubules of the basal body continue as the A and B microtubules of the axoneme while the C tubule terminates between the basal body and the origin of the axoneme, a region termed as the “transition zone” (O'Toole et al., 2003, Pearson and Winey, 2009; Marshall, 2008). Like the axoneme, the basal bodies / centrioles are highly conserved (Pearson and Winey, 2009).

The axoneme is composed of approximately 400 distinct and well conserved proteins (Li et al., 2004; Pazour et al., 2005). Most motile cilia and flagella contain a highly conserved "9+2" axonemal arrangement (Fig. 3). This 9+2 arrangement refers to

the nine outer doublet microtubules and two inner microtubule based structures called the central pair. The central pair complex is composed of the “C1” and “C2” microtubules and associated structures and is part of the signal transduction mechanism (central pair/radial spoke/I1 dynein) that regulates axonemal bending. This mechanism is discussed in more detail below and appears to involve the protein phosphatase PP2A as a downstream component (Warner and Satir, 1974; DePetrillo and Smith, 2010; Mitchell and Sale, 1999; Wargo et al., 2005; Lechtreck and Witman, 2007; Lechtreck et al., 2008). In some cilia types the central pair is missing and has a 9+0 arrangement. Previously cilia missing the central pair were only thought to be non-motile/primary cilia (Satir et al., 2010). However, motile cilia found at the embryonic node lack the central pair and have been shown to move and are critical for left-right axis determination (Hirokawa N. et al, 2006; Feistel K. and Blum M., 2006; Okada Y. et al., 2005; Nonaka et al., 1998). It is also likely the embryonic node bears both motile and primary cilia (McGrath et al., et al., 2003), and that some of the cilia are 9+2 structures (Caspary et al., 2007).

Located between the central pair and outer doublet microtubules are the radial spokes that are anchored on the outer doublet microtubules and transiently contact the central pair projections (Warner and Satir, 1974). The radial spokes are also scaffolds for various signaling molecules such as PKA and calmodulin and transmit signals to the dyneins located on the outer doublets (Hasgawa et al., 1987; Yang et al., 2001, 2004, 2006; Gaillard et al., 2001; Gaillard et al., 2006). It is believed that the central pair contacts the radial spokes during flagellar bending to transmit a signal to the outer doublet microtubules involved in control of waveform (Brokaw et al., 1982; Porter et al., 1992). As discussed in more detail below, part of the function of the radial spokes is to

transmit signals that control phosphorylation, including IC138 in I1 dynein (Wirschell et al., 2007; Elam et al., 2009). The mechanism also appears to require PP2A, the focus of my dissertation.

The outer doublets are composed of an A- and an incomplete B-tubule containing 13 and 11 proto-filaments respectively (Linck and Stephens, 2007). The outer doublet microtubules are connected to one another through nexin links recently shown by Cryo-EM tomography to be what has been referred to as the dynein regulatory complex structure (DRC, Fig., Heuser et al., 2009). The DRC is known to regulate microtubule sliding, including restriction of sliding through the nexin function, resulting in control of axonemal bending (Satir, 1968; Summers and Gibbons, 1971). The mechanism of the DRC is not known, but it appears to alter bending through modulation of the basic sliding microtubule mechanism that drives bending (Heuser et al., 2009).

Located on the A tubule of the doublet are molecular motors called the inner and outer dynein arms (King and Kamiya, 2009). These dynein structures are a family of large, conserved ATPases that convert chemical energy to the mechanical energy that drives microtubule sliding, which is responsible for flagellar bending (Gibbons and Rowe, 1965; Satir, 1968; Summers and Gibbons, 1971, Shingyoji et al., 1977; Brokaw, 1991). As emphasized in the next section, the outer arm dyneins are homogeneous structures responsible for control of beat frequency and power required for movement (Fig. 1.4.; King and Kamiya, 2009). The inner arm dyneins, however, are more complex, composed of at least seven different dynein subspecies precisely organized in a 96-nm repeat pattern along each A-tubule of the axoneme (Fig 5.; Wirschell et al., 2007, Kamiya et al; Porter and Sale, 2000; King and King, 2009). The inner arm dyneins are localized

on the A-tubule in a 96-nm repeat pattern (Goodenough and Heuser, 1985; Porter and Sale, 2000; Heuser et al., 2009; Bui et al., 2009). The inner dynein arms play a key role in regulation of the size and shape of the axonemal bend (Kamiya, 2002; King and Kamiya, 2009). The inner dynein arm called I1 dynein plays a particularly important role and its activity is controlled by phosphorylation (Wirschell et al., 2007). This will be discussed further after discussion of the dynein motors.

IV. Axonemal dyneins

All dynein complexes are very large and have a molecular mass greater than a million Dalton (King 2000 and 2003; Harrison and King, 2000). Dynein subunits can be classified as heavy chains (HC, 400-500 kDa), intermediate chains (IC, 50-150 kDa), and light chains (LC, 8-45 kDa) (Pfister et al., 2006). The heavy chains contain the ATPase activity that convert chemical energy into the mechanical force needed to move along the microtubules and the domain structure has recently been solved (Carter et al., 2011). Dyneins are minus-end directed motors found on microtubules (Sale and Satir, 1977; Fox and Sale, 1987), and generate microtubule sliding in one direction. This observation has led to a "switching" model for bends in the opposite direction: dyneins on one side of the "axis" of the axoneme is active for bending in one direction, whereas the dyneins on the opposite side of the axis must be inactive, with passive microtubule sliding (Fig. 1.5a; Smith, 2007). If all the dyneins were active at the same time on both sides of the axoneme, there would be no movement. Therefore, it is imperative that the dyneins be regulated not only along the length of the axoneme, but also around the circumference to alternate bends.

Based on detailed analysis of *Chlamydomonas* mutants, and pathology of human PCD patients, the outer and inner arms assemble independently of each other and are located at specific sites within the axonemal superstructure organized in a 96nm grouping fashion (Porter and Sale, 2000; Nicastro et al., 2006; Bui et al., 2008, 2009, 2011). Outer arm dyneins repeat at 24-nm intervals along the length of the flagellar axoneme (Fig. 5). The outer dynein arm-docking complex (ODA-DC) is thought to set up the proper binding site for the outer arm structures (Fig. 1.4; Takada and Kamiya, 1994; Wakabayashi *et al.*, 2001). In each organism studied, and based on structure and fractionation, there is only one known species of outer dynein arm, which contains at least 13 polypeptides: 3 heavy chains (HC:α,β,γ), 2 intermediate chains (IC), and several light chains (LC1-8) (Fig. 1.4, DiBella and King, 2001; King and Kamiya, 2009). When viewed by electron microscopy, the *Chlamydomonas* outer arms appear as a bouquet-shaped structure with 3 large heads, each head representing one of the globular domains of the three heavy chains (Goodenough and Heuser, 1983; Oiwa and Sakakibara, 2005; King and Kamiya, 2009). The outer dynein arms are required for normal flagellar beat frequency and provide up to 4/5ths of the power for flagellar movement (Brokaw, 1994). Without this motor structure, flagella beat at a much lower frequency and as a result cells swim with a slow, jerky motion at approximately one-third the speed of wild-type cells. This characteristic swimming phenotype is unique to the outer dynein armless (*oda*) mutants and distinguishes them from other *Chlamydomonas* motility mutants.

The inner dynein arms are more heterogeneous in composition and structure. They are organized in a repeating 96-nm intervals (Fig. 5; Goodenough and Heuser, 1985; Piperno *et al.*, 1990; Porter et al., 1992; Bui et al., 2008; Nicastro et al., 2006). The

inner arm I1 isoform (subspecies f), containing 2 HCs, is the most proximal component of the 96-nm repeat and is found along the entire length of the axoneme. I1 dynein is a major focus of this thesis since, as discussed below, I1 is regulated by phosphorylation. I1 is followed more distally by at least six distinct single-headed (i.e. containing one HC) inner arm dynein motors (King and Kamiya, 2009). The single-headed dyneins, termed subspecies a, b, c, d, e, and g, were defined by fractionation and then subsequently by mutations in genes that encode each individual heavy chain (Table I; Alford et al., 2011; Yagi et al., 2008; Kagami and Kamiya, 1992). Current data supports that different single headed inner arm isoforms are also found in the proximal region of the flagellum as compared to the more distal regions (Yagi et al, 2009). It is undetermined how the inner arm dyneins are targeted to the axoneme. It is predicted that like the outer dynein arms, inner dynein arm-docking complexes (IDA-DCs) are required to target and dock each of the inner arms to their respective sites along the length of the axoneme (Porter and Sale, 2000).

The inner dynein arms are responsible for regulation of the size and shape of the axonemal bend and for the efficient propagation of the flagellar waveform. This conclusion is based on motion analysis of inner dynein arm mutants (*ida*) that have reduced shear amplitude (Brokaw and Kamiya, 1987; Bayly et al., 2010) and as a result swim with a slow, smooth motion. Since different isoforms of single headed inner dynein arms are targeted to specific regions of the axoneme, this suggests that efficient control of waveform requires functionally distinct dynein motors within these different axonemal domains (Piperno and Ramanis, 1991). The understanding of how proteins are targeted to the flagellum and to the axoneme is critical to our understanding of how the

flagellar axoneme is both constructed and how proteins within it are regulated. This theme of targeting, whether it be for dynein motors, kinases or phosphatases, is one of the central themes of this thesis, and is critical to our understanding of flagellar assembly and motility.

V. Sliding-Switching model for ciliary bending

Before proceeding to a discussion of the axonemal kinases and phosphatases and how they might regulate motility, it is important to describe a working model for ciliary bending (Fig. 1.6). As discussed briefly above, work has revealed that the basis for ciliary motility lies in controlled dynein-driven microtubule sliding-a "sliding microtubule" model for ciliary bending (Satir, 1968; Summers and Gibbons 1971; Shingyoji et al., 1977; Brokaw, 1991). In addition, it was determined that the dynein motors generate force in one direction (minus-end direction) relative to microtubule polarity (Sale and Satir, 1977). Thus, since all dyneins are minus-end motors, this observation directly led to a "switching" model for alternating effective (principal/forward) and recovery (reverse) bending: dyneins on one side of a structural and functional axis (Figs. 1.5 and 1.6) of the axoneme are active for bending in one direction. Predictably, when the direction of bending changes or "switches", there is a switch in activity where the previously inactive dyneins, on one side of the axis, are activated, and the formerly active dyneins on the opposite side, are turned off.

The precise mechanism for sensing the end point of each bend direction is not understood but clearly for oscillatory bending, dynein motors must be regulated.

Detailed experimental evidence indicates the basic oscillatory movement, and "switches" in bend direction, are inherent properties of the dynein motors involving microtubule curvature and a mechanical feedback control (Mora and Shingyoji, 2004; Hayashi and Shingyoji, 2009). The switching sensor is not known, but one model includes the outer dynein arm playing a role as a sensor of microtubule curvature (Hayashibe et al., 1997; Patel-King and King, 2009). Thus, the phospho-regulatory mechanism discussed in this thesis is not responsible for the control of the basic oscillatory bending in ciliary axonemes. Rather, the phospho-regulatory mechanism is superimposed on the basic dynein-driven mechanism to modulate the size and shape of the bend, parameters we will refer to as ciliary waveform. So, what is I1 dynein and what is the evidence that I1 dynein is regulated by phosphorylation?

VI. Dynein regulation by phosphorylation

Studies in diverse experimental systems revealed that axonemal motility is regulated by phosphorylation (reviewed in Salathe, 2007). Based on *in vitro* functional studies with isolated axonemes the focus is on the axonemal molecular motor I1 dynein and how phosphorylation alters I1 dynein. Data shows that I1 dynein is directly involved in regulation of bending and phototaxis, and is regulated by phosphorylation (reviewed in Wirschell, 2007).

I1 dynein (also known as dynein f) is an unusual inner arm dynein. First, unlike all other inner arm dyneins, which are single-headed dynein, I1 dynein is a two-headed structure (Goodenough and Heuser, 1985; Piperno et al., 1990; Smith and Sale, 1991).

As indicated in Figure 5, I1 dynein is located at the most proximal end of the 96 nm repeat near radial spoke 1

(Nicastro et al., 2006; Bui et al, 2008). I1 dynein is a large complex, composed of two heavy chains, 1α and 1β; three intermediate chains IC140, IC138, IC97; a light intermediate chain, FAP120; and several light chains (Fig. 4; Piperno et al., 1990; Porter et al., 1991; Yang and Sale, 1998; D. Bella et al., 2004, Hendrickson et al., 2004; Ikeda et al. 2009; Wirschell et al., 2009; Bower et al., 2009). Analysis of *Chlamydomonas* mutants revealed I1 assembly is required for control of axonemal bending (Brokaw and Kamiya, 1997; Bayly et al., 2010) and phototaxis (King and Dutcher, 1997; Okita et al., 2005). In addition, I1 dynein mutants "suppress" paralysis in a central pair mutant (Porter et al., 1992). This result suggested that I1 dynein was regulated by a pathway that linked the central pair and radial spokes for control of motility. The question has been: What is this regulatory mechanism?

In vitro functional assays and biochemistry, taking advantage of wild-type and informative mutant axonemes, confirmed that I1 dynein is important for control of axonemal motility, and that the mechanism of control involved reversible phosphorylation of the intermediate chain IC138 (Fig. 2.; Habermacher and Sale, 1997; King and Dutcher, 1997; Yang and Sale, 2000; Hendrickson et al., 2004; Wirschell et al., 2009). Functional assays demonstrated that increased phosphorylation of IC138 resulted in inhibition of dynein-driven microtubule sliding (Fig. 2). The precise mechanism for how phosphorylation alters dynein activity is not known, but regulation involves the central pair-radial spoke mechanism (Wirschell et al., 2007) and requires the assembly of I1 dynein, (Habermacher and Sale, 1997), the IC138 "complex" (Bower et al., 2009) and

the 1β heavy chain (Toba et al., 2011). Important for this thesis, the protein kinases and phosphatases required for regulation are physically built into the 9+2 axonemal structure.

Ultimately we want to test the hypothesis that IC138 phosphorylation regulates I1 dynein and axonemal bending, this will require the identification of, and mutation of key phosphorylated amino acids. Preliminary data has revealed six candidate phosphorylation sites (Serine (3), Threonine (2), and Tyrosine(1)) within the IC138 subunit, all located at the N-terminal region of the protein (Mittag et al., 2009). The analysis will also require a null mutant in the IC138 gene at the Bop5 locus in *Chlamydomonas* (Hendrickson et al., 2004; Bower et al., 2009; Ikeda et al., 2009).

VII. Proteins kinases – PKA and CK1 - located in the axoneme

The focus on kinases associated with the axoneme began with biochemical and physiological assays using isolated ciliary axonemes. For example, studies using ciliary axonemes or detergent extracted *Tetrahymena* and *Paramecium* cells revealed that cAMP alters reactivated, ATP –induced ciliary beating (Bonini et al., 1988 JCB; Hamasaki et al., 1989). Consistent with the functional and pharmacological analysis, PKA has been isolated and characterized from axonemes (Hochstrasser et al., 1996) and may alter dynein activity in cilia from *Paramecium* (Walczak et al., 1993). Similar studies with ciliary axonemes from mammalian epithelia also reveal that axonemal beating is regulated by increased cyclic nucleotide second messengers and that the ciliary axoneme bears AKAPs and PKA (Kultgen et al., 2002; Salathe, 2007). Part of the mechanism is to control ciliary beat frequency by regulation of the outer dynein arms. Since these

studies make use of the intact, isolated 9+2 axoneme, predictably the key kinases are targeted and anchored in the axoneme near the substrates by specialized scaffold proteins similar to the AKAP model for PKA localization.

As discussed above, genetic and *in vitro* studies using isolated axonemes from *Chlamydomonas* have also revealed that inner arm dynein activity is regulated by phosphorylation and that the key kinases are located in the axoneme. Based upon functional assays and the use of the PKA inhibitor PKI, one of the kinases is PKA (Howard et al., 1994), and, as discussed further below, another axonemal kinase that controls inner arm dynein phosphorylation is CK1 (Yang and Sale, 2000; Gokhale et al. ,2009). As indicated in Fig. 2, there appears to be a correlation between IC138 phosphorylation and regulation of microtubule sliding: inhibition of microtubule sliding correlates with phosphorylation of IC138; active or rescued microtubule sliding correlates with de-phosphorylation of IC138. To date, the only mechanism for localizing PKA in the axoneme is through AKAPs (Gaillard et al., 2001; 2006).

Experimental analysis of isolated *Chlamydomonas* ciliary axonemes has implicated the protein kinase, CK1, in regulation of dynein-driven motility. Using CKI inhibitors, it was shown that the characteristic slow-sliding velocities of paralyzed radial spoke mutant *Chlamydomonas* axonemes were restored to wild-type levels, indicating that CK1 plays a role in dynein-driven ciliary motility (Fig. 1.7;Yang and Sale, 2000; Gokhale et al., 2009). In addition, CK1 inhibitors blocked phosphorylation of IC138, demonstrating a correlation between IC138 phosphorylation and control of microtubule sliding by CK1. These findings implicated an axonemal CK1, in addition to PKA, in regulation of I1 dynein and microtubule sliding. CKI is located in the flagellar axoneme in

Chlamydomonas where it functions in control of IC138 phosphorylation and microtubule sliding (Gokhale, et al., 2009). *In vitro* assays using recombinant CK1 proteins demonstrate that an enzymatically functional CK1 is required to inhibit I1 dynein-dependent microtubule sliding. The results support a model in which CK1 and I1 dynein function together to control flagellar waveform and firmly establish that an axonemal CK1 regulates I1-dynein activity. Thus, CK1 is a downstream component of the central pair-radial spoke mechanism that controls I1-dynein activity.

VIII. Axonemal Phosphatases

The role of PKA and CK1 in regulation of microtubule sliding in axonemes from *Chlamydomonas* was first defined by taking advantage of mutant cells defective in normal control of the kinases and resulting in constitutively active axonemal kinase activity (Fig. 1.7 and 1.8). As a consequence of the mutations, and the constitutively active axonemal kinases, the axonemes are paralyzed presumably due to inhibition of dynein. Consistent with this interpretation, and illustrated in Fig. 1.7, kinase inhibitors "rescued" microtubule sliding in isolated axonemes (Howard et al., 1994; Habermacher and Sale, 1996; 1997; Yang and Sale, 2000). Since protein kinase inhibitors rescued microtubule sliding in isolated axonemes, predictably the axonemes must contain protein phosphatases required for de-phosphorylation of key phospho-proteins and increased microtubule sliding. Consistent with this prediction, Habermacher and Sale (1996), determined that phosphatase inhibitors, including microcystin LR and okadaic acid, when applied before or with the kinase inhibitors, block kinase inhibitor-dependent rescue of microtubule sliding (Fig. 1.8). Subsequent biochemical and molecular analyses revealed

the axoneme contains a highly conserved Protein Phosphatase 1 (PP1) and Protein Phosphatase 2A (PP2A,Yang et al., 2000), while comprehensive proteomic analyses of cilia also identified additional phosphatases (Pazour et al., 2005). My focus is on PP2A as discussed in Chapter 2 of the Thesis. For the remainder of this Introduction, I will review PP2A and then describe the hypothesis that forms the basis of my dissertation.

IX. The protein phosphatase, PP2A

At least 518 putative protein kinases have been identified in the fully sequenced Human genome (Lander et al, 2001; Johnson and Hunter, 2005; Venter et al., 2001). The number of known protein phosphatases is much smaller, with 107 putative tyrosine phosphatases and 30-40 serine/threonine phosphatases (Alonso et al., 2004). The serine/threonine phosphatases are divided into the metal-dependent protein phosphatases (PPM) family and the phosphoprotein phosphatases (PPP) family (Cohen PT, 1997). The PPM family comprises magnesium-dependent protein phosphatases such as PP2C and pyruvate dehydrogenase phosphatase, while the PPP family includes protein phosphatase 1 (PP1), PP2A, PP2B/calceneurin, PP4, PP5, PP6, and PP7. The *Chlamydomonas* flagellar proteome revealed the presence of several phosphatases in the flagellar fractions (Pazour et al., 2005). The challenge is to determine their role in ciliary function.

As stated above and elaborated upon in Chapter 2, the focus of this thesis is on the protein phosphatase 2A (PP2A). PP2A is a serine/threonine phosphatase that plays a role in many vital cellular processes including cell growth, cell cycle, mitosis, cell motility, and apoptosis (Janssens and Goris, 2001, Virshup, 2000, Lechward et al., 2001, Mumby

and Walter, 1993). Additionally, the hyper-phosphorylation of the microtubule associated protein tau has been shown to result in the formation of brain tangles resulting in Alzheimer's disease (AD) (Gotz, 2001; Goedert and Spillantini, 2006). PP2A has been shown to directly bind to and play a major role in the de-phosphorylation of Tau (Gong et al., 1994, Goedert et al., 1995; Sontag et al., 1999; Gong et al., 2000; Bennecib et al., 2000; Kins et al., 2001).

The holoenzyme of PP2A is made up of three different subunits, the A-scaffolding, C-catalytic and the B-regulatory subunits (Fig. 6; Shi, 2009). In human cells there are two different isoforms of the A/PR65- and C-subunits, alpha and beta, which are each expressed by different genes. The A- and C- subunits bind together in the cell to form an obligate heterodimer. The A-subunit is a 65 kDa protein comprised of 15 tandem, α-helical HEAT repeat domains. The A- protein has no catalytic activity, but serves as a platform for binding the B- and C-subunits of the holoenzyme (Xu et al., 2008). Characterization of the A-subunit shows that the catalytic subunit binds to HEAT repeats 11-15, while the regulatory B-subunits bind the amino terminal end (Rudiger R et al., 1992; Ruediger et al., 1994, Zhou et al., 2003; Xing et al., 2006; Xu et al., 2008). As reviewed in Chapter 2, *Chlamydomonas* flagella contain both the PP2A A- and C-subunits (Yang et al., 2000).

The C-subunit is a highly conserved, compact protein and adopts an α/β folding pattern (Xu et al., 2008). Two inhibitors okadaic acid and microcystin-LR bind to the same surface pocket on the catalytic subunit (Xing et al., 2006). The C-subunit can be post-translationally modified by phosphorylation and methylation and these modifications have been shown to play a significant role in the assembly and activity of

the PP2A holoenzyme (Lee et al., 1996; Xie and Clarke, 1994a,1994b,1993; Lee and Stock ,1993). For example, methylation of the carboxy-terminal Leu309 in a conserved $TPDYFL_{309}$ motif of the catalytic subunit has been shown to enhance the affinity of the PP2A core enzyme for some, but not all, regulatory subunits (Xu et al., 2006, Xing et al, 2006 Tolstykh et al., 2000, Wei et al., 2001; Yu et al., 2001; Ogris et al., 1997, Ikehara et al., 2007, Xu et al., 2008). Reversible methylation of PP2A is catalyzed by two PP2A specific enzymes, leucine carboxyl methyltransferase (LCMT1) and PP2A methylesterase (PME-1) (Lee and Stock, 1993; De Baere et al., 1999; Ogris et al., 1999; Lee et al., 1996). PME-1 catalyzes removal of the methyl group, thus reversing the activity of LCMT1 (Lee et al., 1996). It had also been demonstrated that methylation levels of PP2A changed during a cell cycle, suggesting a critical role of methylation in cell cycle regulation (Janssens & Goris, 2001; Turowski et al., 2007; Lee and Pallas, 2007). In our experiments the 1D6, mammalian C-subunit antibody which recognizes the de-methylated form of the PP2A C-subunit, was used for immuno-blot analysis (Yu et al., 2001). Base-treated immuno-blots using the 1D6 antibody containing WT and *pf4* cytoplasmic extracts revealed that there was a detectable change in immuno-staining of the methylated C-subunits in *Chlamydomonas*. Although the result indicated C-subunit methylation, the 1D6 antibody proved to be a useful tool on both base-treated and non-base treated immuno-blots for our experimental analyses of the *Chlamydomonas* PP2A C-subunit. Future studies will include identifying the role of methylated PP2A C-subunits in *Chlamydomonas* and analysis of whether LCMT-1 plays a role in cilia.

The diversity of the phosphatase activity is accomplished by binding of the regulatory B-subunit to the A-subunit (Virshup and , 2009). In mammalian cells four

different families of B-subunits have been identified, (PR55/B/B55, PR61/B'/B56, PR48/PR72/PR130/B'', and PR93/PR110/B''') (Janssens and Goris, 2001). Each family of B-subunits contains at least three different proteins encoded by at least three different genes some of which contain at least two different mRNA splice variants (McCright et al., 1996, Janssens et al., 2001, Lechward et. al, 2001) thus, the total numbers of possible combinations of PP2A subunits is quite large. Although all B-subunit isoforms are able to bind to overlapping regions within the PP2A A-subunit, there is very little sequence or structural homology between the four different B-subunit families. However, within each family the sequences and predicted structures are very similar.

In the remainder of this Introduction, I focus the PP2A B-subunit, and then build upon the case that the ciliary axoneme bears a specialized B-type subunit that is responsible, in part, for localizing the A- and C-subunit dimer. This model can be likened to an AKAP model for localization of PKA (reviewed in Welch et al., 2010; Wong et al., 2004; Beene and Scott, 2007): in the case of PP2A the B-subunits act in targeting the PP2A holoenzyme. These B-subunits vary greatly in their expression patterns within the cell. In addition, published data has identified the B-subunit as being responsible for regulating spatial and temporal expression of the PP2A holoenzyme thereby conferring substrate specificity of the holoenzyme. As a result of the many different configurations of the PP2A holoenzyme and their different roles within the cell, accurate targeting of the phosphatase is essential and likely mediated by special targeting domains within each different B-type subunit.

X. The PR55/B/B55 family of PP2A B- subunits

As discussed in Chapter 2, my work focuses on the PR55/B/B55 family of PP2A B-subunits. This is because out of all the B-type subunits encoded in the *Chlamydomonas* genome, I found this type of B-subunit in the flagellar proteome (Table 1). Members of the PR55/B/B55 family are typically 55kDa proteins that form a seven-bladed β-propeller like structure due to the seven WD-repeats found throughout the protein (Figs. 1.9 and 1.10a; and Xu et al. 2008; Wall et al., 1995; Schmidt et al., 2002, Xu et al., 2008). WD-repeat proteins are scaffolds capable of mediating complex, reversible, protein-protein interactions, making B/PR55 family members appropriate candidates for targeting and anchoring the PP2A holoenzyme to specific subcellular domains. PP2A holoenzymes containing members of the B/PR55 family members are expressed in a wide variety of tissues including the testis, brain, and in some cases associate with microtubules (Sontag et al., 1995; Schmidt et al., 2002, Schild et al., 2006).

There are currently four different human isoforms that make up the B/PR55 family of B-subunits (αβγδ), and each is encoded by a separate gene (Fig. 1.9; Schmidt et al., 2002). Additionally, each isoform has been shown to have multiple splice variants, adding to the complexity of the phosphatase as a whole (Janssens and Goris, 2001, Schmitdt et al., 2002). Different PR55/B transcripts are tightly regulated at the transcriptional level in different cell types in the mammal (Schmidt et al., 2002). Protein alignments show that these B-subunits share a high degree of homology throughout their sequences with diverse amino-terminal ends, possibly responsible for mediating subcellular domain targeting (Fig. 1.9; Xu et al., 2008). For example, it was shown that

only trimeric PP2A forms containing Bα/PR55 or Bβ/PR55 , but not Bγ or B'/PR61, associate with neuronal microtubules, and that this interaction depends on an as yet unidentified anchoring protein (Price et al., 1999).

Recently, the crystal structure of the human Bα subunit has been solved (Fig. 1.10a; Xu et al., 2008). As was predicted, the B-subunit indeed forms a barrel shaped, B-sheet repeat structure (Fig. 1.10a). Based on this structure, the bottom face of the B-subunit was shown to make several extensive contacts with the A-subunit, consistent with a critical role for B- and A-subunits in both organizing and localizing the C-subunit. Additionally, a β-hairpin arm in the second β-sheet blade, extends out of the propeller and attaches to the A-subunit (Fig. 1.10b). Deletion of this β-hairpin arm abolished the interaction between the A- and B-subunits (Xu et al., 2008). The crystal structure of the PP2A holoenzyme containing the Bα subunit has also shown that members of the B55 family make few interactions with the C-subunit unlike members of the B' family which make extensive contacts with the C-subunit (Figs. 1.10 b,c). However, the PP2A holoenzymes containing the Bα isoform have been shown to be the most affected by decreased methylation of the C-subunit (Xu et al., 2006, Xing et al, 2006 Tolstykh et al., 2000, Yu et al., 2001; Wei et al., 2001, Ogris et al., 1997, Ikehara et al., 2007, Xu et al., 2008). The top face of the β-propeller contains a highly acidic groove proximal to the active site of the C-subunit, similar to a previously identified peptide binding site thought to be a putative substrate-binding groove (Fig. 10.10b; Wilson et al., 2005, Xu et al., 2008). Based on these structural features, PP2A holoenzymes containing B55 subunits are thought to have a larger substrate binding site than members of the B' family.

One of the most studied B55 interacting proteins has been the microtubule associated protein, tau. PP2A holoenzymes containing B/PR55 subunits were shown to bind and dephosphorylate tau very efficiently (Goedert et al., 1992; Sontag et al., 1999). An *in vitro* dephosphorylation assay was performed using recombinant tau fragments and Bα containing PP2A holoenzymes containing mutations in various regions of the B-subunit protein. Results show that two non-overlapping microtubule binding sites within tau bind the B-subunit. It was also shown that when certain charged regions of the B-subunit are replaced with neutral or deleted amino acids within the central groove region, tau binding is diminished or abolished (Xu et al., 2008). This critical experiment provides valuable insights into determining how PP2A recognizes and binds to dephosphorylate its substrates. Thus, the B-subunit appears to play multiple roles: targeting PP2A in the cell and organizing the precise interaction between substrate and C-subunits. In this thesis I will present evidence that a specialized ciliary axonemal B-subunit is required to localize PP2A for control of motility. Furthermore, based on mutations in intragenic revertants in the gene that encodes the axonemal B-subunit, that wild-type B-subunit structure is required for PP2A activity in the ciliary axoneme.

XI. Summary and design of the hypothesis

Analyses of isolated axonemes from *Chlamydomonas* by functional, pharmacological and direct biochemical methods have revealed a number of highly conserved, otherwise ubiquitous, protein kinases and phosphatases that are located in the axoneme (Porter and Sale, 2000; Elam et al., 2009). The general mechanism for controlling inner arm dynein activity and regulating microtubule sliding is through phosphorylation of dynein subunits

(e.g. IC138 of I1 dynein), using a network of structures (central pair and radial spokes) and enzymes (CK1, PP2A). Additional important questions include: How and where are these kinases and phosphatases targeted and anchored in the axoneme? The RSP3 AKAP provides an important model (Gaillard et al., 2001; Gaillard et al., 2006) for the targeting of axonemal signaling proteins within the axoneme. How are signals transmitted from the central pair to the radial spoke heads? How are signals from the radial spoke transmitted to the kinases and phosphatases on the outer doublets? How does phosphorylation of dynein subunits alter dynein motor activity? A better understanding of the phospho-regulatory mechanism will require the identification of proteins responsible for anchoring of the kinases/phosphatases to the axoneme. High resolution structural imaging of wild-type and mutant axonemes will define the localization of PP2A in the axoneme, biophysical analyses of dyneins with altered subunit composition and the identification and mutation of the target phospho-residues in the key regulatory proteins will directly test ideas for how IC138 regulates I1 dynein.

As indicated in the next Chapter, functional and biochemical data has revealed that PP2A is localized to the ciliary axoneme and that it plays a role in control of dynein-driven motility (Yang et al., 2000). Furthermore diverse studies indicate that ciliary motility is regulated in part by I1 dynein (reviewed in Wirschell et al., 2009) and that I1 dynein activity is regulated by changes in phosphorylation of IC138 (Habermacher and Sale, 1997; Yang and Sale, 2000; Hendrickson et al., 2004; Ikeda et al., 2009; Bower et al., 2009). Questions include: (1) What is the molecular mechanism for localization of PP2A in the axoneme? (2) What is the precise localization of PP2A in the axoneme? (3) Does the axonemal PP2A play a role in control of IC138 phosphorylation? (4) How does

change in IC138 alter I1 dynein activity? (5) How does I1 dynein contribute to changes in axonemal bending? (6) What are the upstream signals that regulate changes in IC138 phosphorylation? I test the hypothesis that the ciliary axoneme bears a specialized B-type subunit that is required to localize PP2A. I further test the idea that PP2A is part of a network of signaling proteins that controls IC138 phosphorylation.

Fig. 1.1.

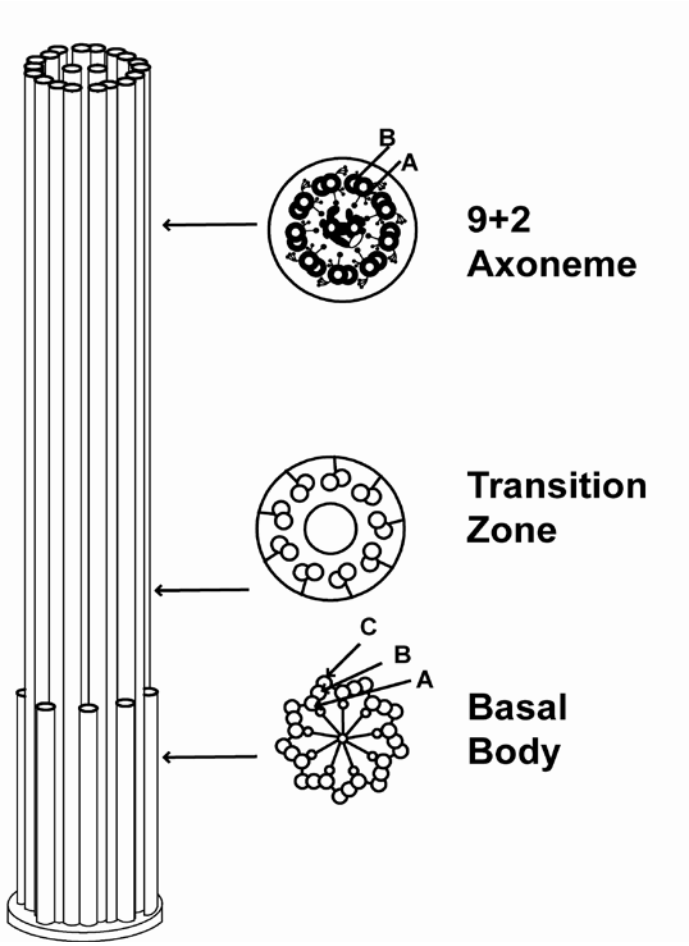

Fig. 1.1: Diagram of the structural organization of the basal body, transition zone, and axoneme. The 9+2 axonemal structure originates at the basal body, a cartwheel-like structure characterized with a 9+3 arrangement of microtubules. While the A and B microtubules of the basal body are continuous with the axonemal A and B microtubules, the C microtubule of the basal body terminates at a region called the transition zone. In addition, a pair of central singlet microtubules originates at the transition zone. [cross sections to the right depict slices through the structure from proximal (basal body) to distal (axoneme)].

Fig. 1.2

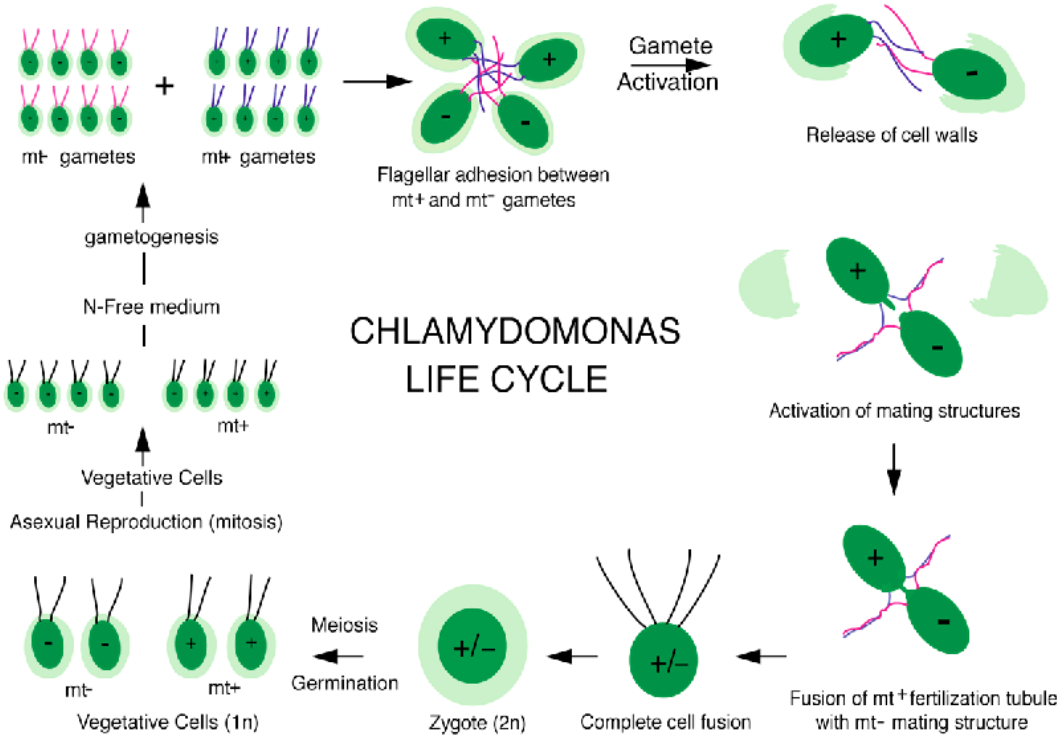
CHLAMYDOMONAS
LIFE CYCLE
mt- gametes
mt+ gametes
Flagellar adhesion between
mt+ and mt- gametes
Gamete
Activation
Release of cell walls
gametogenesis
N-Free medium
mt-
mt+
Vegetative Cells
Asexual Reproduction (mitosis)
Activation of mating structures
Fusion of mt+ fertilization tubule
with mt- mating structure
Complete cell fusion
Zygote (2n)
Meiosis
Germination
mt-
mt+
Vegetative Cells (1n)

Fig. 1.2: The life cycle of *Chlamydomonas* cells. *Chlamydomonas* cells can reproduce sexually or asexually. *Chlamydomonas* cells exist in two mating types "+" and "-". Under nitrogen starvation conditions, the cells can be induced to form gametes. When gametes of opposite mating types are mixed they adhere to one another with their flagella. The cells then release a gametic lytic enzyme to remove their cell walls. Mating structures are then activated forming a fertilization tubule. Fusion of the cells occurs laterally from anterior to posterior to form a quadraflagellate cell. Under favorable conditions zygotes undergo germination and meiotic division to produce four vegetative cells. Vegetative cells undergo mitosis to reproduce.

Fig. 1.3.

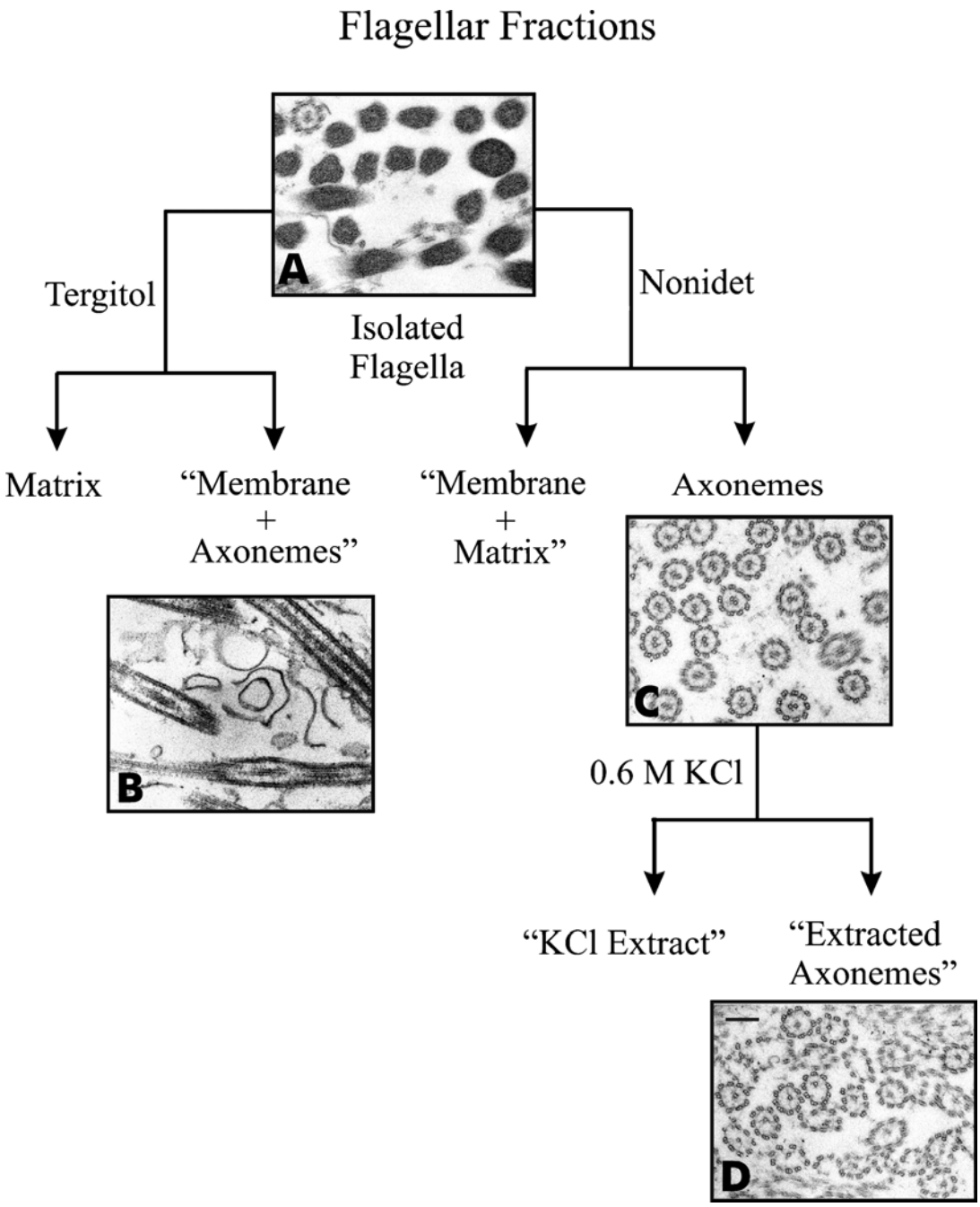
Flagellar Fractions
A
Isolated
Flagella
Tergitol
Nonidet
Matrix
"Membrane
+
Axonemes"
"Membrane
+
Matrix"
Axonemes
B
C
0.6 M KCl
"KCl Extract"
"Extracted
Axonemes"
D

Fig. 1.3: Isolation of *Chlamydomonas* flagellar fractions used for proteomic analysis. (A) Electron micrograph of cross sections of isolated flagella. Isolated flagella from wild-type cells were treated with the detergent Tergitol (left), which disrupts the flagellar membranes without dissolving them, and releases the flagellar matrix. The Tergitol-insoluble fraction (B) was then collected by centrifugation and analyzed by MS. For subsequent analyses (right), flagella were isolated from the outer armless mutant oda1 and treated with the detergent Nonidet, which dissolves the membrane and releases the matrix; the preparation was then centrifuged to yield a supernatant containing the "membrane+matrix" fraction and a pellet containing demembranated axonemes (C). The axonemes were resuspended in 0.6 M KCl and was centrifuged to yield a supernatant containing the "KCl extract" and a pellet containing the "extracted axonemes" (D). The KCl extraction releases numerous axonemal proteins, including those of the inner dynein arms and the C2 central microtubule, which are missing in the extracted axonemes. Images acquired from Pazour et al., 2005.

Fig. 1.4.

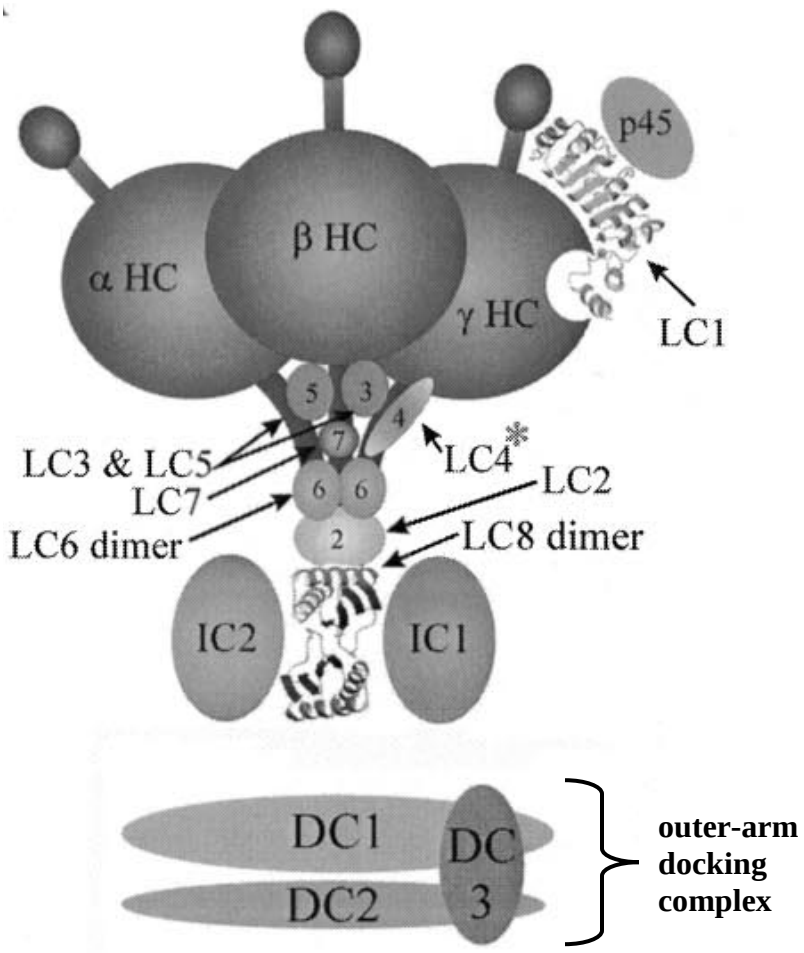
p45
β HC
α HC
γ HC
LC1
5
3
4
7
LC3 & LC5
LC7
LC6 dimer
LC4*
6
6
LC2
2
LC8 dimer
IC2
IC1
DC1
DC2
DC 3
outer-arm docking complex

Fig. 1.4: Molecular model for the outer dynein arm and ODA-DC in *Chlamydomonas*. α, β, and γ denote the three dynein heavy chains; IC1 and IC2 depict the intermediate chains; numbers indicate the light chain subunits (LC1-8). p45 was identified as tubulin. The dynein complex attaches to the A-tubule of the microtubule doublet. This attachment is mediated by a structure termed the Outer Dynein Arm-Docking Complex (ODA-DC), which contains the DC1, DC2, and DC3 subunits.

Fig. 1.5.

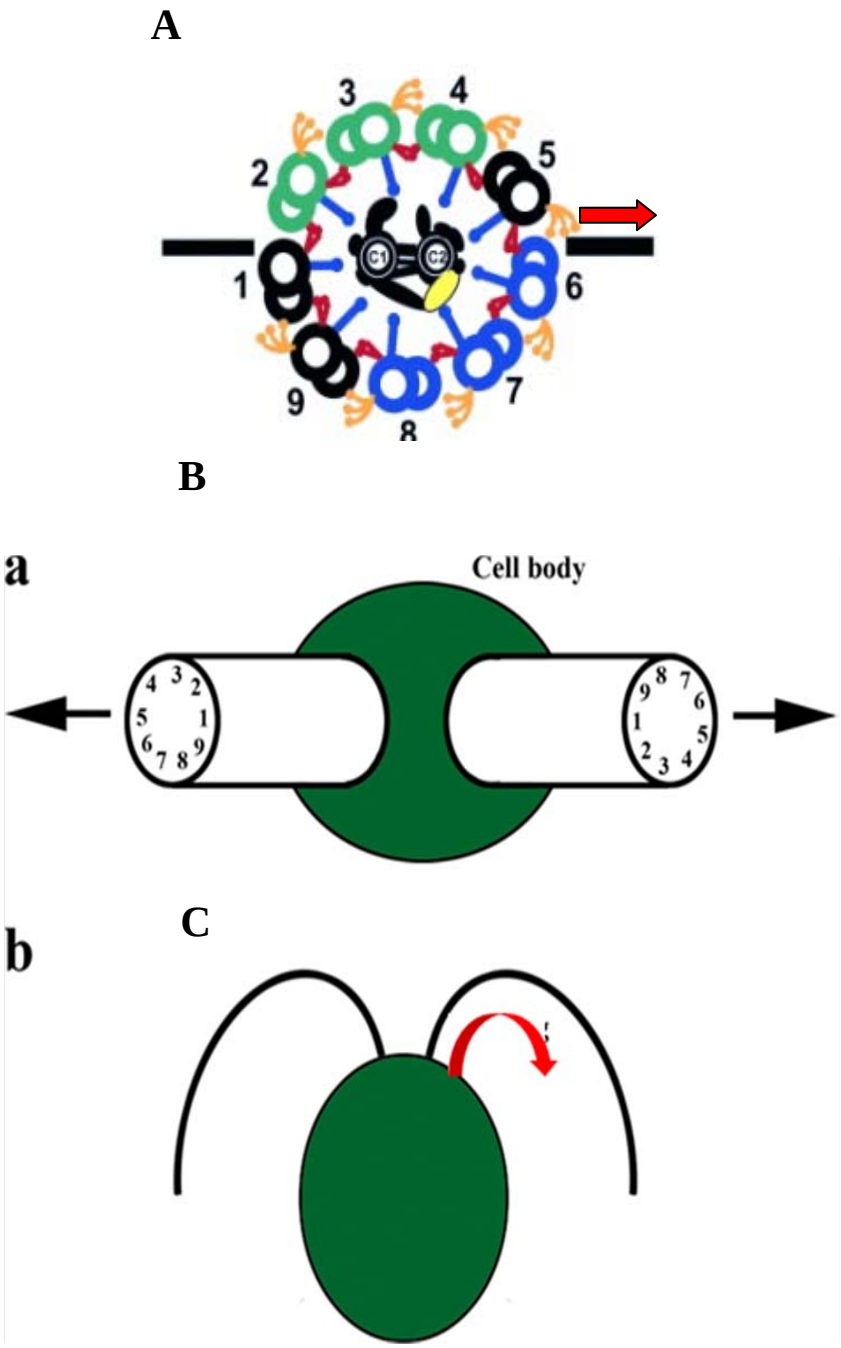

Figs., 1.5 a,b and c: Axis of the axoneme and switching. All arrows represent the plane of the bend **(a)** The plane of bending is illustrated by the black line, and in most cilia, this plane is also defined by a structural and functional axis. The doublet microtubules in blue would be active in the bend to the left and then, at the end of the bend a switch in activity occurs and the doublet microtubules in green become active for the bend in the opposite direction. Fig. a adapted from Smith, 2007. **(b)** Doublet order of flagella at the basal body of *C. reinhardtii* (Hoops and Witman,1983), showing that doublets 1 of the two flagella are facing each other. **(c)** Illustration of the generation of planar asymmetric waveform is shown. Figs b and c adapated from Bui et al., 2009.

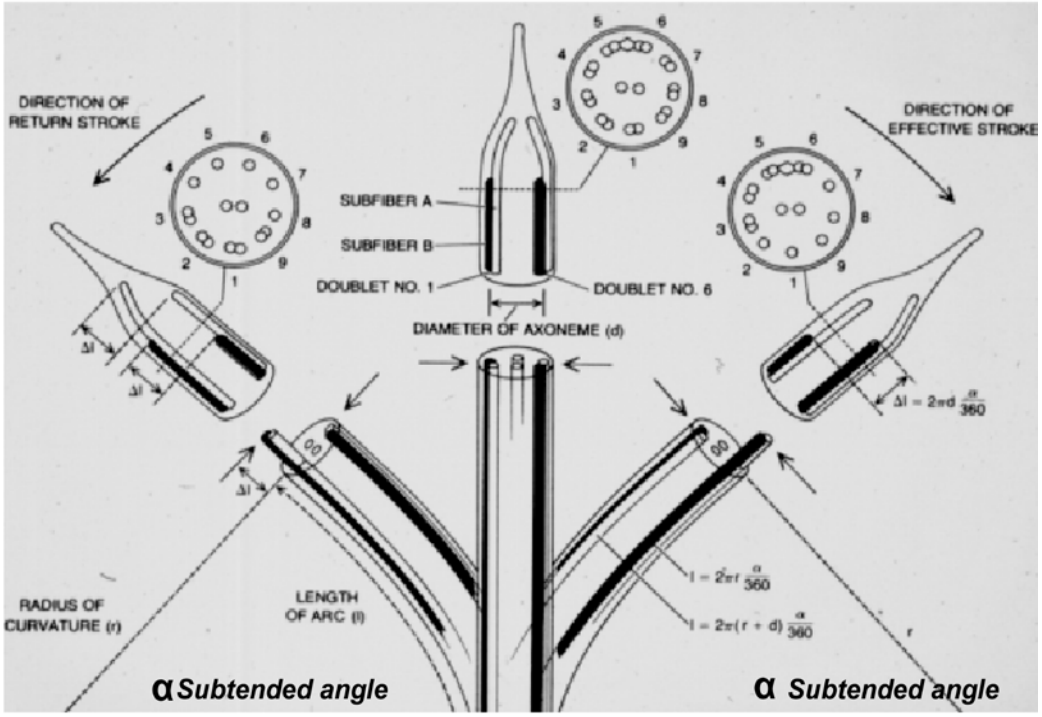
DIRECTION OF
RETURN STROKE
DIRECTION OF
EFFECTIVE STROKE
SUBFIBER A
SUBFIBER B
DOUBLET NO. 1
DOUBLET NO. 6
DIAMETER OF AXONEME (d)
RADIUS OF
CURVATURE (r)
LENGTH
OF ARC (l)
α Subtended angle
α Subtended angle

Fig. 1.6: Microtubule sliding in cilia. This design adapted from Satir, 1968 illustrates that microtubules slide during bending , and that based on simple geometry, microtubule sliding (Δl) can be calculated based on the bend angle (α) and the radius of the bend. Electron microscopy of the tips of cilia in known bend position confound a "sliding filament model' as described in Satir, 1968.

Fig. 1.7.

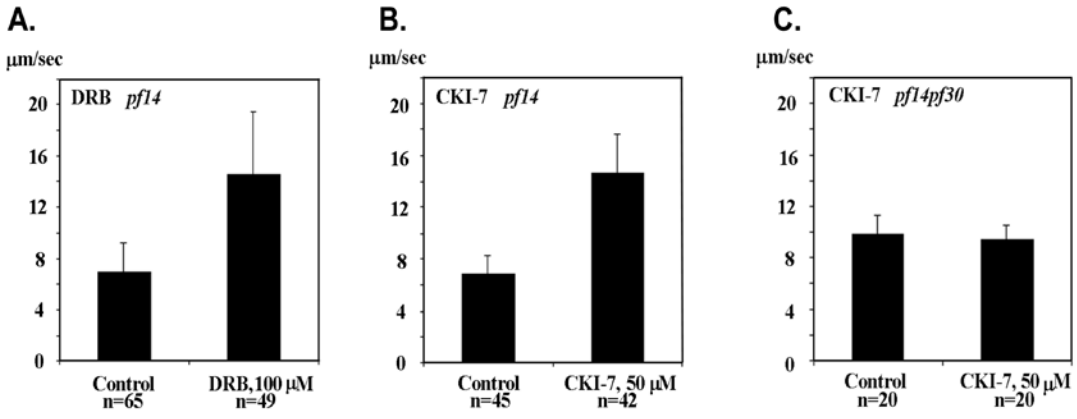
A.
μm/sec
DRB pf14
20
16
12
8
4
0
Control
n=65
DRB,100 μM
n=49
B.
μm/sec
CKI-7 pf14
20
16
12
8
4
0
Control
n=45
CKI-7, 50 μM
n=42
C.
μm/sec
CKI-7 pf14pf30
20
16
12
8
4
0
Control
n=20
CKI-7, 50 μM
n=20

Fig. 1.7: CK1 inhibitors restore dynein activity in paralyzed axonemes lacking the radial spokes. *In-vitro* microtubule sliding assays reveal that dynein activity is greatly reduced in paralyzed axonemes lacking the radial spokes (*pf14*). When these axonemes were treated with CK1 inhibitors DRB (A) and CK1-7(B) dynein-driven microtubule sliding velocity is restored. CK1-7 or DRB fail to rescue dynein activity in a double mutant lacking the radial spokes as well as I1 dynein (C; *pf14pf30*) indicating an essential, positive role for I1 dynein in the regulatory pathway and control of microtubule sliding. The same results were obtained from another radial spoke, paralyzed flagellar mutant, *pf17*. These results provide part of the foundation for my study and hypothesis. Fig. from Yang and Sale, 2000.

Fig. 1.8.

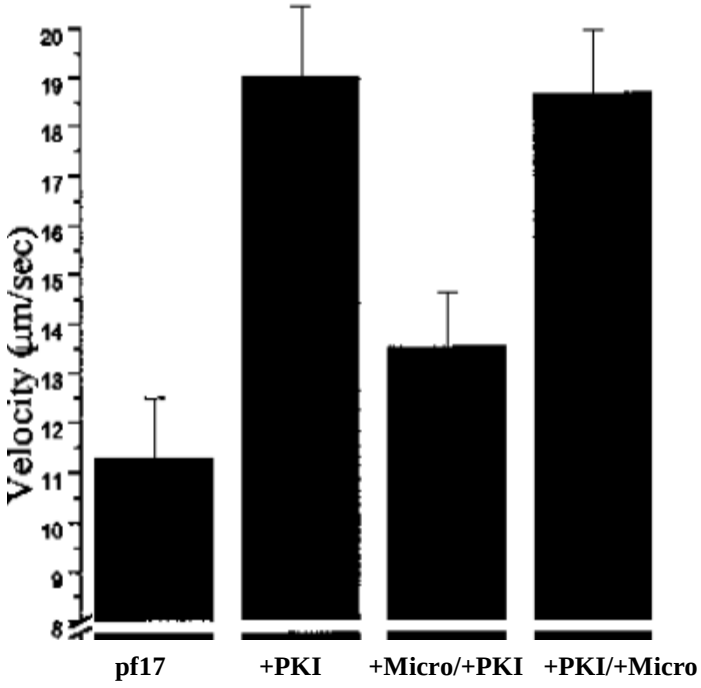
Velocity (μm/sec)
20
19
18
17
16
15
14
13
12
11
10
9
8
pf17
+PKI
+Micro/+PKI
+PKI/+Micro

Fig. 1.8: The protein phosphatase inhibitor microcystin-LR has no effect on the slow microtubule sliding of axonemes lacking spokes and blocks PKI-induced increase in microtubule sliding velocity. Isolated *pf17* axonemes were treated with buffer alone (control, *pf17*), 1 mM microcystin-LR then 100 nM PKI (+Micro/+PKI) or 100 nM PKI followed by 1 mM microcystin-LR (+PKI/+Micro). Figure adapted from Habermacher and Sale, 1996.

Fig. 1.9.


β7D
β1A
β1B
β1C
β1D
Bα MAGAGGGNDIQWCFSQVKGAVDDDVAEADIISTVEFNHSGELLATGDKGGRVVIFQQEQENKIQSHSRGEYNVYST 76
Bβ MEEDIDTRKINNSFLRDHSYA----TEADIISTVEFNHTGELLATGDKGGRVVIFQREQESKNQVHRRGEYNVYST 72
Bγ MGKRDT----------ADIISTVEFNHTGELLATGDKGGRVVIFQREPESKNAPHSQGEYDVYST 55
Bδ1 MAGAGGGNDFQWCFSQVKGAIDEDVAEADIISTVEFNYSGDLLATGDKGGRVVIFQREQENKSRPHSRGEYNVYST 82
Bδ2 M---------- 2
β1
β2
β2A
β2B
β2C
β-hairpin arm
Bα FQSHEPEFDYLKSLEIEEKINKIRWLPQKNAAQFLLSTNDKTIKLWKISERDKRPEGYNLKEEDGRYRDPTTVTTL 152
Bβ FQSHEPEFDYLKSLEIEEKINKIRWLPQQNAAYFLLSTNDKTVKLWKVSERDKRPEGYNLKDEEGRLRDPATITTL 148
Bγ FQSHEPEFDYLKSLEIEEKINKIKWLPQQNAAHSLLSTNDKTIKLWKITERDKRPEGYNLKDEEGKLKDLSTVTSL 131
Bδ1 FQSHEPEFDYLKSLEIEEKINKIRWLPQQNAAHFLLSTNDKTIKLWKISERDKRAEGYNLKDEDGRLRDPFRITAL 158
Bδ2 ---------- 2
β-hairpin arm
β2D
β3A
β3B
β3C
β3D
Bα RVPVFRPMDLMVEASPRRIFANAHTYHINSISINSDYETYLSADDLRINLWHLEITDRSFNIVDIKPANMEELTEV 228
Bβ RVPVLRPMDLMVEATPRRVFANAHTYHINSISVNSDYETYMSADDLRINLWNFEITNQSFNIVDIKPANMEELTEV 224
Bγ QVPVLKPMDLMVEVSPRRIFANGHTYHINSISVNSDCETYMSADDLRINLWHLAITDRSFNIVDIKPANMEDLTEV 207
Bδ1 RVPILKPMDLMVEASPRRIFANAHTYHINSISVNSDHETYLSADDLRINLWHLEITDRSFNIVDIKPANMEELTEV 234
Bδ2 ----------EELTEV 7
β4A
β4B
β4C
β4D
α1
β5A
β5B
Bα ITAAEFHPNSCNTFVYSSSKGTIRLCDMRASALCDRHSKLFEEPEDPSNRSFFSEIISSISDVKFSHSGRYMMTRD 304
Bβ ITAAEFHPHHCNTFVYSSSKGTIRLCDMRASALCDRHTKFFEEPEDPSNRSFFSEIISSISDVKFSHSGRYIMTRD 300
Bγ ITASEFHPHHCNLFVYSSSKGSLRLCDMRAAALCDKHSKLFEEPEDPSNRSFFSEIISSVSDVKFSHSGRYMLTRD 283
Bδ1 ITAAEFHPHQCNVFVYSSSKGTIRLCDMRSSALCDRHSKFFEEPEDPSSRSFFSEIISSISDVKFSHSGRYMMTRD 310
Bδ2 ITAAEFHPHQCNVFVYSSSKGTIRLCDMRSSALCDRHSKFFEEPEDPSSRSFFSEIISSISDVKFSHSGRYMMTRD 83
β5C
β5D
α2
β6A
β6B
β6C
β6D
Bα YLSVKIWDLNMENRPVETYQVHEYLRSKLCSLYENDCIFDKFECCWNGSDSVVMTGSYNNFFRMFDRNTKRDITLE 380
Bβ YLTVKVWDLNMENRPIETYQVHDYLRSKLCSLYENDCIFDKFECVWNGSDSVIMTGSYNNFFRMFDRNTKRDVTLE 376
Bγ YLTVKVWDLNMEARPIETYQVHDYLRSKLCSLYENDCIFDKFECAWNGSDSVIMTGAYNNFFRMFDRNTKRDVTLE 359
Bδ1 YLSVKVWDLNMESRPVETHQVHEYLRSKLCSLYENDCIFDKFECCWNGSDSAIMTGSYNNFFRMFDRDTRRDVTLE 386
Bδ2 YLSVKVWDLNMESRPVETHQVHEYLRSKLCSLYENDCIFDKFECCWNGSDSAIMTGSYNNFFRMFDRDTRRDVTLE 159
β3
β4
β7A
β7B
β7C
Bα ASRENNKPRTVLKPRKVCASGKRKKDEISVDSLDFNKKILHTAWHPKENIIAVATTNNLYIFQDKVN 447
Bβ ASRENSKPRAILKPRKVCVGGKRRKDEISVDSLDFSKKILHTAWHPSENIIAVAATNNLYIFQDKVN 443
Bγ ASRESSKPRAVLKPRRVCVGGKRRRDDISVDSLDFTKKILHTAWHPAENIIAIAATNNLYIFQDKVNSDMH 430
Bδ1 ASRESSKPRASLKPRKVCTGGKRRKDEISVDSLDFNKKILHTAWHPVDNVIAVAATNNLYIFQDKIN 453
Bδ2 ASRESSKPRASLKPRKVCTGGKRRKDEISVDSLDFNKKILHTAWHPVDNVIAVAATNNLYIFQDKIN 226
Side-chain H-bond
Main-chain H-bond
van der Waals contact

Fig. 1.9: Structural Features of the Regulatory B Subunit

Sequence alignment of the four isoforms of the regulatory B subunits from humans.

Conserved residues are highlighted in yellow. The secondary structures of the proteins are listed above the sequences. These secondary structures include seven WD-repeats (β 1-7, blades a-d) (blue); β-hairpin arm (magenta), important for mediating A-subunit binding; and α1, α2 ,β1 and β2, important for mediating substrate interactions (yellow). Residues that H-bond to the A-subunit using side chain and main chain groups are identified with red and green circles respectively, below the sequences. Amino acids that make van der Waals interactions are indicated by blue squares. The sequences shown include all four

Fig. 1.10.

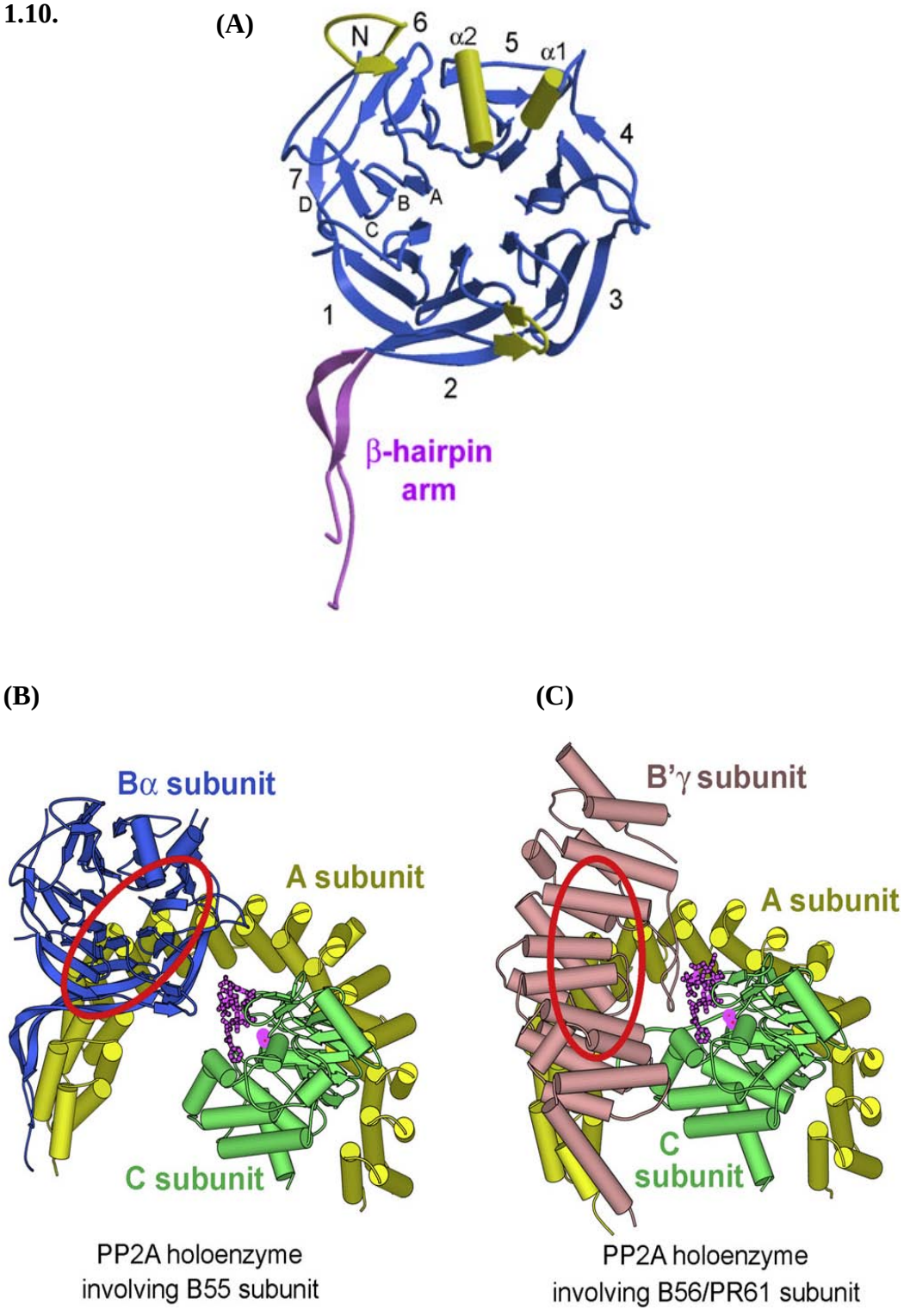
(A)
N
6
α2
5
α1
4
7
D
B
A
C
3
1
2
β-hairpin
arm
(B)
Bα subunit
A subunit
C subunit
PP2A holoenzyme
involving B55 subunit
(C)
B'γ subunit
A subunit
C
subunit
PP2A holoenzyme
involving B56/PR61 subunit

Fig. 1.10: Crystal Structure of PP2A subunits (A) Structure of the Bα subunit. The β propeller core, containing WD-repeats 1-7, made up of blades a-d, is shown in blue; the additional secondary structural elements above the top face are shown in yellow; and the β2C-β2D hairpin arm is highlighted in magenta. **(B and C)** The PP2A holoenzyme consists of three subunits B (blue, or Pink), A (yellow) and C(green). **(B)** The PP2A holoenzyme containing the B/PR55 family member. **(C)** The PP2A holoenzyme containing a B'/PR61 family member. Magenta indicates the site of microcystin binding in the C-subunit. The Red circles indicate the proposed substrate binding sites in the B-subunits. These figures are used with permission

Chapter II: The foundation for the study of PP2A and the identification of the axonemal PP2A B-subunit gene.

Foundation for study of the protein phosphatase PP2A

The initial discovery that dynein-driven microtubule sliding is regulated by posttranslational modifications was based on measurement of microtubule sliding in wild-type and paralyzed flagellar mutants in *Chlamydomonas* (Okagaki and Kamiya, 1986; Smith and Sale, 1992a; 1992b). The sliding assay is founded on the original studies by Barbara and Ian Gibbons (1972) showing that isolated axonemes could be reactivated to beat *in vitro* when ATP is added. These studies demonstrated that all of the components – dynein motors, etc.-are physically localized to the 9+2 axoneme. Notably, these studies were the first to use the nonionic detergents (in this case Triton X 100) to permeabilize or remove the plasma membrane. Gibbons then went on to show that addition of ATP and a small amount of protease to axonemes resulted, not in reactivated oscillatory beating, but rather in sliding between adjacent doublet microtubules driven by the dynein arms (Fig. 2.1; Summers and Gibbons, 1971). This reliable assay was then adapted to study regulation of dynein in axonemes from *Chlamydomonas*. As discussed in the Methods Chapter and illustrated in Fig. 2.2 , flagella can be actively excised by treatment of cells with pH shock or with the drug dibucaine. Purified flagella can then be suspended in a buffer containing a non-ionic detergent, such as triton or nonidet, and axoneme and membrane-matrix fractions separated and recovered by centrifugation.

Elizabeth Smith adopted this assay to measure dynein activity in axonemes from paralyzed flagellar mutants lacking the radial spokes (*pf14* or *pf17*) or the central pair (*pf18*) and discovered that dynein activity is greatly reduced (Smith and Sale, 1992a, 1992b). The reduced sliding was despite the full assembly of each dynein isoform in the

axoneme, suggesting some mechanism was inhibiting the dynein motors. Smith then went on to develop a novel *in vitro* reconstitution assay that, when combined with the sliding assays, revealed the dyneins were regulated by a reversible posttranslational modification (Smith and Sale, 1992). Moreover, using axonemes lacking subsets of dyneins, Smith determined the inner dynein arms were regulated by a reversible change. It was postulated that reduced dynein activity was a consequence of altered phosphorylation.

To test this idea, the Sale lab used a pharmacological approach combined with the dynein assay. The prediction was that inhibition of kinases or phosphatases located in the axoneme would either restore wild type dynein activity or maintain the inhibited state for the dyneins. As predicted, treatment of radial spoke or central pair mutant axonemes with inhibitors of cAMP-dependent protein kinases, (PKA), or inhibitors of CK1, increased microtubule sliding velocities to wild-type levels (Fig. 1.7; Habermacher and Sale, 1996; Howard et al., 1994; Yang et al., 2000). This result demonstrated that the axoneme contains these kinases and that they control dynein activity. Moreover, the results indicated that the constitutively active kinases in axonemes from the mutants resulted in phosphorylation and inhibition of dynein activity.

Additionally, as indicated in the model in Fig. 2, kinase inhibitors rescued dynein activity. This result indicated that the axoneme must also contain protein phosphatases required for reversing phosphorylation and restoring dynein to wild type activity. Consistent with this idea, Habermacher found that treatment of radial spoke or central pair mutant axonemes with the PP1 and PP2A phosphatase inhibitors, okadaic acid and microcystin, blocked rescue dynein activity (Fig. 1.8; Habermacher and Sale, 1996).

From this data we surmised that the rescue of dynein activity depended on the action of the tightly bound axonemal phosphatases – PP1 and PP2A (Habermacher and Sale, 1996; Yang et al., 2000). Thus, pharmacological analyses of microtubule sliding in isolated axonemes provided the initial evidence that conserved kinases and phosphatases are located in the axoneme. As discussed in Chapter 1, Habermacher then went on to determine the key dynein important for regulation in this pathway was the inner dynein arm I1 and that the key phospho-protein is the intermediate chain IC138 (Habermacher and Sale, 1997). This model has since been supported by a number of more recent studies (King and Dutcher, 1997; Yang and Sale, 2000; Hendrickson et al., 2004; Bower et al., 2009; Gokhale et al., 2009).

Based on the pharmacological data, P. Yang and L.A. Fox in the Sale lab sought to identify the microcystin sensitive phosphatase in the axoneme. The phosphatase inhibitor microcystin-LR is a heptapeptide that binds to the C-subunit of PP2A and the catalytic C-subunit of the phosphatase PP1 (PP1c) (Mackintosh, C. 1990; Gulledge B.M., 2002) For the precipitation assay, isolated axonemes were salt extracted (Fig. 2.4a) and microcystin-Sepharose was used to precipitate proteins from the dialyzed extracts (Figs. 2.3 and2.4). Precipitated protein was resolved by SDS-PAGE and the gel was silver stained and controls included addition of free microcystin LR to compete with the microcystin- Sepharose (Fig. 2.3).

Three bands were identified which migrated at 35, 37 and 65 kDa which correspond to PP1c, the catalytic subunit of PP2A and the A-subunit of PP2A respectively (Fig. 2.4a, lane 2). As a competitive control, dialyzed, salt solublized protein was first treated with free microcystin-LR before precipitation with microcystin-

sepharose beads (2.4a lane 1). The band corresponding to the 65kDa band was excised and sent for micro-sequencing (MS/MS analysis was not yet possible since the sequencing of the genome had only just begun and was not yet completed in 1999). Unique peptides were identified that are conserved in the PP2A A-subunit (Yang et al., 2000), and subsequent analysis of the *Chlamydomonas* genome indicated the peptides define a gene model C_1010056 in version 2 of the *Chlamydomonas* flagellar genome. The catalytic C-subunits of PP2A and PP1 were confirmed by immuno-blot analysis using a monoclonal antibody for PP2A and a mouse polyclonal PP1 C-subunit antibody (Fig. 2.4b). Results show that both PP1 and PP2A are abundantly present in the axoneme.

To localize the phosphatases we used flagella and axonemes from *Chlamydomonas* structural mutants missing various axonemal structures and compared them to wild-type axonemes on immuno-blots. *Chlamydomonas* is powerful model genetic system because isolated axonemes from *Chlamydomonas* structural mutants (e.g. axonemes from mutants lacking the entire radial spoke structures, the entire central pair apparatus or the dynein arms) can be used for indirect localization of proteins or enzymes (Fig. 2.5) We used our PP1c antibody, and a mouse monoclonal PP2A C-subunit antibody, 1D6 (Yu et al., 2001) on immuno-blots to detect flagellar and axonemal PP1 and PP2A. Based on immuno-blots, isolated flagella and axonemes from mutants lacking outer or inner arm dyneins, radial spokes, and the dynein regulatory complex all contained WT levels of both PP1 and PP2A (Fig. 2.5; Yang et al., 2000). Immuno-blot analysis shows that PP2A is present in equal amounts in both the flagella and the isolated axonemes of WT and central pair mutant cell lines, but PP1 is missing from the central

pair mutants. Thus, PP1 is mostly localized to the central pair, whereas PP2A is localized to the outer doublets. Therefore, in a model in which a phosphatase interacts directly with the dynein motors, PP2A is the candidate. Notably, as indicated in figure 2.5, the initial immuno-blots showed that PP2A is missing in axonemes from the *pf15* mutant that has a mutation in the microtubule severing protein, katanin, which has been shown to localize to the axoneme (Dymek et al., 2004). However, the basis for the absence of the PP2A C-subunit in this particular immuno-blot is not known. Subsequent analysis using the mouse monoclonal, C-subunit (1D6) and B-subunit antibodies have shown that PP2A is present in the *pf15* mutant.

Thus, in summary, from these data we can predict that PP1 localizes to the central pair apparatus, while PP2A is anchored in the axoneme possibly on the outer doublet microtubules in position to regulate dynein. From this data we designed the hypothesis that there must be a candidate PP2A B-type subunit anchored in the axoneme, and this B-subunit is responsible for targeting the PP2A holoenzyme to the outer doublet microtubules.

Results and Discussion

Identification of the *Chlamydomonas* axonemal PP2A B-subunit gene and protein

To identify a B-type subunit in *Chlamydomonas* flagella, we analyzed the flagellar proteome database and identified a unique peptide that was found in the KCl fraction (Fig. 1.3) of the large-scale mass spectrophotometeric analysis of flagellar proteins performed by Pazour et al., (2005). This unique peptide corresponds to sequence

contained in the candidate PP2A regulatory B-subunit gene model (C_180129) found in version 2 of the *Chlamydomonas* Joint Genome Institute database (http://genome.jgi-psf.org/cgi-bin/browserLoad/46486bc677fb7dfd50acb646). The proteome data indicates the B-subunit is an axonemal protein that is solubilized with 0.6M KCl. The genomic DNA was scanned and the exons were predicted using the genomic model. The full length B-subunit gene is 3792 base pairs with nine exons and eight introns (Fig. 2.6).

BAC clones containing partial DNA sequence were obtained (Clemson University Genomics Institute), sequenced, and aligned using SEQMAN (DNASTAR) to obtain the full length cDNA sequence. This protein was shown to be a conserved member of the B/PR55 family of B-subunits and encodes a highly conserved 52.6-kDa protein with seven WD-repeats that form a seven bladed propeller-like structure (Fig. 2.7) (Xu et al., 2008). The predicted protein also contained the peptide identified from the proteomic analysis. Analysis of the predicted protein sequence by Blastp shows the sequence is most homologous to the B-subunit beta isoform of *Oryza sativa* (rice) being 59% identical and 71% conserved (Fig 2.7). In *Homo sapiens* the *Chlamydomonas* B-subunit is most homologous to the B-subunit delta isoform1 being 54% identical and 67% conserved. While there are other B-type subunits found in the *Chlamydomonas* genome (Table I), only this gene was identified from peptides found in the flagellar proteome. Thus, consistent with my hypothesis, the axonemal B-subunit is targeted to the axoneme where it would then localize the otherwise ubiquitous PP2A A- and C- subunit dimer. Predictably, since PP2A is a ubiquitous and functionally versatile phosphatase (Shi, 2009b), the other, non-flagellar B-type subunit proteins are responsible for targeting

PP2A to other cellular locations in *Chlamydomonas* where they would play non-flagellar functional roles.

To confirm that the identified B-subunit localizes to flagellar axoneme, we generated a B-subunit specific antibody to an N-terminal fusion protein. Following blot affinity purification of the antiserum, the antibodies recognized a ~50-kDa band on immunoblots of isolated flagella and axonemes, consistent with the predicted size of the B-subunit protein and confirming the presence of the B-subunit in the axoneme (Figs. 2.9 and 2.10). The B-subunit antibody is a rabbit polyclonal that was made to the first 134 amino acids of the *Chlamydomonas* PP2A B-subunit. This region of the protein was selected based on its unique sequence within the *Chlamydomonas* genome and predicted high antigenicity. This sequence was cloned into an N-terminal His-tagged protein expression vector. Briefly, expressed bacterial protein was purified over a metal affinity column and the sample containing a large quantity of the 21kDa fusion protein was then injected into two quarantined rabbits for antibody production.(Fig. 2.8, lane 2). Serum obtained from the rabbits was used to screen axonemes for antibody recognition using the pre-immune sera as a negative control (Fig. 2.9, gel B). Serum from the second bleed of one rabbit (#5) recognized a 50kDa band that was similar in size to the predicted *Chlamydomonas* PP2A B-subunit size of 52.6 kDa (Fig. 2.9 gel A lane 3).

As indicated in Yang et al., (2000), the PP2A A- and C-subunits were localized to the axoneme and were salt extractable (Fig. 2.4a). Moreover, the B-subunit derived peptides were found in the KCl fraction in the proteomic analysis (Pazour et al., 2005). To test whether the axonemal PP2A B-subunit was also extractable in high salt buffers, I fractionated the cells into flagellar, membrane matrix, axonemal, 0.6M NaCl soluble, and

0.6M NaCl extracted axonemal fractions and tested which fractions contain the B-subunit (Figs. 2.9 and 2.10). Additional samples containing cytoplasmic extracts were also used to determine if the B-subunit was also enriched in the cell body cytoplasmic fraction. Using the B-subunit antibody on immuno-blots, I found that the B-subunit is present in the cytoplasm and all of the flagellar fractions (Figs 2.9 and 2.10). The B-subunit is partially solubilized with detergent (M+M fraction), while the fraction of the B-subunit in the axoneme is solubilized in high salt buffers, confirming the fractionation profile reported in the flagellar proteome and consistent with the solubility of the axonemal A- and C-subunits (Fig. 2.4a; Pazour et al., 2005; Yang et al., 2000). Since I found a fraction of cellular B-subunit in the cytoplasm and membrane-matrix of the flagellum, it is possible the PP2A B-subunit also plays roles in the cytoplasmic and membrane-matrix compartments. However, since the cytoplasm contains a significant pool of flagellar proteins, enough to make two new half length flagella (Lefebvre and Rosenbaum, 1986) and the membrane–matrix compartment contains axonemal proteins in transit to or from the axoneme by IFT (Pedersen and Rosenbaum, 2008), it is possible that the axonemal B-subunit performs mainly as an axonemal component.

As described in Yang et al., (2000), using the monoclonal antibody 1D6 (Yu et al., 2001), I confirmed that the PP2A C-subunit is also found in the axoneme and is salt extractable. Thus, consistent with my model, both the PP2A C- and B-subunits are found in the same axonemal fractions. To date, we have not found an antibody useful for study of the A-subunit in *Chlamydomonas*, and the analysis of the A-subunit will be part of a future study. Maintaining my focus on the B-subunit function, my next challenge was to test the idea that PP2A is targeted and or anchored in the axoneme by the B-

subunit. As described in the next chapter, I took a molecular genetic approach of mapping the gene that encodes the B-subunit with the hope the gene mapped to a motility mutant. The idea was that mutants defective in the PP2A C-subunit might be lethal since the C-subunit and PP2A play other essential roles cell. In contrast, one of the advantages of genetic approaches for study of flagellar proteins is that the cell can survive without the flagellum. Therefore, I predicted that *Chlamydomonas* mutations in the axonemal PP2A B-subunit may survive and display a flagellar motility phenotype. As predicted, mapping of the gene did reveal a flagellar mutant *pf4* defective in the B-subunit gene.

Fig. 2.1

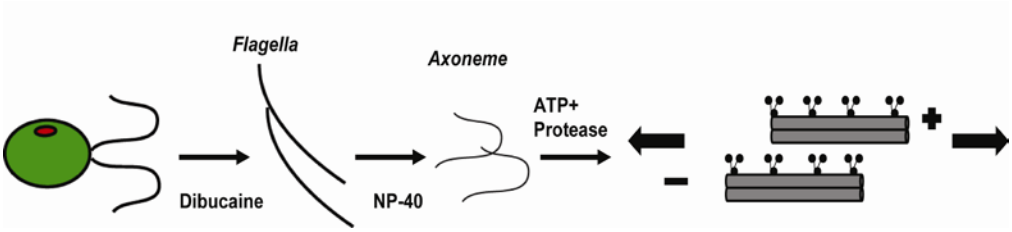

Fig. 2.1: Axonemal isolation and the microtubule sliding assay. Flagella from *Chlamydomonas* cells are obtained after dibucaine treatment, demembranated with non-ionic detergents, such as NP-40, to generate isolated axonemes. Axonemes can then be reactivated to beat in ATP containing buffers or exposed to ATP and proteases to induce interdoublet sliding. Sliding can then be viewed by dark field microscopy and recorded by video for measurement of sliding velocity. The microtubule sliding velocity measurements provide an assay for quantifying dynein activity.

Fig. 2.2

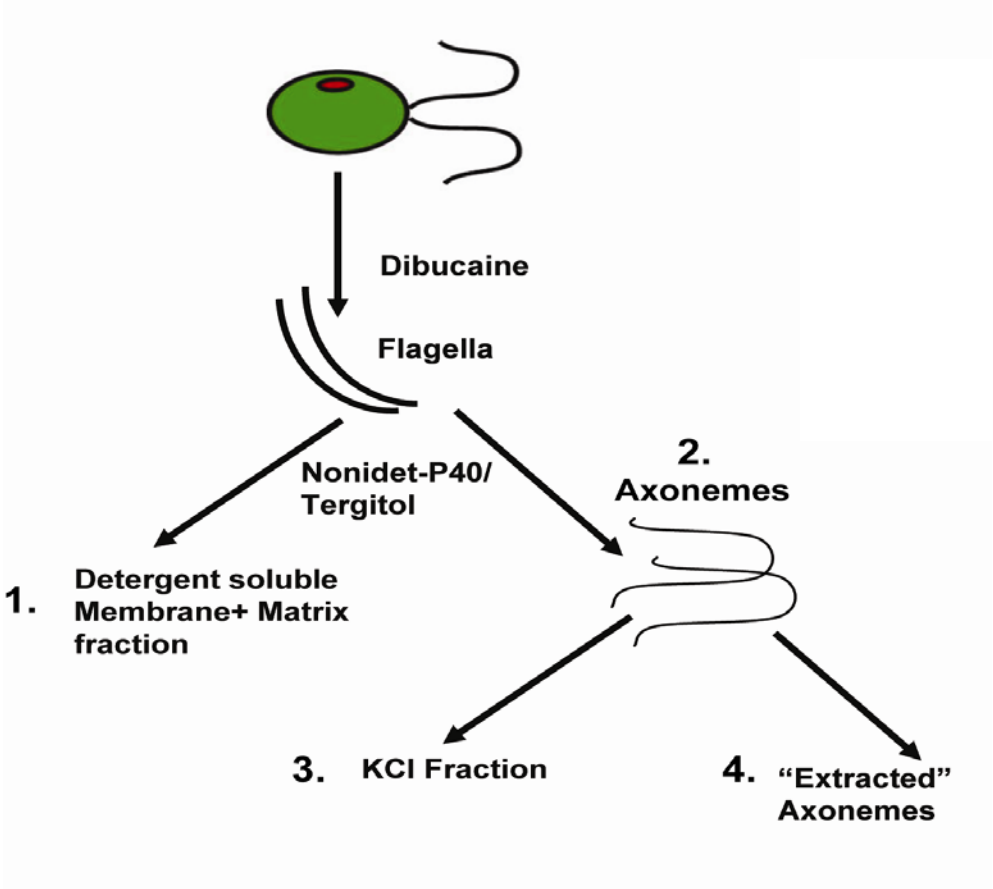
Dibucaine
Flagella
Nonidet-P40/
Tergitol
2.
Axonemes
1.
Detergent soluble
Membrane+ Matrix
fraction
3.
KCl Fraction
4.
"Extracted"
Axonemes

Fig. 2.2: Schematic showing purification of axonemal proteins from *Chlamydomonas* cells. First dibucaine is used to remove the flagella from the cell body. The flagella are demembranated using the non-ionic detergent Nonidet-P40 or tergitol. Proteins are then solubilized from axonemes in high salt using 0.6M KCl.

Fig. 2.3

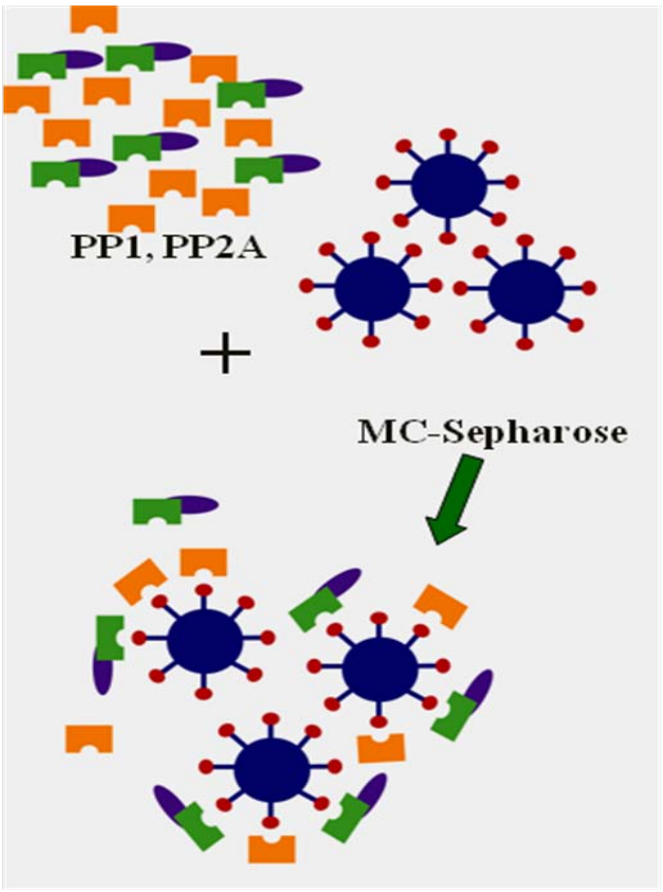

Fig. 2.3: Microcystin conjugated to Sepharose beads was used to precipitate both PP1 and PP2A from salt solubilized axonemes.

Microcystin covalently binds to the catalytic subunits of both PP1 and PP2A (orange and green rectangles, respectively). Microcystin conjugated to Sepaharose beads (blue circles with red extensions) was used to precipitate the A- and C-subunits of PP2A and PP1c.

Fig. 2.4

(A)

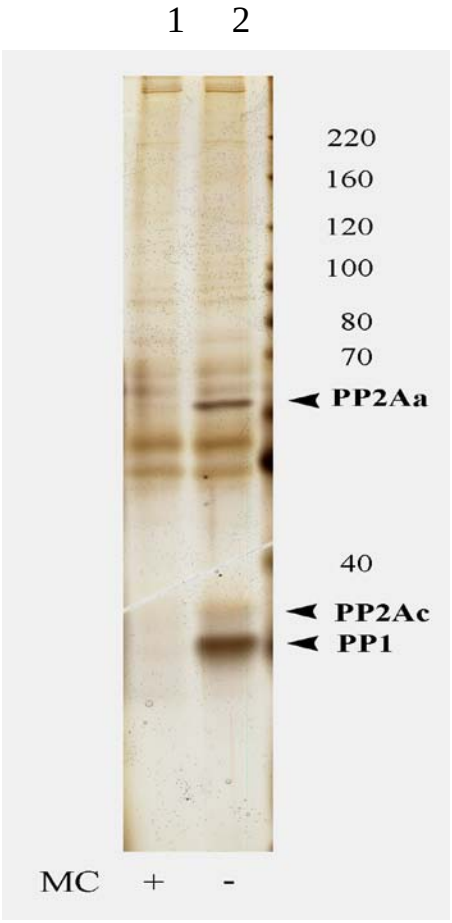
1 2
220
160
120
100
80
70
PP2Aa
40
PP2Ac
PP1
MC + -

(B)

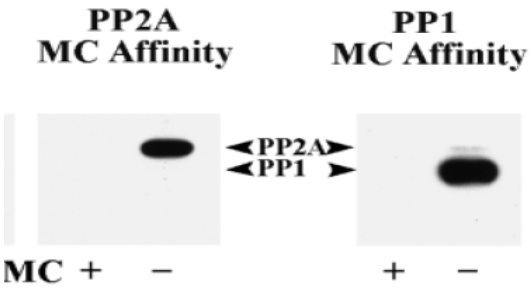
PP2A
MC Affinity
PP1
MC Affinity
PP2A
PP1
MC + − + −

Figs. 2.4: PP2A and PP1 can be precipitated from the axoneme. (A) Silver stain showing axonemal salt extracts precipitated with microcystin-sepharose. Lane 1 was treated with free microcystin before precipitation. Precipitated bands in lane 2 correspond to PP1c (35kDa), and the PP2A A and C subunits which migrate at 65 and 37kDa, respectively. **(B)** is a western blot of the silver stained gel in Fig. 4a, blotted with PP1 and PP2A c-subunit antibodies. Results show that both PP2A and PP1c are located in the axoneme (Yang et al., 2000b).

Fig. 2.5

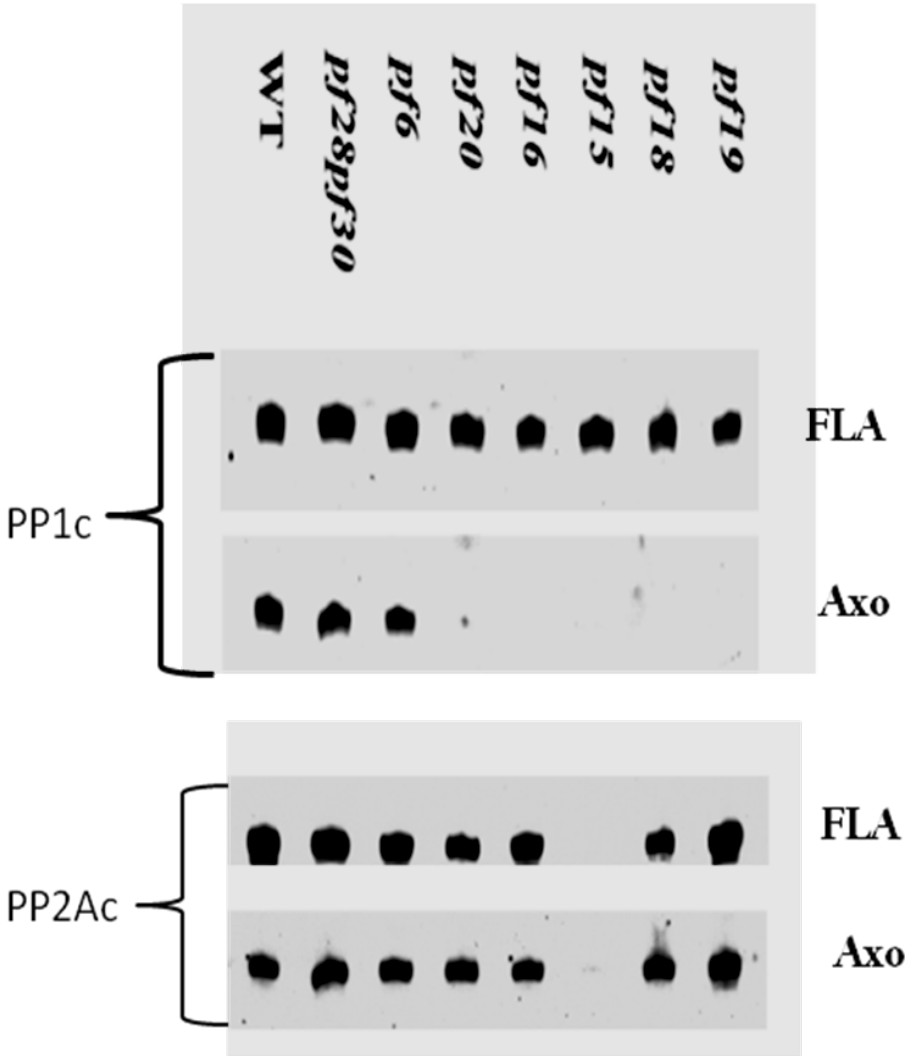
WT
pf28pf30
pf6
pf20
pf16
pf15
pf18
pf19
PP1c
FLA
Axo
PP2Ac
FLA
Axo

Fig. 2.5: Axonemal PP1c is located in the central pair apparatus and PP2A localized to the outer doublet microtubules. (A) Western blot using our PP1c antibody or **(B)** the monoclonal PP2A C-subunit antibody (1D6). Results show that, PP2A is dramatically reduced in *pf15* flagella and axonemes, but not in other central pair mutants (*pf*28pf30, have no C1 microtubule projections; *pf*6, lack a C1 microtubule projection; *pf*20 predominantly lacks central pair components; *pf*16 lack the C1 microtubule and associated projections;*pf*15,*pf*18, and *pf*19 lack the entire central pair apparatus) as compared to wild-type (Yang et al., 2000b).

Fig. 2.6


5'UTR
E1
E2
E3
E4
E5
E6
E7
E8
E9
3'UTR
1
281
79
104
219
144
213
144
171
189
174
755
3792
122
84
69
62
288
217
230
247

Fig. 2.6: The *Chlamydomonas* axonemal B-subunit gene schematic. The entire B-subunit gene, including the 3' and 5' UTRs (blue), is 3792 base pairs. The gene contains nine exons (orange) and eight introns (lines). Numbers represent the base pair size of each predicted intron and exon and UTR.

Fig. 2.7

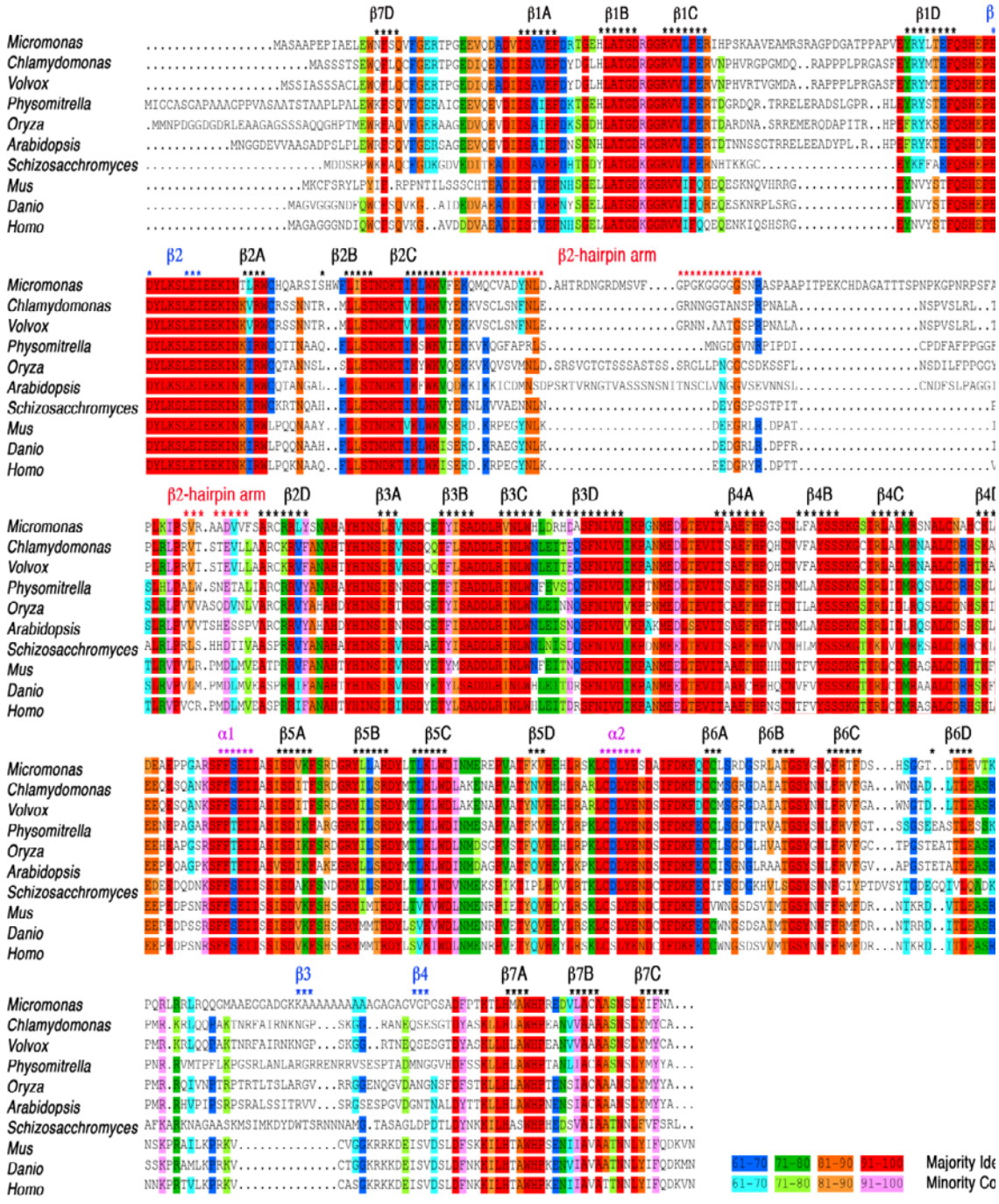
β7D
β1A
β1B
β1C
β1D
Micromonas
Chlamydomonas
Volvox
Physomitrella
Oryza
Arabidopsis
Schizosacchromyces
Mus
Danio
Homo
β2
β2A
β2B
β2C
β2-hairpin arm
β2D
β3A
β3B
β3C
β3D
β4A
β4B
β4C
α1
β5A
β5B
β5C
β5D
α2
β6A
β6B
β6C
β6D
β3
β4
β7A
β7B
β7C
61-70
71-80
81-90
91-100
Majority Ide
Minority Co

Fig. 2.7: The *Chlamydomonas* B-subunit is homologous to B/PR55 subunits found in other orgamisms. The *Chlamydomonas* axonemal B-subunit protein sequence was aligned with B/PR55 family members of other model organisms using the Phylogeny.fr program and colored with Colorfy (http://bifrost.wustl.edu/colorfy). The percent identity and conservation among the proteins is detailed in the colored legend. The secondary structures of the proteins were determined as described in Xu et al. (2008) and are listed above the sequences. These secondary structures include seven WD-repeats domains (labeled β1-7, blades a-d); the β-hairpin arm-important for mediating A-subunit binding; and α1, α2, β1 and β2-important for mediating substrate interactions.

Fig. 2.8

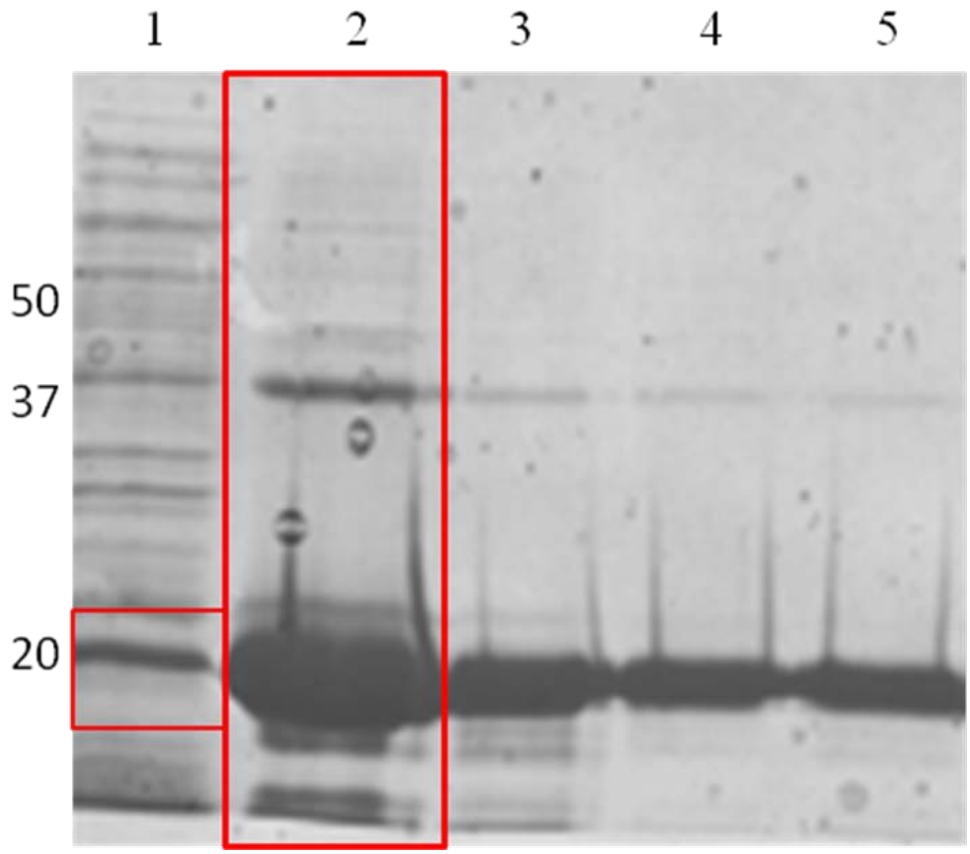

Fig. 2.8: Coomassie stain of the nickel affinity purified His-tagged B-subunit fusion protein. The His-tagged B-subunit fusion protein was induced with IPTG in Bl21 DE3 pLysS E.*coli* cells. The fusion protein was insoluble in bacterial cells, so it was denatured using urea and then purified over a nickel affinity column. The protein was eluted using imidazole and collected in 1ml fractions. 20µl of each fraction was resolved on an SDS-PAGE Gel. **Lane 1** whole cells containing the induced fusion protein. **Lanes 2-5** represent purified fractions. The sample from **lane 2** was sent for antibody production in rabbits.

Fig. 2.9

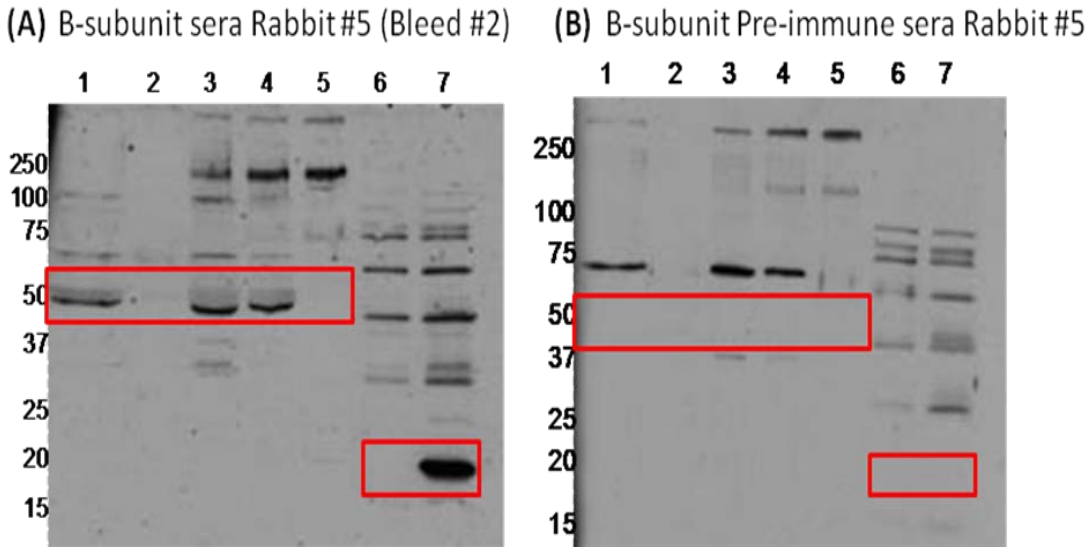
(A) B-subunit sera Rabbit #5 (Bleed #2)
1 2 3 4 5 6 7
250
100
75
50
37
25
20
15
(B) B-subunit Pre-immune sera Rabbit #5
1 2 3 4 5 6 7
250
100
75
50
37
25
20
15

Figs. 2.9: The rabbit polyclonal B-subunit antibody recognizes a 50 kDa band on immuno-blots. WT flagellar samples were fractionated and loaded on onto an SDS-PAGE gel, as described previously. Immuno-blots were performed using rabbit sera from the 2nd bleed (Gel A) and pre-immune sera (Gel B). **Lane 1**, soluble protein after treatment with 0.6M NaCl. **Lane 2**, 0.6M NaCl stripped axonemes. **Lane 3**, axonemes before salt stripping. **Lane 4**, Flagella. **Lane 5**, NP-40 fraction. **Lane 6**, BL21 DE3 pLysS cells containing an uninduced His-tagged B-subunit fusion construct. **Lane 7**, BL21 DE3 pLysS cells containing His-tagged B-subunit fusion construct induced with IPTG. The B-subunit antibody recognizes a band in axonemes at 50kDa slightly lower than that of the 52.6kDa predicted mass (see lanes 1,3 and 4 of Gel A). Red boxes used to compare immunesera to preimmune for flagellar fraction and for fusion protein.

Fig. 2.10

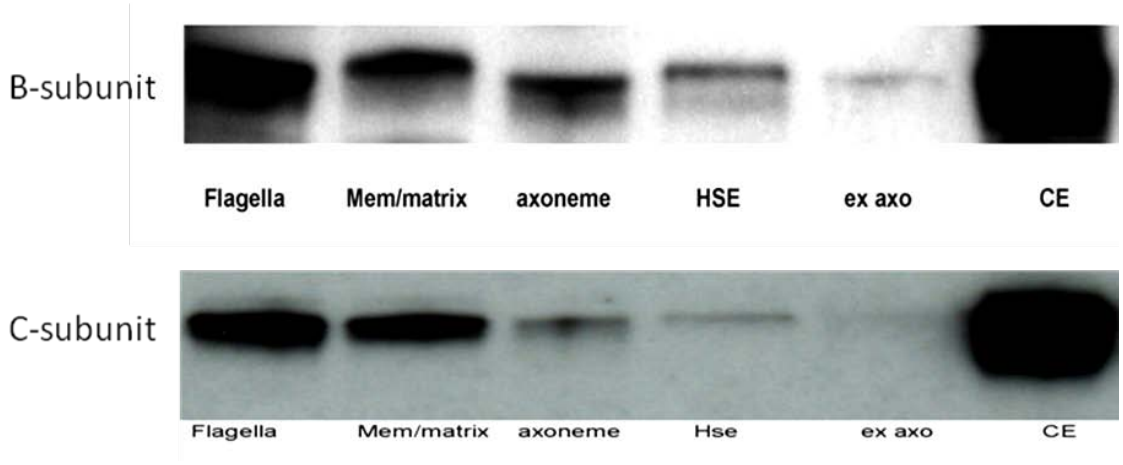
B-subunit
Flagella
Mem/matrix
axoneme
HSE
ex axo
CE
C-subunit
Flagella
Mem/matrix
axoneme
Hse
ex axo
CE

Fig. 2.10: The B-subunit and C-subunits of PPA localize to the axoneme and are salt extractable. (A) Cellular fractionation of *Chlamydomonas* cells. WT and cells were fractionated into flagella (Fla), membrane matrix (M/M), Axonemes (Axo), high salt extract (HSE), and extracted axoneme fractions (Ex. Axo.). Equivalent protein amounts were loaded based on a starting volume of 5µg of flagellar protein. Westerns were performed using our polyclonal B-subunit antibody and the C-subunit antibody (1D6). Ponceau A staining showing tubulin at 50 kDa was used as a loading control.

Table I: PP2A subunits in the *Chlamydomonas* Genome Database.

Type	Name[1]	Protein ID[2]	Domain/Motif/Family[3]	Flagellar Proteome[4]
A (Scaffold)	**PP2A-2r**	**131550**	**HEAT**	**YES**
	FAP14	**194683**	**HEAT**	**YES**
B, B', B'', B''' (Regulatory)	**PP2A-1r (B'')**	**112343**	**---**	**NO**
	PP2A2 (B')	**127638**	**B56**	**NO**
	TAP42-like protein	**148948**	**TAP42**	**NO**
		185509	**WD repeats**	**YES**
	PP2A1/*PF4*(B)	**405966**	**---**	**NO**
	Not annotated (B'')			
C (Catalytic)	**PP2A3**	**807**	**Metallophosphatase/PP2Ac**	**NO**
	PP2A-c4	**132486**	**Metallophosphatase/PP2Ac**	**YES**
	PPA1	**144867**	**Metallophosphatase/PP2Ac**	**NO**
	PP2A-1c	**193562**	**Metallophosphatase/PP2Ac**	**NO**

[1] Name and/or description in JGI *Chlamydomonas reinhardtii* v4.
[2] Protein ID in JGI *Chlamydomonas reinhardtii* v4.
[3] Domain, motif, and family found in SMART and/or pfam analyses.
[4] Presence or absence in flagellar proteome (Pazour *et al*., 2005).

Table I: PP2A subunits in the *Chlamydomonas* Genome Database.

Analysis of the *Chlamydomonas* Genome Database (JGI version 4) reveals several PP2A subunits including 2 A-subunits, 4 C-subunits and 5 B-type subunits. Both A-subunits and one of the C-subunits were found in the *Chlamydomonas* flagellar proteome (Pazour et al., 2005). Of the five B-type subunits in the genome, only one, PP2A1, was identified in the flagellar proteome. This gene is defective in the *pf4* mutant.

Chapter III: The mutant *pf4* reveals that assembly of axonemal PP2A requires the B-subunit and that this B-subunit is required for normal ciliary motility

As indicated in Chapter 2, the next goal was to more directly test the idea that the B-subunit is required for PP2A localization in the axoneme. A flagellar mutant lacking the B-subunit through a mutation would also lack the entire PP2A holoenzyme in the axoneme. Thus, the first goal was to map the B-subunit gene. This could have been a protracted mapping project, but I was very lucky. In collaboration with Susan Dutcher at Washington University, St. Louis, we found the gene to the B-subunit, based on sequence alone, in a genomic scaffold that mapped to a BAC that had been previously mapped.

Results and Discussion

The flagellar mutant, *pf4*, is defective in the B-subunit gene.

The B-subunit gene was mapped to LG1 using BAC clone, 14G12, identified in the *Chlamydomonas* genome database (http://genome.jgi-psf.org/Chlre4/Chlre4.home.html). The gene maps near the *pf4* mutant (Levine and Goodenough, 1970; McVittie, 1972), a slow-swimming mutant that otherwise had not been characterized (Fig. 3.1). To determine whether *pf4* was defective in the B-subunit gene, I sequenced the gene in both the plus and minus mating types for the entire gene. The primer pairs used for sequencing are listed in the Methods Chapter. Sequence analysis revealed that *pf4* contains a base pair substitution/deletion at positions 2239 and 2240 in exon seven of the B-subunit gene (Fig. 3.2). This mutation predicts a F306A change in the fifth WD repeat and a frame-shift resulting in the coding of a premature stop codon; the mutation predicts a 37-kDa truncated protein product (Fig. 3.3).

The original *pf4* cells were isolated from the R.P. Levine laboratory (Levine and Ebersold, 1960; Ebersold and Levine, 1962) and are often palmelloid, grow short flagella, and display a slow, smooth swimming phenotype. The palmelloidy phenotype is characterized by a failure in *Chlamydomonas* cells to hatch from the mother cell wall after undergoing mitosis. This phenotype is often displayed in our mutant cell lines that have short flagella or a slow swimming phenotype, like *pf4* cells. Hatching of the cells is often promoted by re-suspending cells in water or using a purified lytic enzyme formed by gametic *Chlamydomonas* cells called autolysin. Other problems for my study of *pf4* were that the cells were in an unknown genetic background (records were incomplete) and the cells were stored in the *Chlamydomonas* collection for many years. To address these issues, it was therefore important to perform crosses with wild type cells.

To verify the phenotype associated with defects in the B-subunit gene, we backcrossed *pf4* to wild-type cells three times and selected one progeny, *pf4 9-1*, as the representative *pf4*-mutant strain for all experiments. In order to confirm that the *pf4 9-1* cells contained the *pf4* mutation, we PCR amplified a region of the B-subunit gene containing the *pf4* mutation. The resulting PCR product was digested with the restriction enzyme CviKi-1, an enzyme that produces detectable differences in banding patterns between WT and *pf4* mutant DNA (Fig. 3.4). Based on restriction analysis, the *pf4 9-1* cells were shown to contain the original *pf4* mutation. From here on we will refer to *pf4 9-1* as *pf4*. The *pf4* mutant displayed full-length flagella and same reduced swimming speed as originally observed. Moreover, *pf4* cells, although motile, failed to phototax in the presence of white light (Witman, 1993). As described above, this is a phenotype characteristic of mutants that fail to assemble I1 dynein (King and Dutcher, 1997; Okita

et al., 2005), and similar in phenotype to I1 dynein mutants. Thus, consistent with our model (Fig. 2) that I1 dynein is part of a regulatory pathway that includes PP2A, we speculated I1 dynein and *pf4* mutants could have a similar phenotype (see below).

The B-subunit is required for targeting of PP2A to the axoneme

Based on these data, we predicted that the B-subunit would be missing in *pf4* cells and axonemes and, as a consequence, based on our model, the entire PP2A complex would fail to assemble in the *pf4* axoneme. To test these ideas, both WT and *pf4* cells were fractionated, as mentioned above, and immunoblots were performed using our B-subunit antibody. Results show that the B-subunit is absent in all flagellar fractions and the cytoplasm (Fig. 3.5). We did not see any evidence of a truncated B-subunit protein indicating that this mutation is effectively a null allele (data not shown). To determine if the PP2A holoenzyme fails to target to axonemes in the absence of the B-subunit, we repeated the immuno-blots with a mammalian C-subunit antibody. Importantly, we found that the C-subunit fails to target to the flagellum in the absence of the B-subunit, although the C-subunit is found in the cytoplasm of the *pf4* cells (Fig. 3.5). Given that the A- and C-subunits are an obligate heterodimer and consistent with our model, these data indicate that assembly of the B-subunit is necessary for localization of the PP2A C-, and presumably A-, subunits to the outer doublet microtubules. To our surprise, we also found that the C-subunit was often drastically reduced in the cytoplasm of the *pf4* cells (Fig. 3.5b). This data indicates that expression of the B-subunit protein is necessary for both the proper localization of and possibly the stability of the entire PP2A holoenzyme.

The *pf4* mutant has defective motility and fails to perform phototaxis.

The *pf4*-swimming phenotype is similar to the phenotype of mutant cells lacking I1 dynein (Fig. 3.6); *pf4*-swimming velocities are reduced to velocities exhibited by *ida3* mutants (shown here and Bayly et al., 2010) and other I1-dynein mutants including *ida7* (Perrone et al., 1998). One possibility in *pf4* was that in the absence of PP2A there is also a failure in assembly of dynein arms. To test this, we performed immuno-blot analysis and thin section electron microscopy to determine whether the dynein arms and other axonemal strucutres are assembled in *pf4* axonemes. Immunoblots determined the dynein arms and radial spokes are fully assembled in *pf4* axonemes (Fig.3.7a). Transmission electron microscopy also confirmed that there are no obvious structural defects in the dynein arms, radial spokes or central pair apparatus (Fig. 3.7b). Thus, the motility phenotype in *pf4* appears to be solely a consequence of a failure in PP2A assembly that, in turn, results in a failure in regulation of dynein motor function.

Diverse genetic and pharmacological evidence has revealed an axonemal phospho-regulatory mechanism that involves I1 dynein (Porter and Sale, 2000; Wirschell et al., 2007). As indicated above, like the *pf4* mutants, mutations that lead to a failure in assembly of I1 dynein results in a slow-swimming phenotype (Fig. 3.6) (Bower et al., 2009; Hendrickson et al., 2004; Myster et al., 1997; Myster et al., 1999; Perrone et al., 2000; Perrone et al., 1998; Porter et al., 1992; Toba et al., 2011) and defective phototaxis (Fig. 3.8) (King and Dutcher, 1997; Okita et al., 2005). To test whether PP2A may be part of the regulatory pathway that controls I1 dynein and control of flagellar bending, we examined phototaxis in *pf4* cells. Like the I1 dynein mutants, the photo-accumulation assay revealed that *pf4* cells do not undergo phototaxis; failing to accumulate on one side

of a dish, demonstrating that *pf4* mutant cells are defective in phototaxis (Fig. 3.8). (This failure in phototaxis was not due to the slow-swimming phenotype in pf4: other slow swimming cells do not necessarily have a defect in phototaxis (see *ida4*). Thus, assembly of PP2A is required for normal motility and phototaxis. One model is that PP2A is part of the phospho-regulatory mechanism that regulates I1 dynein by control of the regulatory phosphoprotein IC138 (discussed below and see Bower et al., 2009; Habermacher and Sale, 1997; Hendrickson et al., 2004; King and Dutcher, 1997).

Intragenic *pf4* revertants restore PP2A assembly, rescue phototaxis and near wild-motility.

To further verify that the defect in the B-subunit gene is responsible for the *pf4*-mutant phenotype and to potentially define an axonemal regulatory pathway that includes PP2A, we performed a suppressor screen. The idea was to use UV mutagenesis (Dutcher et al., 1998) and assess swimming phenotypes of the surviving cells, looking for cells that appear to swim better or faster than *pf4*. The hope was to recover both intragenic revertants that recover the PP2A B-subunit through a second site mutation, and restore the B-subunit reading frame, or new mutations in other genes that presumably encode proteins that are part of the same regulatory pathway and can suppress the *pf4* phenotype. We recovered two intragenic *pf4*-revertant strains, *pf4rV5* and *pf4rV11*, that harbor a second site mutation in the *PF4* gene. Importantly, this screen also resulted in recovery of a number of new mutants, that improve *pf4* swimming (suppressors) but that did not map to the PF4 locus. Thus, for the future we have a library of new mutants that will help define the PP2A dependent pathway that controls motility. Predictably, these

mutants could include new mutant alleles of the BOP5 gene that encodes IC138 (Hendrickson et al., 2004; Bower et al., 2009).

Sequence analysis of both revertants revealed a 7-bp insertion (AGAAGAA) upstream of the original *pf4* mutation which restores the reading frame (Fig. 3.9). To confirm the original *pf4* mutation in the *pf4* revertant we sequenced the entire B-subunit gene and performed restriction analysis on genomic DNA using the enzyme CviKi-1 as described previously, (data not shown). The new sequence in the *pf4rV5* and *pf4rV11* revertants predicts changes in amino acids 300-308 with the insertion of a valine and a proline, and the alteration of an alanine to a glycine. Notably, these amino acid changes may introduce alterations in the B-subunit structure compared to WT (Figs. 3.10 a,b).

To determine whether the *pf4* revertant cells assemble PP2A, isolated axonemes were fractionated as described previously, and analyzed by immunoblots using the PP2A B- and C-subunit antibodies. The revertant PP2A B-subunit and C-subunit were fully assembled at wild-type levels in *pf4*-revertant axonemes (Fig. 3.11). This result confirmed that the B-subunit rescued the B-subunit mutation and provided additional evidence that the B-subunit is required for localization of the PP2A C-subunit to the axonemal structure. Notably, the revertant B-subunit migrates slightly slower on SDS-PAGE gels compared to the wild-type B-subunit (Figs 3.11). This observation is consistent with the prediction that the revertant protein differs slightly from the wild-type protein. However, despite this new mutation, the B-subunit retains the ability to localize the PP2A holoenzyme in the axoneme.

Since the axonemes from the *pf4* revertant cells have restored PP2A, we predicted that phototaxis and motility would also be restored in the *pf4*-revertant cells. As

predicted, photo-accumulation assays demonstrate that the revertant cells have restored phototaxis (Fig. 3.12). The revertants were identified based on their ability to swim better than *pf4* cells. Consistent with this, the revertants have increased swimming velocities relative to the *pf4* mutation alone (Fig. 3.13). However, the swimming velocities were not restored to wild-type levels; which possibly indicates that the modified B-subunit expressed in *pf4rV5* and *pf4rV11* is partially defective. As indicated above, the revertant B-subunit contains a VP insertion, an A302G substitution and several additional amino acid substitutions in the fifth WD repeat which may disrupt the β-sheet structure (Figs. 1.9,1.10 and 3.10). Perhaps PP2A is accessible only to a subset of its axonemal substrates or the function of PP2A is partially compromised in the revertants. Consistent with this idea, a B-type subunit has been shown to interact with tau to promote its dephosphorylation (Xu et al., 2008). Thus, the inability to fully restore wild-type swimming is most likely a direct result of the modified B-subunit protein. These data also suggest that the phototaxis pathway may be separate from the pathway controlling swimming velocity. Consistent with this interpretation, recent analysis of *Chlamydomonas* null mutations in the IC138 gene (*bop5*) revealed that IC138 is required from normal flagellar bending, but not required for phototaxis (See Discussion below and unpublished data, M.E. Porter, University of Minnesota, R. Kamiya, University of Tokyo, and W.S. Sale).

The *pf4* double mutants display more severe phenotypes.

To better understand the role of PP2A in regulation of motility, we generated double mutants between *pf4* and dynein arm mutants. As discussed, diverse evidence suggest

PP2A may function in a conserved signaling pathway that involves the central pair, radial spokes and at least one ciliary dynein motor, the inner arm I1 dynein (Porter and Sale, 2000; Smith and Yang, 2004; Wirschell et al., 2007). The *pf4*-motility phenotype is consistent with defects in regulation of the inner dynein arms; *pf4* and inner dynein arm mutations exhibit slow-smooth swimming phenotypes. If the motility defect in *pf4* is due to a mis-regulation of I1 dynein, then we predict the motility phenotype of a *pf4*, I1dynein double mutant will be similar to or no worse than the parental motility phenotypes and failure in phototaxis. Furthermore, we predict that double mutants between *pf4* and inner arm dynein motors that are unaffected by PP2A will display a more severe phenotype.

Table II lists the *pf4,* inner dynein arm double mutants generated in this study and lists their motility phenotypes. Notably, when the *pf4* defect is combined with defects in inner arm dyneins a, c, and d (*ida4*) and inner arm dynein e (*ida6*), or with defects in regulation of I1 dynein (*mia1*, *mia2*), the resulting phenotypes were significantly worse than the parental phenotypes. These results indicate that PP2A does not play a unique role in regulation of the single headed inner dynein arms and that axonemal PP2A does not function in regulatory mechanisms unique to the pathways defined by the *mia1* and *mia2* mutants. To our surprise, we could not isolate double mutants between *pf4* and any I1-dynein mutant (*ida1*, *ida7*, *bop5*) in spite of several attempts. The significance of this result is unclear, but is possibly technical or that the combinations are lethal for unknown reasons. Notably, other combinations of *pf4* and inner arm dynein mutants were successful. It is possible we may be revealing additional essential functions for the PP2A B-subunit and I1 dynein.

Based on pharmacological evidence for a role for PP2A in regulation of I1 dynein and our current results, PP2A may operate, at least in part, in a pathway that includes I1 dynein and possibly IC138 (Bower et al., 2009; Wirschell et al., 2007). As indicated in the model in

Figure 2, failure in a phosphatase such as PP2A would result in altered or increased phosphate incorporation in IC138. Consistent with this hypothesis, we determined that IC138 is highly phosphorylated in *pf4* axonemes compared to wild-type axonemes; a phenotype similar to that observed for mutants that are defective in the phospho-regulatory pathway that controls I1 dynein (Fig. 3.14 and Fig. 2). In the same assay, IC138 also appears to be highly phosphorylated in *pf4* revertant axonemes (Fig. 3.14). As discussed above, this observation may also indicate that the revertant PP2A B-subunit differs in structure from wild-type, and as a consequence, IC138 is abnormally phosphorylated in the revertants resulting in only partial restoration of swimming speed. To date, the key phospho-residues in I1 dynein are not known and, thus, sites of phosphorylation in IC138 may differ in *pf4* axonemes compared to the *pf4* revertants. Further tests of this model will require identification of specific IC138 phospho-residues and detailed analysis of point mutations in these residues. Nevertheless, these results are consistent with a role for PP2A in regulation of I1 dynein.

Fig. 3.1

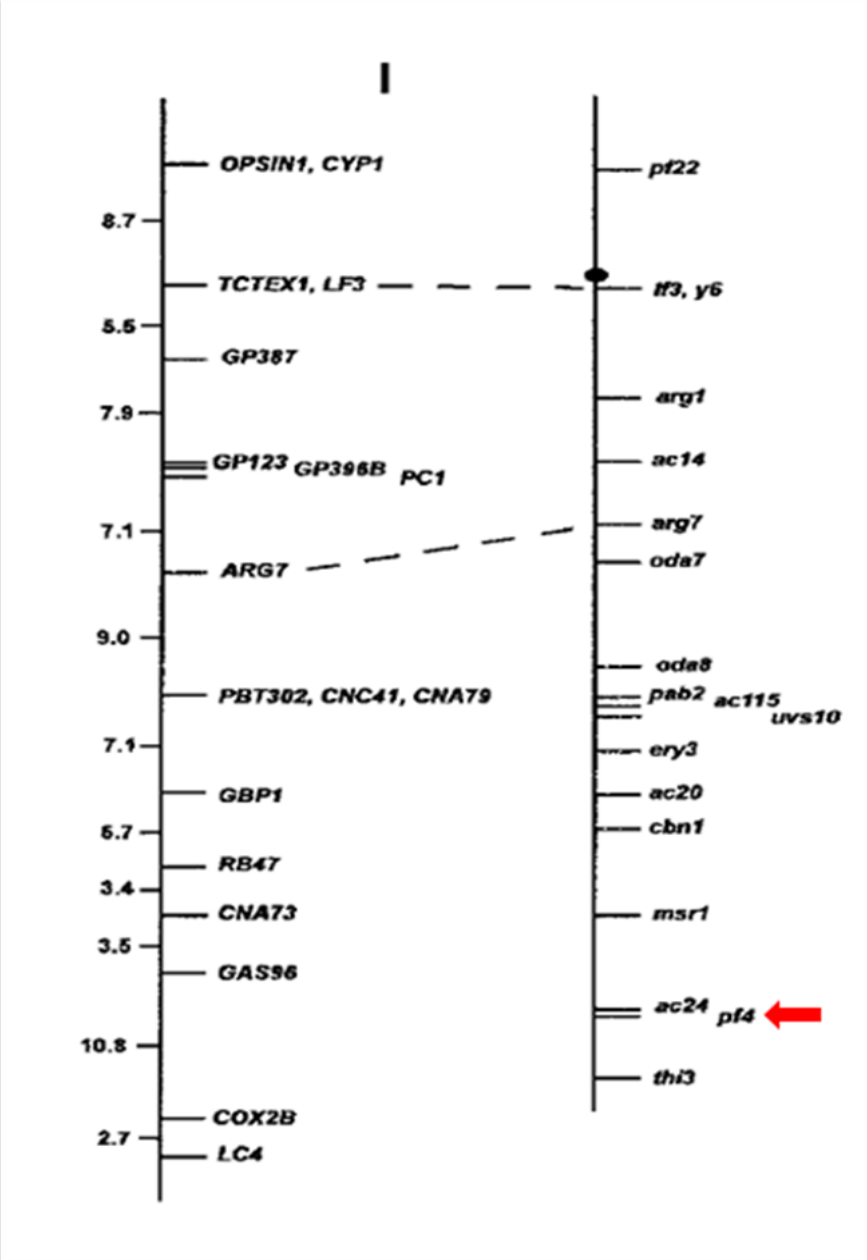
I
OPSIN1, CYP1
8.7
TCTEX1, LF3
5.5
GP387
7.9
GP123 GP396B PC1
7.1
ARG7
9.0
PBT302, CNC41, CNA79
7.1
GBP1
5.7
RB47
3.4
CNA73
3.5
GAS96
10.8
COX2B
2.7
LC4
pf22
lf3, y6
arg1
ac14
arg7
oda7
oda8
pab2 ac115
uvs10
ery3
ac20
cbn1
msr1
ac24 pf4
thi3

Fig. 3.1: The B-subunit of PP2A maps near the flagellar mutant *pf4*. The *pf4* mutant was isolated in the Levine laboratory and maps to linkage group I in the *Chlamydomonas* genome. Image adapted from Kathir, P. et al., 2003.

Fig. 3.2

(A)

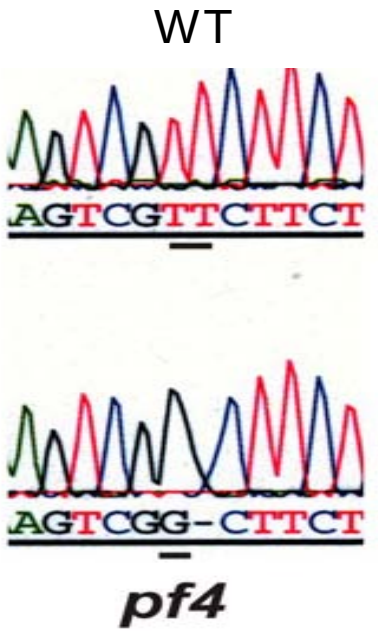
WT
AGTCGTTCTTCT
AGTCGG-CTTCT
pf4

(B)

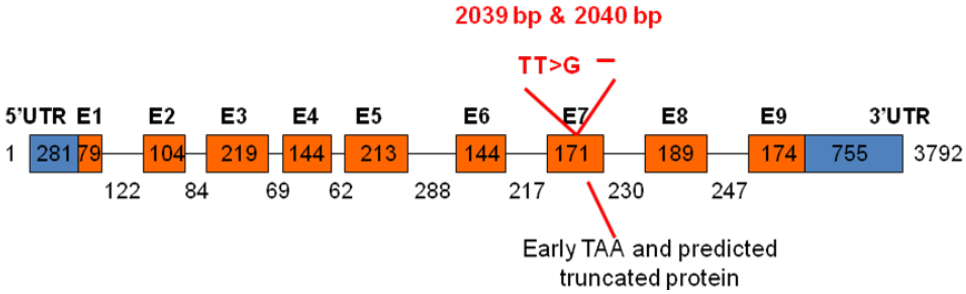
2039 bp & 2040 bp
TT>G
5'UTR E1 E2 E3 E4 E5 E6 E7 E8 E9 3'UTR
1 281 79 104 219 144 213 144 171 189 174 755 3792
122 84 69 62 288 217 230 247
Early TAA and predicted truncated protein

Fig. 3.2: (A) A DNA sequence chromatogram showing that the *pf4* mutant contains a base pair substitution/deletion (TT>G-) at positions 2239 and 2240. **(B)** A B-subunit gene schematic showing the location of the *pf4* mutation in exon seven of the B-subunit gene.

Fig. 3.3

(A)

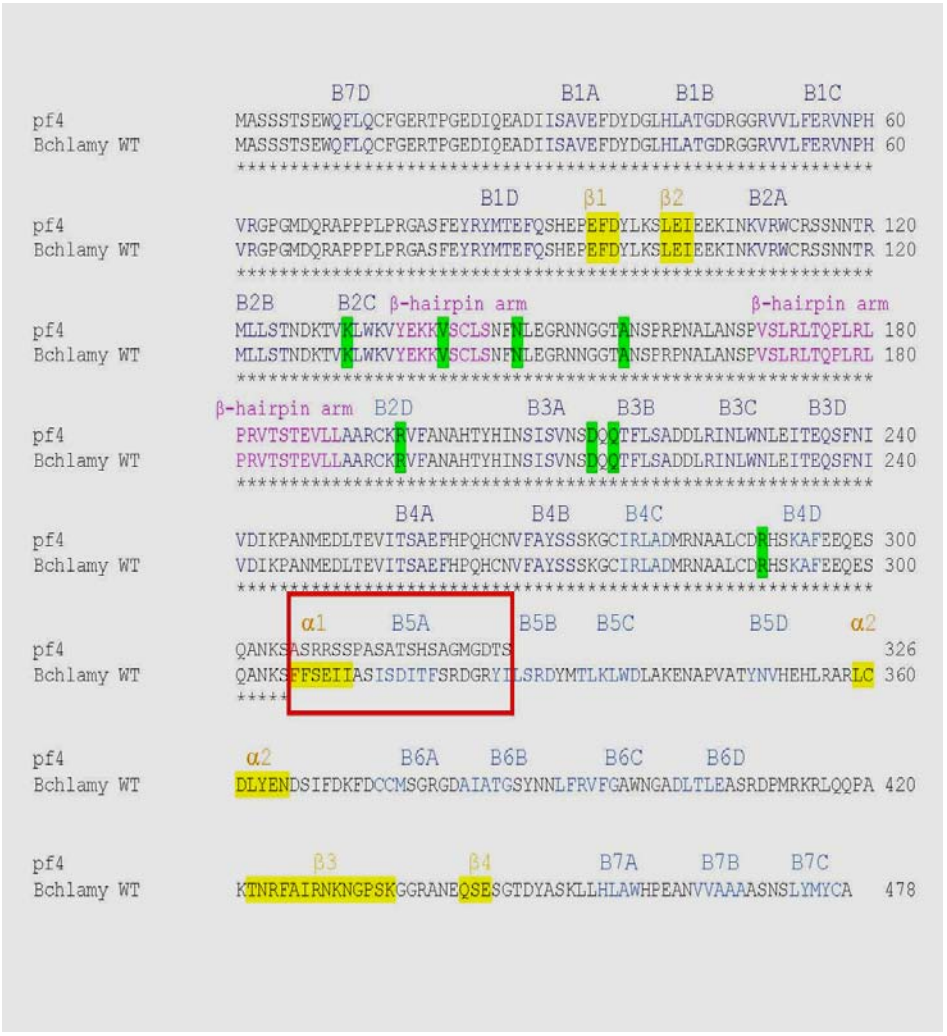
B7D B1A B1B B1C
pf4 MASSSTSEWQFLQCFGERTPGEDIQEADIISAVEFDYDGLHLATGDRGGRVVLFERVNPH 60
Bchlamy WT MASSSTSEWQFLQCFGERTPGEDIQEADIISAVEFDYDGLHLATGDRGGRVVLFERVNPH 60
B1D β1 β2 B2A
pf4 VRGPGMDQRAPPPLPRGASFEYRYMTEFQSHEPEFDYLKSLEIEEKINKVRWCRSSNNTR 120
Bchlamy WT VRGPGMDQRAPPPLPRGASFEYRYMTEFQSHEPEFDYLKSLEIEEKINKVRWCRSSNNTR 120
B2B B2C β-hairpin arm β-hairpin arm
pf4 MLLSTNDKTVKLWKVYEKKVSCLSNFYLEGRNNGGTANSPRPNALANSPVSLRLTQPLRL 180
Bchlamy WT MLLSTNDKTVKLWKVYEKKVSCLSNFYLEGRNNGGTANSPRPNALANSPVSLRLTQPLRL 180
β-hairpin arm B2D B3A B3B B3C B3D
pf4 PRVTSTEVLLAARCKRVFANAHTYHINSISVNSDQGTFLSADDLRINLWNLEITEQSFNI 240
Bchlamy WT PRVTSTEVLLAARCKRVFANAHTYHINSISVNSDQGTFLSADDLRINLWNLEITEQSFNI 240
B4A B4B B4C B4D
pf4 VDIKPANMEDLTEVITSAEFHPQHCNVFAYSSSKGCIRLADMRNAALCDRHSKAFEEQES 300
Bchlamy WT VDIKPANMEDLTEVITSAEFHPQHCNVFAYSSSKGCIRLADMRNAALCDRHSKAFEEQES 300
α1 B5A B5B B5C B5D α2
pf4 QANKSASRRSSPASATSHSAGMGDTS 326
Bchlamy WT QANKSFFSEIIASISDITFSRDGRYILSRDYMTLKLWDLAKENAPVATYNVHEHLRARLC 360
α2 B6A B6B B6C B6D
pf4
Bchlamy WT DLYENDSIFDKFDCCMSGRGDAIATGSYNNLFRVFGAWNGADLTLEASRDPMRKRLQQPA 420
β3 β4 B7A B7B B7C
pf4
Bchlamy WT KTNRFAIRNKNGPSKGGRANEQSESGTDYASKLLHLAWHPEANVVAAAASNSLYMYCA 478

(B)

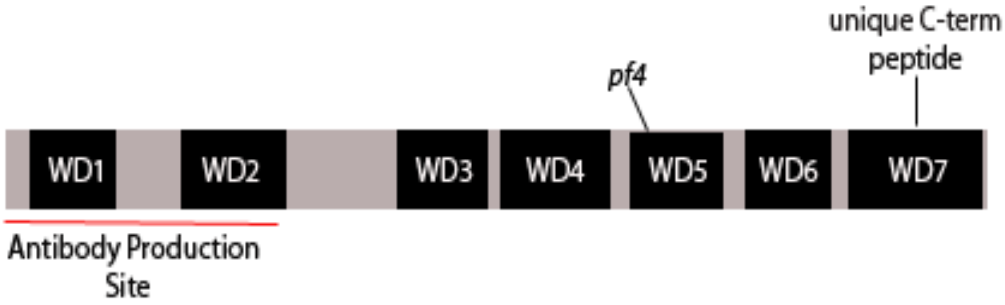
unique C-term peptide
pf4
WD1
WD2
WD3
WD4
WD5
WD6
WD7
Antibody Production Site

Fig. 3.3: (A) Sequence alignment of the WT axonemal *Chlamydomonas* B-subunit and the truncated *pf4* B-subunit. The *pf4* mutation contains an F>A amino acid change at position 306 and the subsequent amino acids are changed from the original protein leading to an early stop codon (TAA) at position 327, resulting in a C-terminal truncation of the protein.

(B) Schematic of the predicted *Chlamydomonas* PP2A B-subunit protein containing the *pf4* mutation.

Fig. 3.4

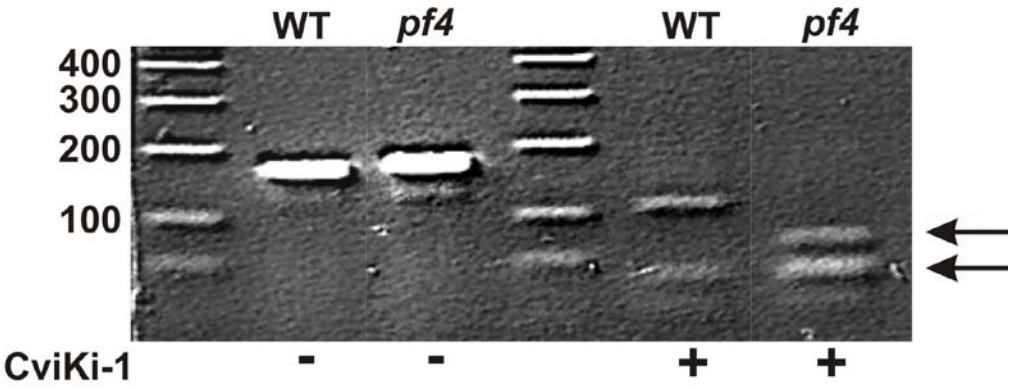

Fig. 3.4: Confirmation of the *pf4* mutation in genomic DNA by restriction enzyme digestion. Undigested(-) and CviKi digested(+) PCR products were resolved on a 2% agarose gel shown in 3D. The samples contain a 175 base pair PCR product spanning the region where the predicted *pf4* mutation was identified. Results show that when digested with CViKi-1, DNA from *pf4* cells produces a banding pattern distinctly different from WT (arrows) thus confirming the mutation within this region.

Fig. 3.5

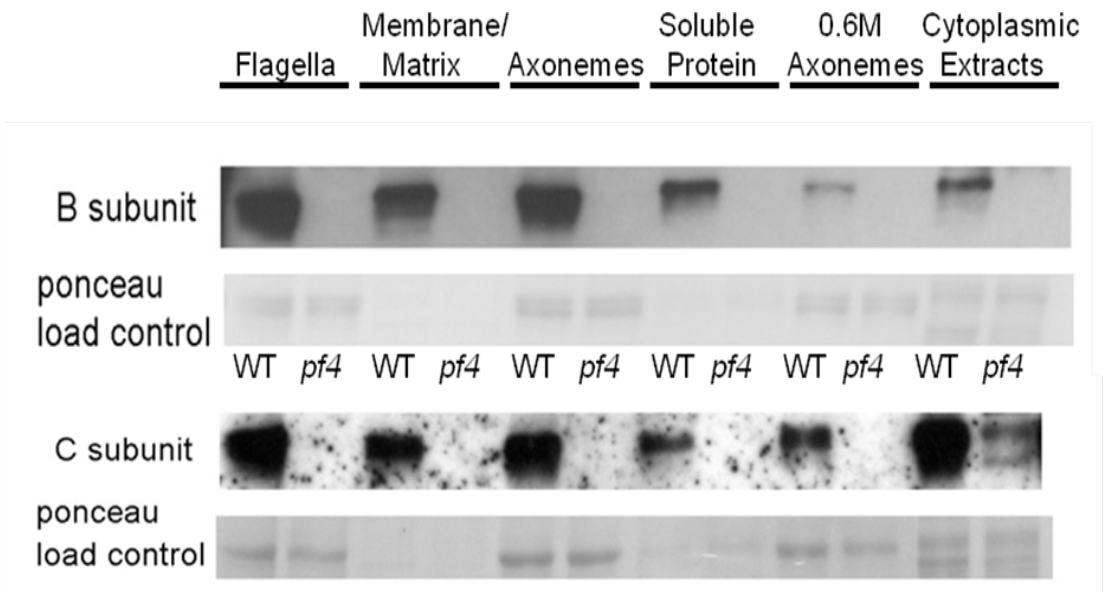
Flagella
Membrane/ Matrix
Axonemes
Soluble Protein
0.6M Axonemes
Cytoplasmic Extracts
B subunit
ponceau load control
WT pf4 WT pf4 WT pf4 WT pf4 WT pf4 WT pf4
C subunit
ponceau load control

Fig. 3.5: The B-subunit gene is mutated in *pf4* cells and the PP2A holenzyme fails to target to the axoneme. (A) Cellular fractionation of Chlamydomonas cells. WT and *pf4* cells were fractionated into flagella, membrane matrix, Axonemes, Soluble protein, and 0.6M salt extracted axoneme fractions. Equivalent protein amounts were loaded based on a starting volume of 5µg of flagellar protein. Westerns were performed using our polyclonal B-subunit antibody and the C-subunit antibody (1D6). Ponceau A staining showing tubulin at 50 kDa was used as a loading control.

Fig. 3.6

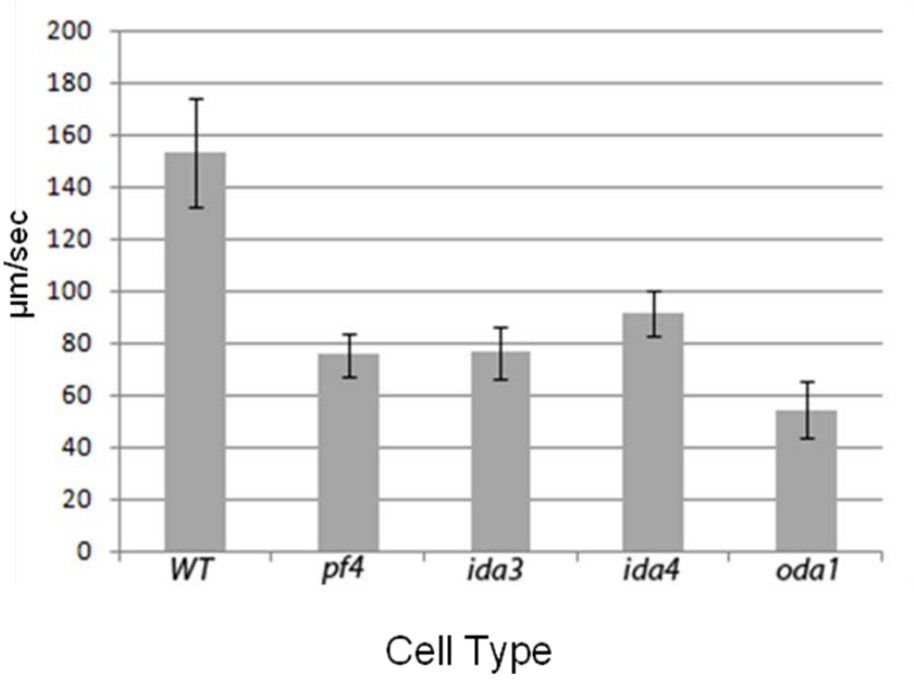
200
180
160
140
120
100
80
60
40
20
0
µm/sec
WT
pf4
ida3
ida4
oda1
Cell Type

Fig. 3.6: Swimming velocities of wild-type and mutant cells were analyzed. The *pf4* mutant has a reduced swimming velocity that is comparable to mutants lacking I1 dynein (*ida3*). Also analyzed are *ida4*-a mutant lacking inner arms a, c, and d, and *oda1*—lacking the outer dynein arm.

Fig. 3.7

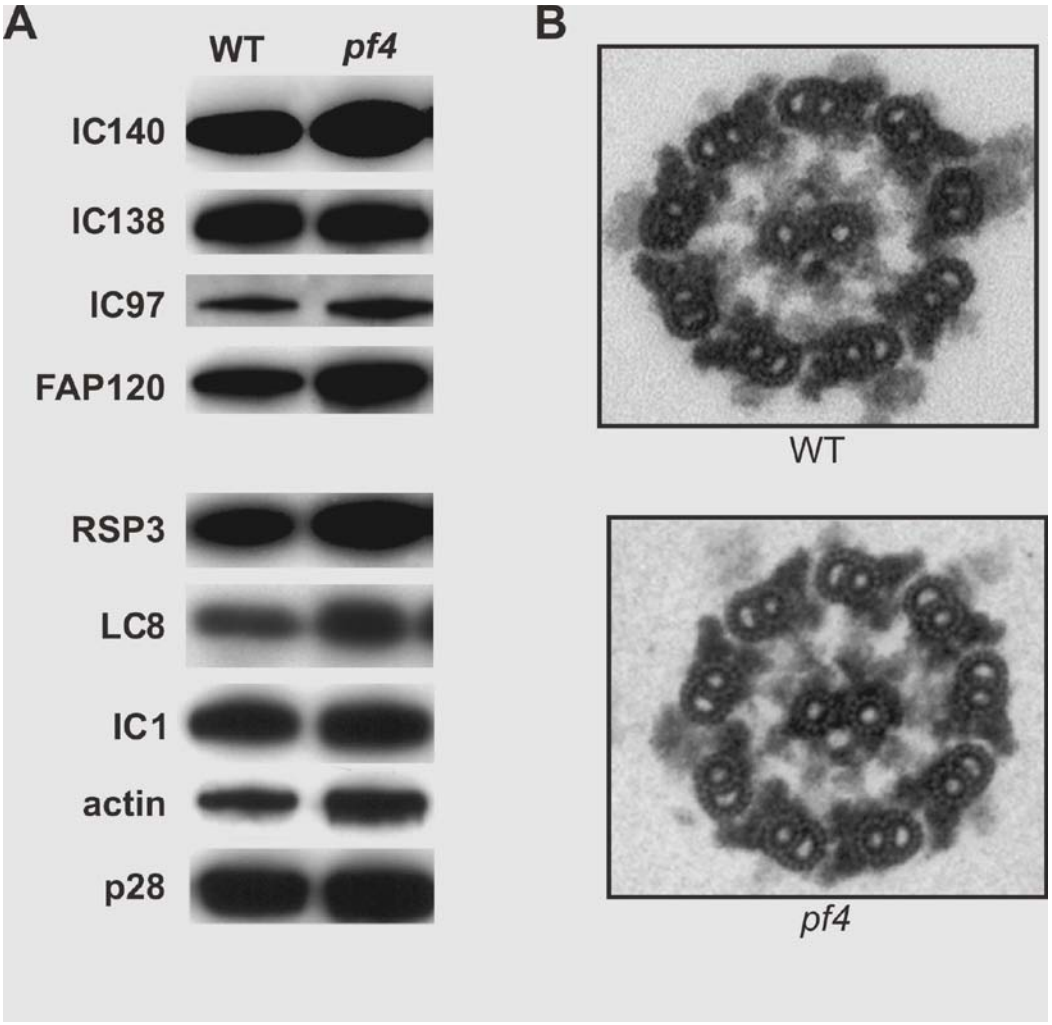
A
WT
pf4
IC140
IC138
IC97
FAP120
RSP3
LC8
IC1
actin
p28
B
WT
pf4

Fig. 3.7: (A) Immnoblots of wild-type and *pf4* axonemes using antibodies to various components of the axonemal dynein motors show that dyneins are assembled in *pf4* including I1 dynein (IC140, IC138, IC97, FAP120), dyneins a, b, c, d, e, and g (actin and p28) and the outer dynein arm (IC1). In addition, there are no defects in assembly of the radial spokes (RSP3). LC8 levels are also unaltered (LC8 is a component of I1, the outer arm and the radial spoke). **(B)** Transmission electron microscopy of wild-type and *pf4* axonemes demonstrates that *pf4* assembles all the major axonemal structures including the central pair, the radial spokes, the dynein arms and the outer doublet microtubules.

Fig. 3.8

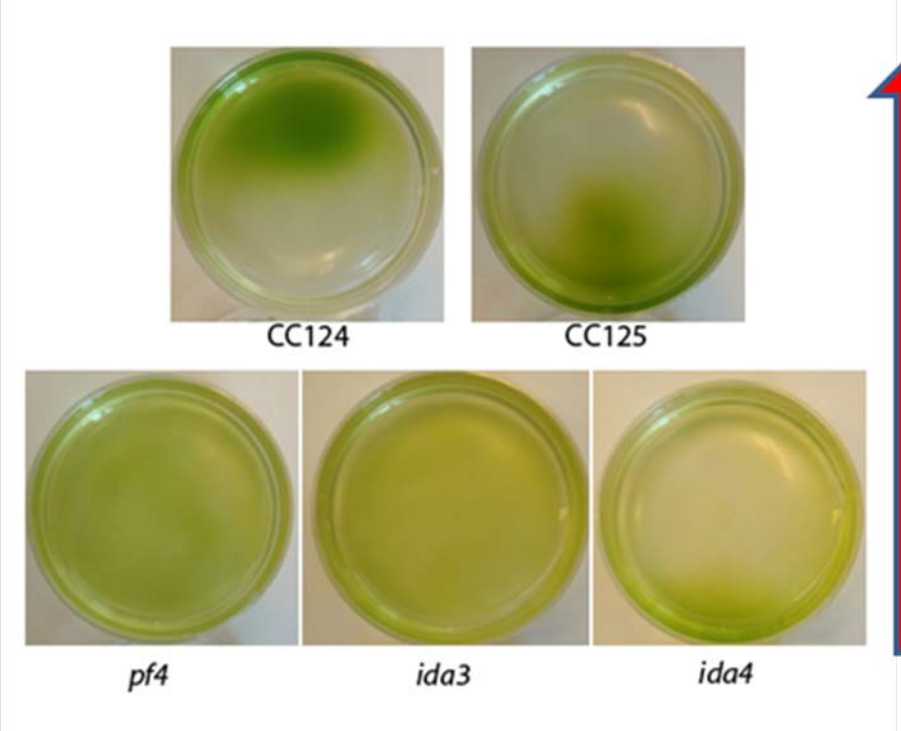

Fig. 3.8: Photo-accumulation assays reveal that *pf4* is defective in phototaxis. Wild-type cells swim towards (CC125+; *AGG1*) or away (CC124-, *agg1*) from a light source (red arrow) and accumulate on one side of a culture dish, whereas *pf4* cells do not. This defect is also present in *ida3, mia1* and *mia2* mutants—defective in I1 dynein assembly or regulation, but is not a consequence of slow swimming, as another inner arm mutant and an outer arm mutant (*ida4* and *oda1*(not shown) respectively) photo-accumulate with wild-type kinetics.

Fig. 3.9 (A)

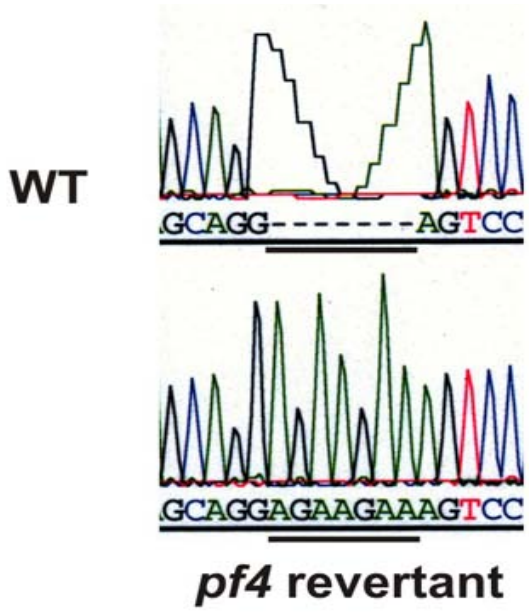
WT
GCAGG-------AGTCC
GCAGGAGAAGAAAGTCC
pf4 revertant

(B)

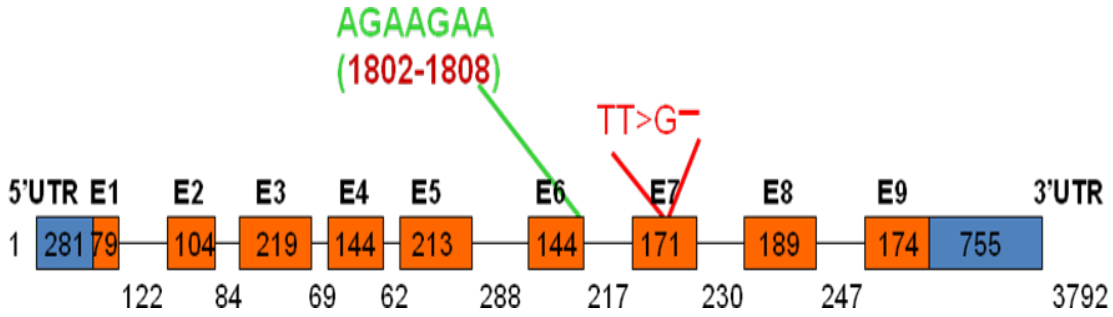
AGAAGAA
(1802-1808)
TT>G
5'UTR E1 E2 E3 E4 E5 E6 E7 E8 E9 3'UTR
1 281 79 104 219 144 213 144 171 189 174 755
122 84 69 62 288 217 230 247 3792

Fig. 3.9: Schematic of the *Chlamydomonas* PP2A B-subunit gene in the intragenic revertants *pf4rV5* and *pf4rV11*. The original *pf4* mutation is a base pair substitution/deletion (TT>G-) at positions 2239 and 2240 found in exon seven. The *pf4* revertants, V5 and V11, contain a seven base pair insertion (AGAAGAA) which consists of base pairs 1802-1808 in exon six, upstream of the original *pf4* mutation. This isnsertion is expected to restore the reading frame of the B-subunit, resulting in a full-length B-subunit protein product.

Fig. 3.10

(A)

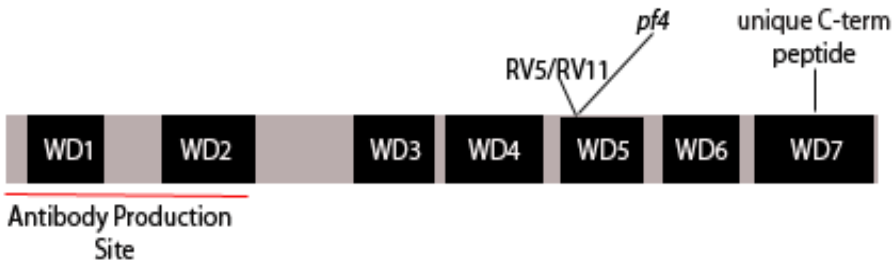

(B)

WT B-sub	(293)	KAFEEQESQ--ANKSFFSEIIASIS	(315)
rV5/V11 B-sub	(293)	KAFEEQEKKVPGEQVGFSEIIASIS	(317)

Fig. 3.10: Schematic of the predicted *Chlamydomonas* PP2A B-subunit protein of the intragenic revertants *pf4rV5* and *pf4rV11*. The seven base pair insertion into the gene results in amino acid changes at positions 300-308 including a valine and proline insertion. The insertion is predicted to produce a full length B-subunit protein product.

Fig. 3.11

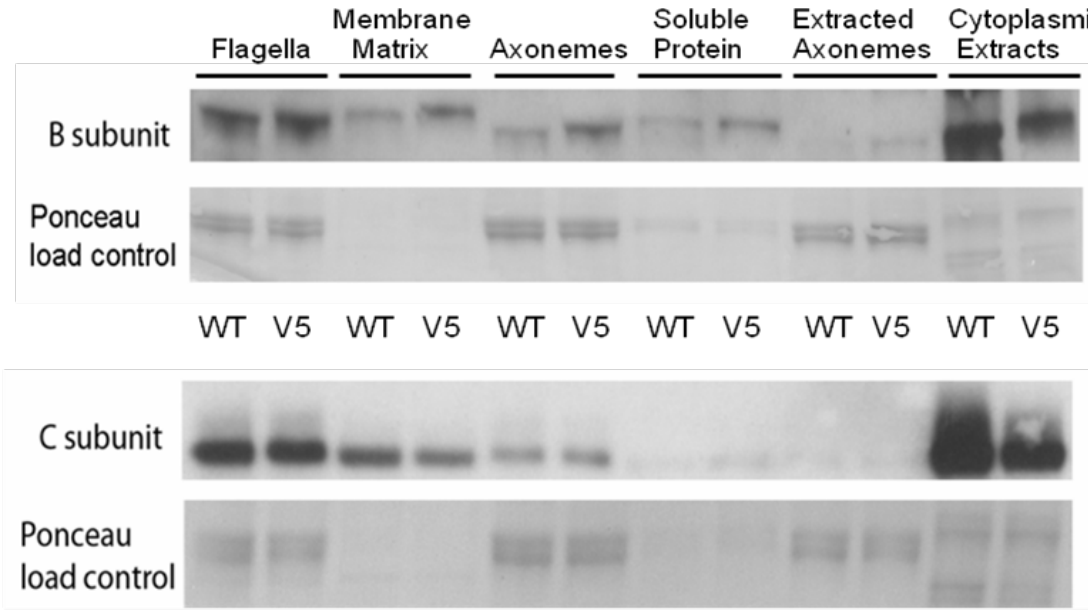
Flagella
Membrane Matrix
Axonemes
Soluble Protein
Extracted Axonemes
Cytoplasmi Extracts
B subunit
Ponceau load control
WT V5 WT V5 WT V5 WT V5 WT V5 WT V5
C subunit
Ponceau load control

Fig. 3.11: The B- and C-subunits are expressed at WT levels in the *pf4* revertant cells and flagella. Cellular fractionation of C*hlamydomonas* cells. Wild-type (WT), and *pf4rV5*cells were fractionated into flagella, membrane matrix, Axonemes, Soluble protein, and 0.6M salt extracted axoneme fractions. Equivalent protein amounts were loaded based on a starting volume of 5µg of flagellar protein. Westerns were performed using our polyclonal B-subunit antibody and the C-subunit antibody (1D6). Ponceau stains showing tubulin at 50 kDa were used as loading controls.

Fig. 3.12

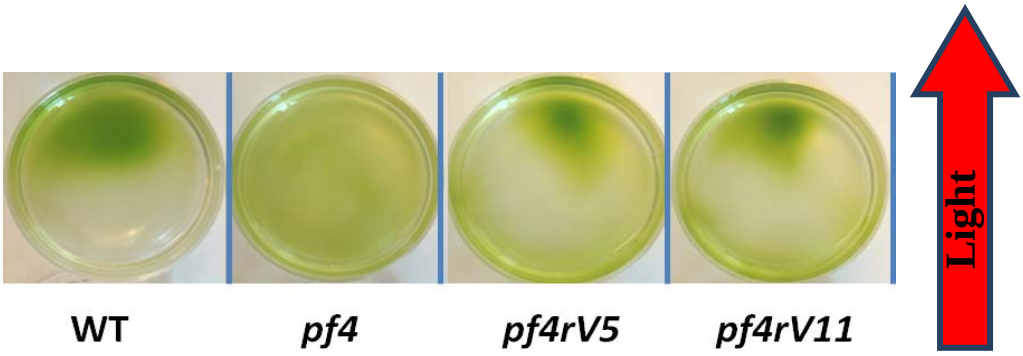

Fig. 3.12: Photoaccumulation of *Chlamydomonas* cells. WT (CC124), *pf4*, and the *pf4* suppressor mutants *pf rV5* and *pf4rV11* were plated in tissue culture dishes and allowed to phototax in the presence of ambient sunlight. The CC124 cells phototax away from the light because they are defective in the *agg1* gene responsible for directional control of phototaxis. The *pf4* cells are unable to phototax in the presence of light. The ability to phototax is restored in the *pf4* suppressor mutants *pf4rV5* and *pf4rV11*.

Fig. 3.13

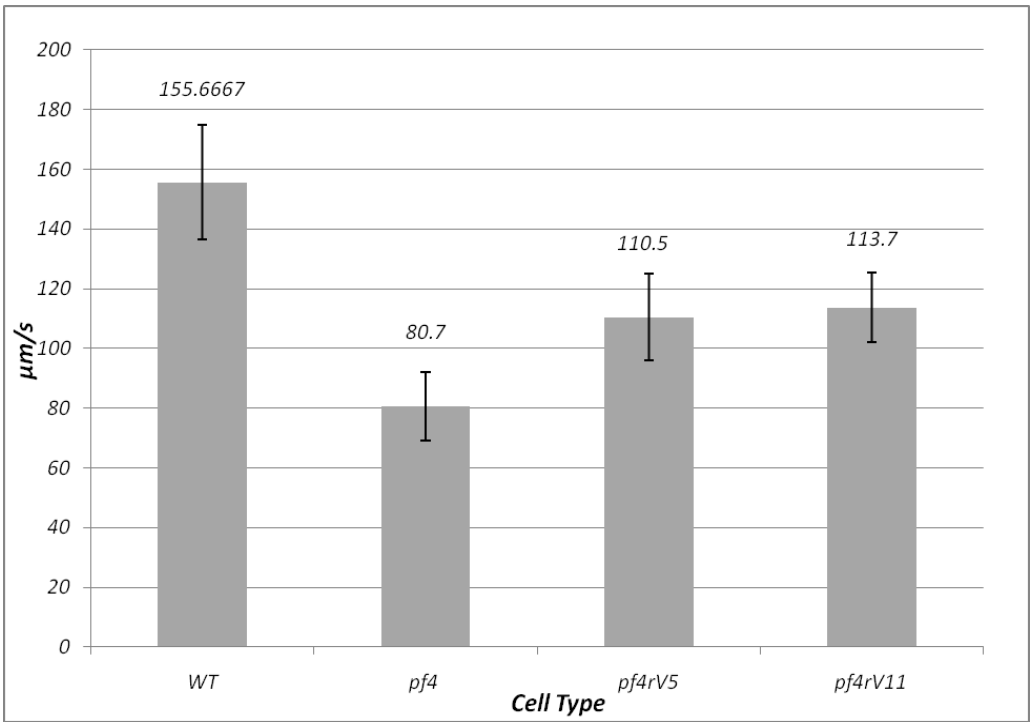
200
180
160
140
120
100
80
60
40
20
0
µm/s
155.6667
80.7
110.5
113.7
WT
pf4
pf4rV5
pf4rV11
Cell Type

Fig. 3.13: The *pf4* revertant cells *pf4rV5* and *pf4 rV11* swim with a velocity intermediate between Wt and *pf4* cells. Swimming velocities of, WT (CC124), *pf4 9-1*, and the *pf4* suppressor mutants *pf4rV5* and *pf4rV11* were determined by measuring distance traveled in a straight path over time. Data shown is an experiment representing the typical result of at least 3 experiments with an n=20 for each individual experiment analyzed. Error bars represent the standard deviation of the measured velocities. A student's t-test ($P<0.05$) shows that swimming velocities between WT and the suppressor mutants and between *pf4* and suppressor mutants are significantly different.

Fig. 3.14

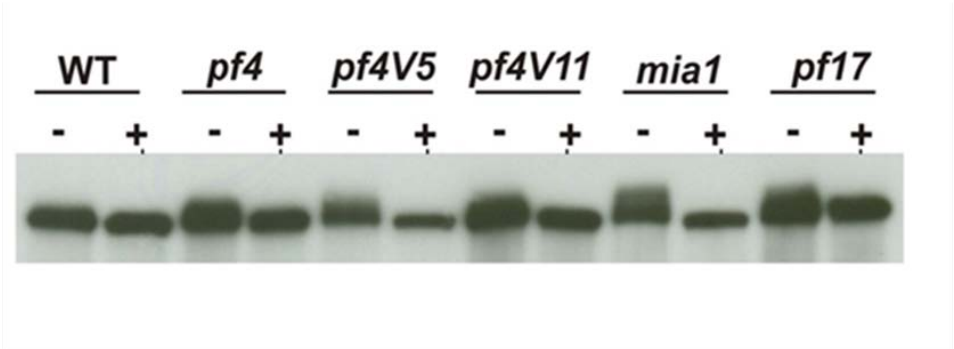

Fig. 3.14: Immunoblots of axonemes treated with buffer alone or CIP were probed with the IC138 antibody as described (Hendrickson et al. 2004; Wirschell et al. 2009). Wild-type axonemes display relatively little IC138 phosphorylation (compare axonemes treated with CIP (calf-intestinal alkaline phosphatase) to untreated axonemes) while axonemes from mutants defective in regulation of I1 dynein (*mia1*, *pf17*) show excessive IC138 phosphorylation due to a global inactivation of I1-dynein activity. Axonemes from *pf4* and the *pf4* revertants also show increased IC138 phosphorylation, consistent with a role for PP2A in regulation of I1

Table II: Phenotype of *pf4* double mutants.

Mutant	**Defect**	**Phenotype**
pf4	PP2A	Slow swimming
pf4 x ida4	PP2A, Dynein a, c, and d	slower swimmer than *pf4* or *ida4*
pf4 x ida6	PP2A, Dynein e	slower swimmer than *pf4* or *ida6*
pf4 x ida9	PP2A, Dynein c	slower swimmer than *pf4* or *ida9*
pf4 x mia1	PP2A, Mia1p	slower swimmer than *pf4* or *mia1*
pf4 x mia2	PP2A, Mia2p	slower swimmer than *pf4* or *mia2*

Table II: Phenotype of *pf4*-double mutants: The *pf4* mutant phenocopies I1-dynein mutants which are defective in assembly or regulation of I1 dynein. Double mutants generated between *pf4* and other dynein deficiencies show more severe phenotypes indicating that PF4 does not work in a pathway that controls single headed inner dynein arms. Rather the results are consistent with the observation that PP2A is involved in a phospho-regulatory pathway that controls I1 dynein.

Chapter 4: Discussion and New Questions

Summary and opportunities:

The work presented in this dissertation is founded on pharmacological and functional studies that determined the presence of PP2A in the ciliary axoneme (Yang et al., 2000). The goal of my work was to identify a PP2A B-type subunit in the axoneme and test the role of axonemal PP2A in regulation of dynein and ciliary motility. My principal objective was to test the hypothesis that a PP2A B-type subunit is responsible for targeting the PP2A holoenzyme to the axoneme. I also tested the hypothesis that PP2A regulates I1 dynein activity and control of phosphorylation of a regulatory protein - IC138. The main results of this work include:

[1] B-subunit localization of PP2A: The axoneme contains a highly conserved B/PR55 subunit of the serine/threonine protein phosphatase, PP2A, which is anchored to the outer doublet microtubules. I was able to confirm that the PP2A B-subunit identified in this study was identical to the axonemal B-subunit identified in the KCl fraction of the flagellar proteome (Pazour et al., 2005). Interestingly, several other B-type subunits were identified in the *Chlamydomonas* genome, however peptides corresponding to these proteins were not identified in the flagellar proteome (Table I). Based on the presence of the other B-subunits, clearly PP2A is quite versatile in other *Chlamydomonas* cellular functions.

One key question is: How is PP2A targeted to distinct subcellular positions to perform distinct functions? The prediction is that the B-subunits bind to specific docking proteins unique to specific organelles to target and anchor PP2A. Therefore, the axoneme can be used as a model system to define mechanisms by which PP2A may be targeted to

the outer doublet microtubules and may involve a class of PP2A anchoring proteins. The *Chlamydomonas* axoneme, thus, offers opportunities to possibly define a class of proteins that anchor PP2A to the cytoskeleton.

[2] The PP2A B-subunit is necessary for normal flagellar motility. This advance was made possible by the identification of the flagellar mutant, *pf4*,that fails to express the B-subunit protein. I also showed that in the absence of B-subunit, the PP2A catalytic subunit fails to assemble in the *pf4* axoneme, and that the *pf4* cells had a reduced swimming velocity and failed to phototax, revealing a motility phenotype. The isolation of two intragenic suppressors of *pf4* was a critical advance providing very strong proof that the *pf4* phenotype is due to the mutation in the gene that encodes the B-subunit: each revertant restored PP2A to the axoneme and displayed partially restored swimming velocity and fully restored phototaxis.

Although the exact role of PP2A in regulation of motility is yet to be determined, the evidence indicates that PP2A plays a role in control of I1 dynein. As predicted the IC138 subunit was abnormally phosphorylated in the *pf4* cells. Somewhat surprisingly, the revertants also contain a hyperphosphorylated IC138 subunit. These data lend support to the idea that the pathways for the regulation of swimming speed and phototaxis may involve a common pathway for PP2A and I1 dynein involving IC138. Therefore, identification of key phospho-residues in IC138 that are responsible for the regulation of each motility phenotype is necessary. Each of the above mentioned goals can be addressed using the *Chlamydomonas* model system and the available array of structural mutants as well as the tools and biochemical reagents developed in this work.

Role of PP2A in the regulation of ciliary motility:

Among the major challenges is to determine the role of PP2A in controlling ciliary motility. The immediate focus is on control of I1 dynein activity in the flagellar axoneme. This is due in part to similar phenotypes in *pf4* and the I1 dynein mutants *ida1, ida2, ida3, ida7* and *bop5*. The current model is that in wild-type axonemes, I1 dynein is locally regulated, on single or a small subset of doublet microtubules, in response to chemical or mechanical signals that, presumably, originate at the central pair, and are directed to specific outer doublet microtubules by the radial spokes (Fig. 3; reviewed in Wirschell *et al.*, 2007). This prediction is founded on the structural asymmetry inherent to the central pair apparatus, discussed in Chapter 1, and the requirement for central pair and radial spoke assembly and a functional link to I1 dynein (Porter et al., 1992; Smith and Yang, 2004; Wirschell *et al.*, 2007). The idea is that an asymmetric signal from one of the central pair microtubules, and its associated proteins, is transmitted via the radial spokes to the outer doublets. These signals presumably are mediated by axonemal kinases including, CK1 and PKA, and the phosphatase, PP2A, that regulate the phosphorylation state of IC138, and consequent changes in I1 dynein activity and microtubule sliding. Predictably, such local changes in microtubule sliding, on one side of an axonemal axis, must alter the pattern of bending (Fig. 1.5). Further tests of this idea will require site directed mutagenesis in IC138, transformation of the IC138 null mutants *bop5-3* and analysis of motility.

Our model states that abnormal phosphorylation of the IC138 subunit of I1 dynein by axonemal kinases decreases dynein-driven microtubule sliding velocities resulting in a disruption of proper flagellar waveform. Further data from our microtubule

sliding assays shows that phosphatases are necessary for the recovery of I1 dynein activity. Consistent with this idea our microtuble sliding data show that axonemes isolated from *pf4* cells display a slow sliding velocity similar to other mutants that contain an abnormally phosphorylated IC138 subunit (Figs. 4.1 A,B). Again, based on our model we predicted that in the presence of kinase inhibitors, we would not be able to rescue microtubule sliding in *pf4* axonemes. Surprisingly, as described at the end of this chapter, microtubules in *pf4* axonemes treated with kinase inhibitors were able slide at WT velocities. This data suggests that PP2A may not be the only phosphatase in the axoneme that regulates dyneins and that I1 dynein may not be the only dynein motor in the axoneme regulated by phosphorylation.

Where does PP2A localize in the axoneme? What is the axonemal B-subunit docking protein?

One prediction of my model is that PP2A is precisely localized in the axoneme near I1 dynein. This prediction can be tested by immuno-electron microscopy using antibodies to PP2A subunits and colloidal gold labeled secondary antibodies. In cross section, I predict that PP2A will be found associated with all of the outer doublet microtubules since I1 dynein is found on all 9 outer doublets (Bui et al., 2009). However, equally or more interesting would be the asymmetrically localized PP2A on only a subset of doublet microtubules. Such a result would be of extraordinary interest indicating that I1 dynein is regulated by PP2A on only a subset of doublet microtubules. Such a discovery would need to be validated by alternative approaches, and would likely become a major focus of work in the lab.

In longitudinal views, I predict PP2A localization would repeat at 96 nm along the doublet microtubules, presumably in register with I1 dynein. However, immuno-gold analysis may not be able to resolve this localization of PP2A relative to I1 dynein with the required precision. A very exciting alternative approach to localize PP2A is to perform cryo EM tomography on axonemes from *pf4*, compared to wild-type, look for a deficiency in structure near the I1 dynein complex. The world's expert, Daniella Nicastro (Brandeis University), has offered to work with us on study of pf4 axonemal structure (see Heuser et al., 2009).

Another prediction is that the PP2A B-subunit must interact with an axonemal docking protein located in the outer doublet repeating at 96 nm. Presumably in the structure of the B-subunit there are domains that not only interact with the A-subunit, but also the postulated docking / targeting protein. Thus, identification of B-subunit interacting proteins is a high priority for future study. Identification of such a protein could be achieved by chemical cross linking in axonemes, an approach that has proven quite successful in the Sale lab (e.g. Wirschell et al., 2009). In addition, as described in Chapter 3, suppressor analysis of *pf4* has yielded not only the intragenic revertants that I characterized, but also a number of extragenic suppressors of *pf4*. These new mutants could include by-pass suppressors that define new proteins required for PP2A function and a regulatory pathway that controls I1 dynein. The new suppressor mutations could be back-crossed to see if a new phenotype is revealed in each suppressor (e.g. slow swimming or failure in phototaxis) and then the new gene mapped. One example of a possible outcome is that one of the suppressors is a new mutation in the substrate IC138 that leads to suppression of *pf4* phenotype.

Microtubule sliding analysis with axonemes from the *pf4* mutant reveals a novel phospho-regulatory pathway that controls dynein

As a further test of the function of PP2A in regulation of axonemal motility, we used a "sliding disintegration assay" (see Methods and Okagaki and Kamiya, 1986; Smith and Sale, 1992) to measure the velocity of microtubule sliding in axonemes from *pf4*. As illustrated in Figure 4.1, in axonemes from *pf4*, microtubules slide at about 50% of the velocity in wild-type axonemes. Thus, microtubules in *pf4* axonemes slide at a reduced velocity similar to the reduced velocity of microtubule sliding in axonemes defective in assembly of the radial spokes (*pf17*, Fig. 4.1 A, B), central pair or subsets of the dynein arms including I1 dynein mutants (e.g. Bower et al., 2009; Toba et al., 2009). In contrast, microtubule sliding is restored in axonemes from the *pf4* revertant cells, *pf4rV5* and *pf4rV11* (Fig. 4.1 C). Thus, consistent with the slowed swimming speed for *pf4* cells, microtubule sliding is also reduced.

We then tested whether kinase inhibitors would restore microtubule sliding velocity as had been found in studies of axonemes from cells defective in radial spoke or central pair assembly (reviewed in Porter and Sale, 2000; Smith and Yang, 2004; Wirschell et al., 2007). Based on the assumption that PP2A is required for rescue of microtubule sliding in the assays, and the assumption that there is a single phospho-pathway for regulation of microtubule sliding, we predicted that kinase inhibitors would fail to rescue microtubule sliding. As described before, control experiments revealed that addition of the kinase inhibitors PKI (Fig. 4.1 A) and DRB (Fig. 4.1 B) rescued microtubule sliding in axonemes from the radial spoke mutant *pf17*. Addition of the

phosphatase inhibitor microcystin LR ("MC"), blocked kinase-dependent rescue of microtubule sliding in axonemes from *pf17* (Fig. 4.1 A,B). These kinase inhibitors PKI and DRB also restored the velocity of microtubule sliding in axonemes from *pf4* (Fig. 5 A, B). Moreover, addition of microcystin LR failed to block rescue of the velocity of kinase-dependent microtubule sliding in axonemes from *pf4*.

The simplest interpretation of this result is that there must be a separate phospho-regulatory pathway in the axoneme that does not require PP2A and is not sensitive to microcystin-LR. This alternative pathway is revealed in axonemes from *pf4* that fully assemble the central pair, radial spokes and I1 dynein but fail to assemble PP2A. Thus, we predict, this pathways requires another, yet to be identified axonemal protein phosphatase, and that the phosphatase is not sensitive to microcystin LR at the concentration used. The flagellar proteome and previous biochemical studies have revealed the axoneme contains other phosphatases, including PP1, that are candidates (Pazour et al., 2005; Yang et al., 2000). However, due to its sensitivity to microcystin LR and its apparent primary localization in the central pair apparatus (Yang et al., 2000), it seems PP1 is not the most likely candidate. Furthermore, the regulatory pathway may impinge on control of dyneins other than I1 dynein including the outer dynein arm. This idea may be testable by functional analysis of double mutants in *pf4* and mutants defective in assembly selected subsets of axonemal dyneins.

Fig. 4

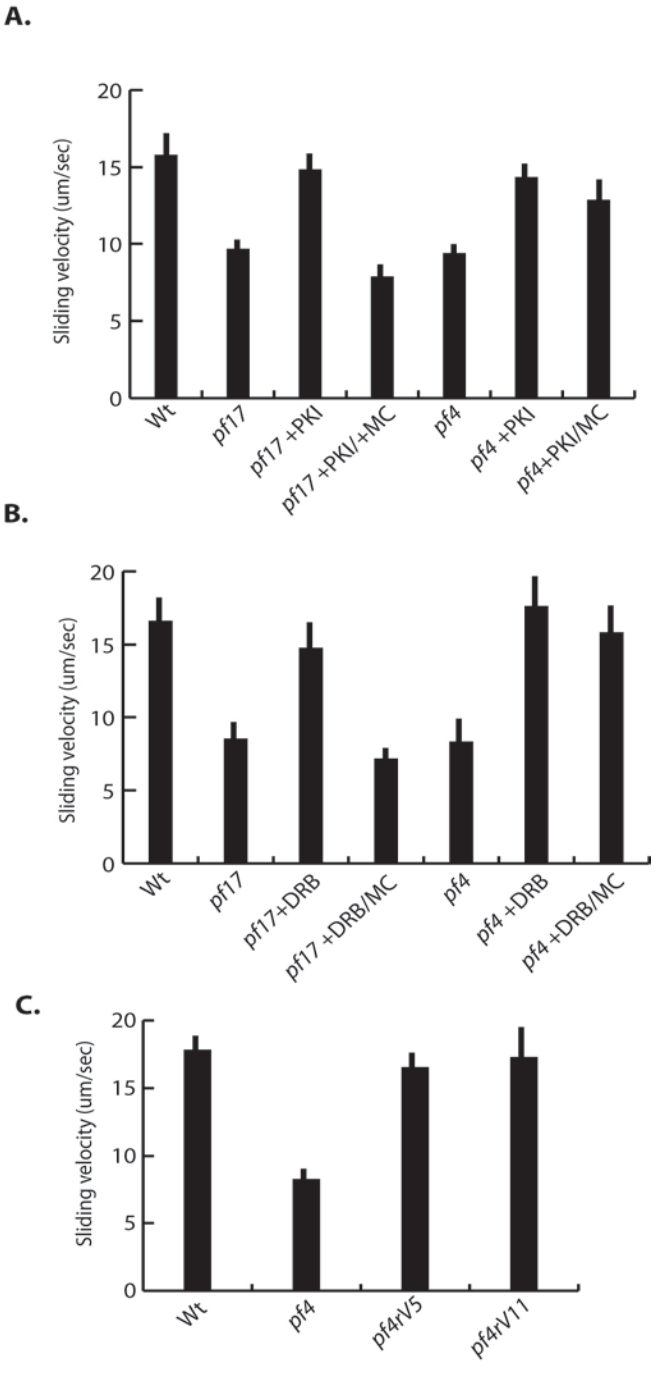
A.
Sliding velocity (um/sec)
20
15
10
5
0
Wt
pf17
pf17 +PKI
pf17 +PKI/+MC
pf4
pf4 +PKI
pf4+PKI/MC
B.
Sliding velocity (um/sec)
20
15
10
5
0
Wt
pf17
pf17+DRB
pf17 +DRB/MC
pf4
pf4 +DRB
pf4 +DRB/MC
C.
Sliding velocity (um/sec)
20
15
10
5
0
Wt
pf4
pf4rV5
pf4rV11

Figure 4.1 Microtubule sliding in *pf4* axonemes reveals other, non-PP2A axonemal, MC-insensitive phosphatases. Isolated axonemes from wild-type, *pf17* and *pf4* were treated with protease and ATP. The velocities of microtubule sliding were measured during axoneme disintegration *in vitro*. A) Axonemes were treated with 100nM PKI or a mixture of PKI and 2 µM Microscystin-LR (MC). Notably, PKI restored sliding in *pf4* axonemes. ; B)Axonemes were treated with 50µM DRB or a mixture of DRB and MC. DRB also restored sliding in *pf4* axonemes. C) Revertant cell, *pf4rV5* and *pf4rV1* display Wt sliding velocities. An average N= 25 for each cell type or treatment .

Chapter 5: Materials and Methods

Strains, genetic analyses and culture conditions:

Chlamydomonas reinhardtii strains used include CC124 (wild-type), *pf4-* (CC-880), *pf4+* (CC-1027) from the *Chlamydomonas* Genetics Center (Univ. of MN, St. Paul, MN), *pf4 9-1* (recovered from a parental tetrad between wild type and *pf4* crosses), *pf4rV5* and *pf4rV11* (recovered from non-parental tetrad, see below). All experiments utilized the backcrossed progeny *pf4 9-1*.

Backcrosses and tetrad dissection were performed as described (Dutcher, 1995). Cells harboring the *pf4* mutation are palmelloid, which is a phenotype often displayed in mutants with short flagella or a slow-swimming phenotype. Suppressors of *pf4* were generated by treating *pf4* cells with a UV light dose of 700 $\mu J/cm^2$ and selecting for cells that hatched. In addition to the two intragenic revertants described here, several extragenic suppressor mutations were isolated and will be characterized elsewhere.

Hatching of the palmelloid cells was promoted by resuspending *pf4* cells in water or gametic autolysin for 1-2 hours. Cells were grown in Sager's minimal media (L- media) with aeration on a 14:10 hr light: dark cycle.

Molecular Biology. A restriction fragment containing the first 134 amino acids of the B-subunit was cloned into the pET28A vector (EMD) using *Bam*HI and *Xho*I to create pCEBsub134 and protein expression induced with 1mM IPTG. The expressed fusion protein was purified using a metal affinity resin (Clontech, Mountain View, CA) and used as an antigen for production of a B-subunit antibody (Spring Valley Labs, Inc, Woodline, MD). B-subunit antibodies were blot purified using the fusion protein and

specific antibodies eluted using 100 mM citric acid pH 3.0 followed by neutralization with 100 mM Tris pH 9.0.

Genomic DNA was isolated from CC125, *pf4 9-1*, *pf4rV5* and *pf4rV11* cells. All primers were designed using Primer3 program (http://frodo.wi.mit.edu/primer3/). Clones with inserts were sequenced (Iowa State DNA Sequencing Facility (http://www.dna.iastate.edu/) and analyzed using DNAstar Megalign (Lasergene). Overlapping PCR primers (PR55 #1-7) were developed to sequence the entire PP2A B-subunit gene (JGI V4 scaffold 23, gene model 185509). Each PCR reaction was performed using Hot Star Taq DNA polymerase kit (Qiagen). PCR products were resolved on 1% agarose gels, and screened for the appropriate sized band. Appropriate sized bands were gel purified and cloned into the TOPO PCR 2.1 vector and colonies were selected following the manufacturer's instructions (Invitrogen).

Primers (PF4-1F,cct tgt ggg aac cca gtg; PF4-1R,gaa tgt gat gtc gct gat gc) were developed to sequence the *B-subunit* gene region (base pairs 2106-2280) containing the *pf4* mutation (JGI V4 scaffold 23, gene model 185509). The 175-bp PCR product was gel purified and digested with the restriction enzyme *CviKi-1* (New England BioLabs, Inc.). The digested product was resolved on a 2% agarose gel stained with ethidium bromide. Gel images were acquired with an Alpha Innotech Corporation gel imager using 3D filter settings.

Flagella Isolation.

Flagella were isolated from three liters of cells as described (Witman, 1986) and resuspended in Na-low buffer (30mM HEPES, pH 7.4; 5mM $MgSO4 \cdot 7H_20$; 1mM DTT; 0.5mM EDTA; 30Mm NaCl; 1mM PMSF; 0.6 trypsin inhibitory unit [TIU] Aprotinin).

NP-40 was added to a final concentration of 1% and axonemes and detergent soluble membrane-matrix fractions separated by centrifugation. To extract the PP2A B-subunit, axonemes were extracted with 0.6 M NaCl for 30 min and the salt-soluble protein and extracted axonemes separated by centrifugation. Samples from each step were saved for SDS-PAGE analysis.

Antibody preparation

The first 134 amino acids of the PP2A B-subunit was cloned into the pET28A vector (EMD) using the restriction enzymes BamHI and XhoI. The resulting construct pCEBsub134 was used to transform BL21-Gold (DE3) pLysS competent cells (Agilent Technologies). Protein expression was induced using 1mM IPTG. The subsequent His-tagged protein was purified using the Talon cobalt metal affinity resin (Clontech Laboratories, Inc.). Purified protein was used as an antigen to inoculate rabbits for poly-clonal antibody production (Spring Valley Laboratories, Inc.) Rabbits were chosen after pre-screening. The strategy for antibody production and selection of rabbits is illustrated in figure 2.9. Briefly, axonemal proteins were prepared for immunoblot analysis, as previously described, and incubated with serum from candidate non-immunized rabbits diluted 1:500. Some of the candidate rabbits showed cross-reactivity with axonemal proteins and were not selected. Only rabbits that showed little to no cross-reactivity were chosen to be immunized with the PP2A antigen (rabbit #5 , Fig. 2.9).

The PP2A antibodies were subsequently blot affinity purified using the pCEBsub His-tagged protein product used to make the antibody. The PP2A fusion protein was run on a 10% SDS PAGE gels and ponceau stained to identify the protein. The strip was cut out,

blocked with 5% nonfat dry milk in TBS, pH 7.4 and incubated overnight at 4°C with the whole sera in the 5% milk/TBS. The antibody was eluted from the strip by incubation in 100mM Citric acid, pH 3.0 for 5 minutes at room temperature and neutralized with 1.0M Tris, pH 9.0. The purified antibody was then used at 1:50 on immuno-blots and stored at 4°C.

SDS-PAGE and immuno-blot analysis.

Axonemal protein samples were separated by SDS-PAGE and either stained by Coomassie blue or transferred to a nitrocellulose membrane (Bio-Rad, Hercules, CA) for immunoblot analysis. The membrane was blocked with 5% nonfat dry milk in TBS followed by incubation with primary antibodies (anti-PP2A serum diluted 1:10,000 or affinity purified antibodies diluted as cited above), then HRP-conjugated goat anti-rabbit secondary antibodies (1:10,000, Bio-Rad). The antibody reactivity was detected with the Pierce Western ECL blotting substrate (Thermo Scientific, Waltham, MA).

For analysis of the fractionation, equivalent sample loads of each flagellar fraction were loaded and probed using the affinity purified PP2A B-subunit antibody (1:50) and the C-subunit antibody, 1D6 that recognizes de-methylated C-subunits (1:200, Upstate, Lake Placid, N.Y.) Immunoblots to verify the assembly of the I1, outer arm dynein and other axonemal structures were probed with the following antibodies: IC140 (1:10,000), IC138 (1:10,000), IC97 (1:10,000), FAP120 (1:1000), RSP3 (1:1000), LC8 (1:50), IC1 (1:1000), actin (1:100) and p28 (1:250). For analysis of IC138 phosphorylation, axonemes were treated with calf intestinal phosphatase (CIP) as described (Hendrickson et al., 2004) or buffer alone and resolved on 5% gels and analyzed by immunoblots using the IC138 antibody.

Motility analyses.

Swimming velocity measurements were determined as described (Elam et al., 2009). Briefly, cells were placed on a microscope perfusion chamber and visualized using a 10X Plan-Apochromat lens (Carl Zeiss, Inc.) and a darkfield condenser using an Axiovert 35 inverted light microscope (Carl Zeiss, Inc.). Cells were recorded using a silicon intensified camera (VE-1000; Dage-MTI) and converted to a digital format using Labview 7.1 software (National Instruments). Swimming velocity was calculated using manual tracings of twenty cells for each strain and the swimming velocity shown is the average of three independent experiments.

Photo-accumulation assays were performed as follows: cells (2.5×10^6 cells/ml in 35 mm petri dishes) were dark adapted for 10 min, then exposed to either ambient or fluorescent light located 30 cm away (2 W/m^2) with the same photo-accumulation results. Dishes were photographed after 5 min to determine relative photo-accumulation ability.

Electron Microscopy.

Electron microscopy samples were prepared as described previously by Mitchell and Sale, 1999. Briefly, pelleted axonemes were fixed in 1% tannic acid, pH 7.0 , 1% glutaraldehyde (Ted Pella, Redding, CA); and 0.1 M NaCacodylate for 1hr at room temperature. The buffer was aspirated and fixative #2 (1% glutaraldehyde and 0.1M NaCacodylate) was added for overnight fixation at 4°C. Fixed samples were washed with 0.1 M NaCacodylate, followed by fixation in 1% osmium tetroxide (Ted Pella) and 0.1 M NaCacodylate for 30 min. at room temperature. The fixed samples were washed using 0.1 M Na-cacodylate followed dehydration using sequential washes of 50, 70, 90, 95, and 100% ethanol. Fixed axonemes were mixed with a solution of 1:1 100% ethanol:

propylene oxide for 10min at room temperature. The ethanol: propylene oxide mixture was removed and samples were mixed with 1:1 solution of epoxy embedding medium (Eponate 12 with BDMA; Ted Pella) and propylene oxide overnight at 23°C, with gentle mixing. Axonemal pellets were transferred to molds containing fresh epoxy embedding medium and were baked at 60°C for 48 h. Embedded axonemes were thin sectioned and stained with lead citrate and uranyl acetate. Thin-sectioned axonemes were viewed using a Hitachi H-7500 Transmission Electron Microscope. Images were acquired using a Gatan 792 BioScan CCD camera (Gatan Digital Micrograph) and adjustments were made using Adobe Photoshop (Adobe Systems, Mountain View, CA).

Microtubule Sliding Assays

Microtubule sliding velocities were measured using the method of Okagaki and Kamiya (Okagaki and Kamiya, 1986), and as previously described (Howard *et al.*, 1994; Habermacher and Sale, 1996, 1997; Hendrickson *et al.*, 2004; Bower *et al.*, 2009; Gokhale *et al.*, 2009; Wirschell *et al.*, 2009). Briefly, isolated flagella were resuspended in buffer without protease inhibitors, demembranated with buffer containing 0.5% Nonidet-P-40 in 10 mM Hepes, pH 7.4, 5 mM $MgSO_4$, 1 mM DTT, 0.5 mM EDTA, 1% polyethylene glycol (20,000 MW), 25 mM potassium acetate. The axonemes were added to a perfusion chamber, and microtubule sliding was initiated by the addition of buffer containing 1 mM ATP and 5 μg/ml subtilisin A Type VIII protease (Sigma Aldrich, St. Louis, MO). For inhibition studies, PKI (100nM) , DRB (50 μM), or a mixture of DRB or PKI and MC (2 μM) was introduced to the perfusion chamber, and sliding was then initiated with 1 mM ATP and subtilisin (5 μg/ml) Sliding was recorded using a Zeiss Axiovert 35 microscope equipped with dark field optics, 40X Plan-Apo lens (Zeiss) and a

silicon intensified camera (VE-1000, Dage-MTI, Michigan City, IN). The video images were converted to a digital format using Labview 7.1 software (National Instruments, Austin, TX), and sliding velocity was determined manually by measuring microtubule displacement on tracings calibrated with a micrometer.

References:

Alonso, A., J. Sasin, N. Bottini, I. Friedberg, A. Osterman, A. Godzik, T. Hunter, J. Dixon, and T. Mustelin. 2004. Protein tyrosine phosphatases in the human genome. *Cell*. 117:699-711.

Basu, B., and M. Brueckner. 2008. Cilia multifunctional organelles at the center of vertebrate left-right asymmetry. *Curr Top Dev Biol*. 85:151-174.

Bayly, P.V., B.L. Lewis, P.S. Kemp, R.B. Pless, and S.K. Dutcher. 2010. Efficient spatiotemporal analysis of the flagellar waveform of Chlamydomonas reinhardtii. *Cytoskeleton (Hoboken)*. 67:56-69.

Beene, D.L., and J.D. Scott. 2007. A-kinase anchoring proteins take shape. *Curr Opin Cell Biol*. 19:192-198.

Bennecib, M., C.X. Gong, I. Grundke-Iqbal, and K. Iqbal. 2000. Role of protein phosphatase-2A and -1 in the regulation of GSK-3, cdk5 and cdc2 and the phosphorylation of tau in rat forebrain. *FEBS Lett*. 485:87-93.

Berbari, N.F., A.K. O'Connor, C.J. Haycraft, and B.K. Yoder. 2009. The primary cilium as a complex signaling center. *Curr Biol*. 19:R526-535.

Bloodgood, R.A. 2010. Sensory reception is an attribute of both primary cilia and motile cilia. *J Cell Sci*. 123:505-509.

Boesger, J., V. Wagner, W. Weisheit, and M. Mittag. 2009. Analysis of flagellar phosphoproteins from Chlamydomonas reinhardtii. *Eukaryot Cell*. 8:922-932.

Bonini, N.M., and D.L. Nelson. 1988. Differential regulation of Paramecium ciliary motility by cAMP and cGMP. *J Cell Biol*. 106:1615-1623.

Bower, R., K. VanderWaal, E. O'Toole, L. Fox, C. Perrone, J. Mueller, M. Wirschell, R. Kamiya, W.S. Sale, and M.E. Porter. 2009. IC138 defines a subdomain at the base of the I1 dynein that regulates microtubule sliding and flagellar motility. *Mol Biol Cell*. 20:3055-3063.

Broadhead, R., H.R. Dawe, H. Farr, S. Griffiths, S.R. Hart, N. Portman, M.K. Shaw, M.L. Ginger, S.J. Gaskell, P.G. McKean, and K. Gull. 2006. Flagellar motility is required for the viability of the bloodstream trypanosome. *Nature*. 440:224-227.

Brokaw, C.J. 1991. Microtubule sliding in swimming sperm flagella: direct and indirect measurements on sea urchin and tunicate spermatozoa. *J Cell Biol*. 114:1201-1215.

Brokaw, C.J. 1994. Control of flagellar bending: a new agenda based on dynein diversity. *Cell Motil Cytoskeleton*. 28:199-204.

Brokaw, C.J., and R. Kamiya. 1987. Bending patterns of Chlamydomonas flagella: IV. Mutants with defects in inner and outer dynein arms indicate differences in dynein arm function. *Cell Motil Cytoskeleton*. 8:68-75.

Brokaw, C.J., and D.J. Luck. 1983. Bending patterns of chlamydomonas flagella I. Wild-type bending patterns. *Cell Motil*. 3:131-150.

Brokaw, C.J., D.J. Luck, and B. Huang. 1982. Analysis of the movement of Chlamydomonas flagella:" the function of the radial-spoke system is revealed by comparison of wild-type and mutant flagella. *J Cell Biol*. 92:722-732.

Bui, K.H., G. Pigino, and T. Ishikawa. 2011. Three-dimensional structural analysis of eukaryotic flagella/cilia by electron cryo-tomography. *J Synchrotron Radiat*. 18:2-5.

Bui, K.H., H. Sakakibara, T. Movassagh, K. Oiwa, and T. Ishikawa. 2008. Molecular architecture of inner dynein arms in situ in Chlamydomonas reinhardtii flagella. *J Cell Biol*. 183:923-932.

Bui, K.H., H. Sakakibara, T. Movassagh, K. Oiwa, and T. Ishikawa. 2009. Asymmetry of inner dynein arms and inter-doublet links in Chlamydomonas flagella. *J Cell Biol*. 186:437-446.

Carter, A.P., C. Cho, L. Jin, and R.D. Vale. 2011. Crystal structure of the dynein motor domain. *Science*. 331:1159-1165.

Casey, D.M., K. Inaba, G.J. Pazour, S. Takada, K. Wakabayashi, C.G. Wilkerson, R. Kamiya, and G.B. Witman. 2003. DC3, the 21-kDa subunit of the outer dynein arm-docking complex (ODA-DC), is a novel EF-hand protein important for assembly of both the outer arm and the ODA-DC. *Mol Biol Cell*. 14:3650-3663.

Caspary, T., C.E. Larkins and K.V. Anderson. 2007. The graded response to Sonic Hedgehog depends on cilia architecture. *Dev. Cell* 12: 767-778

Cohen, P.T. 1997. Novel protein serine/threonine phosphatases: variety is the spice of life. *Trends Biochem Sci*. 22:245-251.

Craige, B., C.C. Tsao, D.R. Diener, Y. Hou, K.F. Lechtreck, J.L. Rosenbaum, and G.B. Witman. 2010. CEP290 tethers flagellar transition zone microtubules to the membrane and regulates flagellar protein content. *J Cell Biol*. 190:927-940.

De Baere, I., R. Derua, V. Janssens, C. Van Hoof, E. Waelkens, W. Merlevede, and J. Goris. 1999. Purification of porcine brain protein phosphatase 2A leucine carboxyl methyltransferase and cloning of the human homologue. *Biochemistry*. 38:16539-16547.

DiBella, L.M., and S.M. King. 2001. Dynein motors of the Chlamydomonas flagellum. *Int Rev Cytol*. 210:227-268.

DiBella, L.M., M. Sakato, R.S. Patel-King, G.J. Pazour, and S.M. King. 2004a. The LC7 light chains of Chlamydomonas flagellar dyneins interact with components required for both motor assembly and regulation. *Mol Biol Cell*. 15:4633-4646.

DiBella, L.M., E.F. Smith, R.S. Patel-King, K. Wakabayashi, and S.M. King. 2004b. A novel Tctex2-related light chain is required for stability of inner dynein arm I1 and motor function in the Chlamydomonas flagellum. *J Biol Chem*. 279:21666-21676.

DiPetrillo, C.G., and E.F. Smith. 2010. Pcdp1 is a central apparatus protein that binds Ca(2+)-calmodulin and regulates ciliary motility. *J Cell Biol*. 189:601-612.

Dunahay, T.G. 1993. Transformation of Chlamydomonas reinhardtii with silicon carbide whiskers. *Biotechniques*. 15:452-455, 457-458, 460.

Dutcher, S.K. W. Gibbons and W. Inwood. 1988. A genetic analysis of supporessors of the PF10 mutation. *Genetics* 120: 965-976.

Dutcher, S.K. 1995. Mating and tetrad analysis in Chlamydomonas reinhardtii. *Methods Cell Biol*. 47:531-540.

Dutcher, S.K. 2003. Elucidation of basal body and centriole functions in Chlamydomonas reinhardtii. *Traffic*. 4:443-451.

Dymek, E.E., P.A. Lefebvre, and E.F. Smith. 2004. PF15p is the chlamydomonas homologue of the Katanin p80 subunit and is required for assembly of flagellar central microtubules. *Eukaryot Cell*. 3:870-879.

Ebersold, W.T. 1967. Chlamydomonas reinhardi: heterozygous diploid strains. *Science*. 157:447-449.

Ebersold, W.T., R.P. Levine and M. Olmsted. 1962. Linkage maps in Chlamy. *Genetics* 47: 531-543.

Elam, C., M. Wirschell, R. Yamamoto, L.A. Fox, R. Kamiya, S. Dutcher, and W.S. Sale. 2011. An axonemal B-subunit is required for PP2A localization and flagellar motility. *Cytoskeleton*. manuscript submitted.

Elam, C.A., W.S. Sale, and M. Wirschell. 2009. The Regulation of Dynein-Driven Microtubule Sliding in Chlamydomonas Flagella by Axonemal Kinases and Phosphatases. *In* Methods in Cell Biology. Vol. Volume 92. M.K. Stephen and J.P. Gregory, editors. Academic Press. 133-151.

Emmer, B.T., D. Maric and D. Engman. 2010. Protein and lipid targeting to ciliary membranes. *J. Cell Sci.* 123: 529-536.

Feistel, K., and M. Blum. 2006. Three types of cilia including a novel 9+4 axoneme on the notochordal plate of the rabbit embryo. *Dev Dyn*. 235:3348-3358.

Flegg, C.P., M. Sharma, C. Medina-Palazon, C. Jamieson, M. Galea, M.G. Brocardo, K. Mills, and B.R. Henderson. 2010. Nuclear export and centrosome targeting of the protein phosphatase 2A subunit B56alpha: role of B56alpha in nuclear export of the catalytic subunit. *J Biol Chem*. 285:18144-18154.

Fox, L.A., and W.S. Sale. 1987. Direction of force generated by the inner row of dynein arms on flagellar microtubules. *J Cell Biol*. 105:1781-1787.

Gaillard, A.R., D.R. Diener, J.L. Rosenbaum, and W.S. Sale. 2001. Flagellar radial spoke protein 3 is an A-kinase anchoring protein (AKAP). *J Cell Biol*. 153:443-448.

Gaillard, A.R., L.A. Fox, J.M. Rhea, B. Craige, and W.S. Sale. 2006. Disruption of the A-kinase anchoring domain in flagellar radial spoke protein 3 results in unregulated axonemal cAMP-dependent protein kinase activity and abnormal flagellar motility. *Mol Biol Cell*. 17:2626-2635.

Gerdes, J.M., E.E. Davis, and N. Katsanis. 2009. The vertebrate primary cilium in development, homeostasis, and disease. *Cell*. 137:32-45.

Gibbons, B.H., and I.R. Gibbons. 1972. Flagellar movement and adenosine triphosphatase activity in sea urchin sperm extracted with triton X-100. *J Cell Biol*. 54:75-97.

Gibbons, I.R. and A.J. Rowe. 1965. Dynein: a protein with ATPase activity in cilia. *Science* 149: 424-426.

Goedert, M., E.S. Cohen, R. Jakes, and P. Cohen. 1992. p42 MAP kinase phosphorylation sites in microtubule-associated protein tau are dephosphorylated by protein phosphatase 2A1. Implications for Alzheimer's disease [corrected]. *FEBS Lett*. 312:95-99.

Goedert, M., R. Jakes, Z. Qi, J.H. Wang, and P. Cohen. 1995. Protein phosphatase 2A is the major enzyme in brain that dephosphorylates tau protein phosphorylated by proline-directed protein kinases or cyclic AMP-dependent protein kinase. *J Neurochem*. 65:2804-2807.

Goedert, M., and M.G. Spillantini. 2006. A century of Alzheimer's disease. *Science*. 314:777-781.

Goetz, S.C., and K.V. Anderson. 2010. The primary cilium: a signalling centre during vertebrate development. *Nat Rev Genet*. 11:331-344.

Gokhale, A., M. Wirschell, and W.S. Sale. 2009. Regulation of dynein-driven microtubule sliding by the axonemal protein kinase CK1 in Chlamydomonas flagella. *J Cell Biol*. 186:817-824.

Gong, C.X., I. Grundke-Iqbal, and K. Iqbal. 1994. Dephosphorylation of Alzheimer's disease abnormally phosphorylated tau by protein phosphatase-2A. *Neuroscience*. 61:765-772.

Gong, C.X., T. Lidsky, J. Wegiel, L. Zuck, I. Grundke-Iqbal, and K. Iqbal. 2000. Phosphorylation of microtubule-associated protein tau is regulated by protein phosphatase 2A in mammalian brain. Implications for neurofibrillary degeneration in Alzheimer's disease. *J Biol Chem*. 275:5535-5544.

Goodenough, U.W., and J.E. Heuser. 1985a. Outer and inner dynein arms of cilia and flagella. *Cell*. 41:341-342.

Goodenough, U.W., and J.E. Heuser. 1985b. Substructure of inner dynein arms, radial spokes, and the central pair/projection complex of cilia and flagella. *J Cell Biol*. 100:2008-2018.

Gotz, J., and R.M. Nitsch. 2001. Compartmentalized tau hyperphosphorylation and increased levels of kinases in transgenic mice. *Neuroreport*. 12:2007-2016.

Green, J. A. and K. Mykytyn. 2010. Neuronal ciliary signaling in hoeostasis and disease. *Cell. Mol. Life Sci*. 67: 3287-3297.

Grossman, A.R., E.E. Harris, C. Hauser, P.A. Lefebvre, D. Martinez, D. Rokhsar, J. Shrager, C.D. Silflow, D. Stern, O. Vallon, and Z. Zhang. 2003. Chlamydomonas reinhardtii at the crossroads of genomics. *Eukaryot Cell*. 2:1137-1150.

Gulledgea, B.M., J.B. Aggena, H.B. Huangb, A.C. Nairnc, and A.R. Chamberlin. 2002. The microcystins and nodularins: cyclic polypeptide inhibitors of PP1 and PP2A. *Curr Med Chem*. 9:1991-2003.

Habermacher, G., and W.S. Sale. 1996. Regulation of flagellar dynein by an axonemal type-1 phosphatase in Chlamydomonas. *J Cell Sci*. 109 (Pt 7):1899-1907.

Habermacher, G., and W.S. Sale. 1997. Regulation of flagellar dynein by phosphorylation of a 138-kD inner arm dynein intermediate chain. *J Cell Biol*. 136:167-176.

Hamasaki, T., T.J. Murtaugh, B.H. Satir, and P. Satir. 1989. In vitro phosphorylation of Paramecium axonemes and permeabilized cells. *Cell Motil Cytoskeleton*. 12:1-11.

Harris, E. 2009. Chlamydomonas in the Laboratory. *In* The Chlamydomonas Sourcebook. Vol. 1. E. Harris, editor. Academic Press, Kidlington, Oxford. 241-301.

Harrison, A., and S.M. King. 2000. The molecular anatomy of dynein. *Essays Biochem*. 35:75-87.

Hasegawa, E., H. Hayashi, S. Asakura, and R. Kamiya. 1987. Stimulation of in vitro motility of Chlamydomonas axonemes by inhibition of cAMP-dependent phosphorylation. *Cell Motil Cytoskeleton*. 8:302-311.

Hatano, Y., H. Shima, T. Haneji, A.B. Miura, T. Sugimura, and M. Nagao. 1993. Expression of PP2A B regulatory subunit beta isotype in rat testis. *FEBS Lett*. 324:71-75.

Hayashi, S., and C. Shingyoji. 2009. Bending-induced switching of dynein activity in elastase-treated axonemes of sea urchin sperm--roles of Ca2+ and ADP. *Cell Motil Cytoskeleton*. 66:292-301.

Hayashibe, K., C. Shingyoji, and R. Kamiya. 1997. Induction of temporary beating in paralyzed flagella of Chlamydomonas mutants by application of external force. *Cell Motil Cytoskeleton*. 37:232-239.

Hendrickson, T.W., C.A. Perrone, P. Griffin, K. Wuichet, J. Mueller, P. Yang, M.E. Porter, and W.S. Sale. 2004. IC138 is a WD-repeat dynein intermediate chain required for light chain assembly and regulation of flagellar bending. *Mol Biol Cell*. 15:5431-5442.

Heuser, T., M. Raytchev, J. Krell, M.E. Porter, and D. Nicastro. 2009. The dynein regulatory complex is the nexin link and a major regulatory node in cilia and flagella. *J Cell Biol*. 187:921-933.

Hiraki, M., Y. Nakazawa, R. Kamiya, and M. Hirono. 2007. Bld10p constitutes the cartwheel-spoke tip and stabilizes the 9-fold symmetry of the centriole. *Curr Biol*. 17:1778-1783.

Hirokawa, N., Y. Tanaka, Y. Okada, and S. Takeda. 2006. Nodal flow and the generation of left-right asymmetry. *Cell*. 125:33-45.

Hochstrasser, M., G.L. Carlson, C.E. Walczak, and D.L. Nelson. 1996. Paramecium has two regulatory subunits of cyclic AMP-dependent protein kinase, one unique to cilia. *J Eukaryot Microbiol*. 43:356-362.

Howard, D.R., G. Habermacher, D.B. Glass, E.F. Smith, and W.S. Sale. 1994. Regulation of Chlamydomonas flagellar dynein by an axonemal protein kinase. *J Cell Biol*. 127:1683-1692.

Hu, Q., L. Milenkovic, H. Jin, M.P. Scott, M.V. Nachury, E.T. Spiliotis, and W.J. Nelson. 2010. A septin diffusion barrier at the base of the primary cilium maintains ciliary membrane protein distribution. *Science*. 329:436-439.

Ikeda, K., R. Yamamoto, M. Wirschell, T. Yagi, R. Bower, M.E. Porter, W.S. Sale, and R. Kamiya. 2009. A novel ankyrin-repeat protein interacts with the regulatory proteins of inner arm dynein f (I1) of Chlamydomonas reinhardtii. *Cell Motil Cytoskeleton*. 66:448-456.

Ikehara, T., S. Ikehara, S. Imamura, F. Shinjo, and T. Yasumoto. 2007. Methylation of the C-terminal leucine residue of the PP2A catalytic subunit is unnecessary for the catalytic activity and the binding of regulatory subunit (PR55/B). *Biochem Biophys Res Commun*. 354:1052-1057.

Insinna, C., and J.C. Besharse. 2008. Intraflagellar transport and the sensory outer segment of vertebrate photoreceptors. *Dev Dyn*. 237:1982-1992.

Janssens, V., and J. Goris. 2001. Protein phosphatase 2A: a highly regulated family of serine/threonine phosphatases implicated in cell growth and signalling. *Biochem J*. 353:417-439.

Jin, H., S.R. White, T. Shida, S. Schulz, M. Aguiar, S.P. Gygi, J.F. Bazan, and M.V. Nachury. 2010. The conserved Bardet-Biedl syndrome proteins assemble a coat that traffics membrane proteins to cilia. *Cell*. 141:1208-1219.

Johnson, S.A., and T. Hunter. 2005. Kinomics: methods for deciphering the kinome. *Nat Methods*. 2:17-25.

Kagami, O., and R. Kamiya. 1992. Translocation and rotation of microtubules caused by multiple species of Chlamydomonas inner-arm dynein. *J Cell Sci*. 103:653-664.

Kamiya, R. 2002. Functional diversity of axonemal dyneins as studied in Chlamydomonas mutants. *Int Rev Cytol*. 219:115-155.

Kamiya, R., E. Kurimoto, and E. Muto. 1991. Two types of Chlamydomonas flagellar mutants missing different components of inner-arm dynein. *J Cell Biol*. 112:441-447.

Kindle, K.L. 1990. High-frequency nuclear transformation of Chlamydomonas reinhardtii. *Proc Natl Acad Sci U S A*. 87:1228-1232.

Kindle, K.L., R.A. Schnell, E. Fernandez, and P.A. Lefebvre. 1989. Stable nuclear transformation of Chlamydomonas using the Chlamydomonas gene for nitrate reductase. *J Cell Biol*. 109:2589-2601.

King, S.J., and S.K. Dutcher. 1997. Phosphoregulation of an inner dynein arm complex in Chlamydomonas reinhardtii is altered in phototactic mutant strains. *J Cell Biol*. 136:177-191.

King, S.M. 2000. The dynein microtubule motor. *Biochim Biophys Acta*. 1496:60-75.

King, S.M. 2003. Organization and regulation of the dynein microtubule motor. *Cell Biol Int*. 27:213-215.

King, S.M., and R. Kamiya. 2009. Axonemal dyneins: Assembly, Structure, and Force Generation. *In* The Chlamydomonas Sourcebook. Vol. 3. G.B. Witman, editor. Academic Press, Kidlington, Oxford. 131-208.

Kins, S., A. Crameri, D.R. Evans, B.A. Hemmings, R.M. Nitsch, and J. Gotz. 2001. Reduced protein phosphatase 2A activity induces hyperphosphorylation and altered compartmentalization of tau in transgenic mice. *J Biol Chem*. 276:38193-38200.

Koutoulis, A., G.J. Pazour, C.G. Wilkerson, K. Inaba, H. Sheng, S. Takada, and G.B. Witman. 1997. The Chlamydomonas reinhardtii ODA3 gene encodes a protein of the outer dynein arm docking complex. *J Cell Biol*. 137:1069-1080.

Kultgen, P.L., S.K. Byrd, L.E. Ostrowski, and S.L. Milgram. 2002. Characterization of an A-kinase anchoring protein in human ciliary axonemes. *Mol Biol Cell*. 13:4156-4166.

Lander, E.S., L.M. Linton, B. Birren, C. Nusbaum, M.C. Zody, J. Baldwin, K. Devon, K. Dewar, M. Doyle, W. FitzHugh, R. Funke, D. Gage, K. Harris, A. Heaford, J. Howland, L. Kann, J. Lehoczky, R. LeVine, P. McEwan, K. McKernan, J. Meldrim, J.P. Mesirov, C. Miranda, W. Morris, J. Naylor, C. Raymond, M. Rosetti, R. Santos, A. Sheridan, C. Sougnez, N. Stange-Thomann, N. Stojanovic, A. Subramanian, D. Wyman, J. Rogers, J. Sulston, R. Ainscough, S. Beck, D. Bentley, J. Burton, C. Clee, N. Carter, A. Coulson, R. Deadman, P. Deloukas, A. Dunham, I. Dunham, R. Durbin, L. French, D. Grafham, S. Gregory, T. Hubbard, S. Humphray, A. Hunt, M. Jones, C. Lloyd, A. McMurray, L. Matthews, S. Mercer, S. Milne, J.C. Mullikin, A. Mungall, R. Plumb, M. Ross, R. Shownkeen, S. Sims, R.H. Waterston, R.K. Wilson, L.W. Hillier, J.D. McPherson, M.A. Marra, E.R. Mardis, L.A. Fulton, A.T. Chinwalla, K.H. Pepin, W.R. Gish, S.L. Chissoe, M.C. Wendl, K.D. Delehaunty, T.L. Miner, A. Delehaunty, J.B. Kramer,

L.L. Cook, R.S. Fulton, D.L. Johnson, P.J. Minx, S.W. Clifton, T. Hawkins, E. Branscomb, P. Predki, P. Richardson, S. Wenning, T. Slezak, N. Doggett, J.F. Cheng, A. Olsen, S. Lucas, C. Elkin, E. Uberbacher, M. Frazier, et al. 2001. Initial sequencing and analysis of the human genome. *Nature*. 409:860-921.

Lechtreck, K.F., P. Delmotte, M.L. Robinson, M.J. Sanderson, and G.B. Witman. 2008. Mutations in Hydin impair ciliary motility in mice. *J Cell Biol*. 180:633-643.

Lechtreck, K.F., and G.B. Witman. 2007. Chlamydomonas reinhardtii hydin is a central pair protein required for flagellar motility. *J Cell Biol*. 176:473-482.

Lechward, K., O.S. Awotunde, W. Swiatek, and G. Muszynska. 2001. Protein phosphatase 2A: variety of forms and diversity of functions. *Acta Biochim Pol*. 48:921-933.

Lee, J., Y. Chen, T. Tolstykh, and J. Stock. 1996. A specific protein carboxyl methylesterase that demethylates phosphoprotein phosphatase 2A in bovine brain. *Proc Natl Acad Sci U S A*. 93:6043-6047.

Lee, J. and J. Gleeson. 2011. Cilia in the nervous system: linking cilia and neurodevelomental disorders. *Curr Opin. Neourl.* 24: 98-105.

Lee, J., and J. Stock. 1993. Protein phosphatase 2A catalytic subunit is methyl-esterified at its carboxyl terminus by a novel methyltransferase. *J Biol Chem*. 268:19192-19195.

Lee, J.A., and D.C. Pallas. 2007. Leucine carboxyl methyltransferase-1 is necessary for normal progression through mitosis in mammalian cells. *J Biol Chem*. 282:30974-30984.

Lefebvre, P. and J. Rosenbaum. 1986. Regulation of assembly of flagella during regeneration. *Ann. Rev. Cell Biol.* 2: 517-546.

Leigh, M.W., J.E. Pittman, J.L. Carson, T.W. Ferkol, S.D. Dell, S.D. Davis, M.R. Knowles, and M.A. Zariwala. 2009a. Clinical and genetic aspects of primary ciliary dyskinesia/Kartagener syndrome. *Genet Med*. 11:473-487.

Leigh, M.W., M.A. Zariwala, and M.R. Knowles. 2009b. Primary ciliary dyskinesia: improving the diagnostic approach. *Curr Opin Pediatr*. 21:320-325.

Levine, R.P. and W.T. Eversold. 1960. Genetics of Chlamydomonas. *Ann. Rev. Micro.* 14: 197-216.

Levine, R.P., and U.W. Goodenough. 1970. The genetics of photosynthesis and the chloroplast in Chlamydomonas reinhardi. *Annu. Rev. Genet.* . 4:397-408.

Li, J.B., J.M. Gerdes, C.J. Haycraft, Y. Fan, T.M. Teslovich, H. May-Simera, H. Li, O.E. Blacque, L. Li, C.C. Leitch, R.A. Lewis, J.S. Green, P.S. Parfrey, M.R. Leroux, W.S. Davidson, P.L. Beales, L.M. Guay-Woodford, B.K. Yoder, G.D. Stormo, N. Katsanis, and S.K. Dutcher. 2004. Comparative genomics identifies a flagellar and basal body proteome that includes the BBS5 human disease gene. *Cell*. 117:541-552.

Lin, H., A.L. Kwan, and S.K. Dutcher. 2010. Synthesizing and salvaging NAD: lessons learned from Chlamydomonas reinhardtii. *PLoS Genet*. 6.

Linck, R.W., and R.E. Stephens. 2007. Functional protofilament numbering of ciliary, flagellar, and centriolar microtubules. *Cell Motil Cytoskeleton*. 64:489-495.

MacKintosh, C., K.A. Beattie, S. Klumpp, P. Cohen, and G.A. Codd. 1990. Cyanobacterial microcystin-LR is a potent and specific inhibitor of protein

phosphatases 1 and 2A from both mammals and higher plants. *FEBS Lett*. 264:187-192.

Marshall, W.F. 2008. Basal bodies platforms for building cilia. *Curr Top Dev Biol*. 85:1-22.

Matre, P., C. Meyer, and C. Lillo. 2009. Diversity in subcellular targeting of the PP2A B'eta subfamily members. *Planta*. 230:935-945.

Mayer, R.E., P. Hendrix, P. Cron, R. Matthies, S.R. Stone, J. Goris, W. Merlevede, J. Hofsteenge, and B.A. Hemmings. 1991. Structure of the 55-kDa regulatory subunit of protein phosphatase 2A: evidence for a neuronal-specific isoform. *Biochemistry*. 30:3589-3597.

McCright, B., A.M. Rivers, S. Audlin, and D.M. Virshup. 1996. The B56 family of protein phosphatase 2A (PP2A) regulatory subunits encodes differentiation-induced phosphoproteins that target PP2A to both nucleus and cytoplasm. *J Biol Chem*. 271:22081-22089.

McEwen, D.P., P.M. Jenkins, and J.R. Martens. 2008. Olfactory cilia: our direct neuronal connection to the external world. *Curr Top Dev Biol*. 85:333-370.

McGrath, J., S. Somlo, S. Makova and M. Brueckner. 2003. Two populations of node monocilia intiate left-right asymmetry in the mouse. *Cell* 114: 61-73.

McVittie, A. 1972. Flagellum mutants of Chlamydomonas reinhardii. *J Gen Microbiol*. 71:525-540.

Merchant, S.S., S.E. Prochnik, O. Vallon, E.H. Harris, S.J. Karpowicz, G.B. Witman, A. Terry, A. Salamov, L.K. Fritz-Laylin, L. Marechal-Drouard, W.F. Marshall, L.H. Qu, D.R. Nelson, A.A. Sanderfoot, M.H. Spalding, V.V. Kapitonov, Q. Ren, P.

Ferris, E. Lindquist, H. Shapiro, S.M. Lucas, J. Grimwood, J. Schmutz, P. Cardol, H. Cerutti, G. Chanfreau, C.L. Chen, V. Cognat, M.T. Croft, R. Dent, S. Dutcher, E. Fernandez, H. Fukuzawa, D. Gonzalez-Ballester, D. Gonzalez-Halphen, A. Hallmann, M. Hanikenne, M. Hippler, W. Inwood, K. Jabbari, M. Kalanon, R. Kuras, P.A. Lefebvre, S.D. Lemaire, A.V. Lobanov, M. Lohr, A. Manuell, I. Meier, L. Mets, M. Mittag, T. Mittelmeier, J.V. Moroney, J. Moseley, C. Napoli, A.M. Nedelcu, K. Niyogi, S.V. Novoselov, I.T. Paulsen, G. Pazour, S. Purton, J.P. Ral, D.M. Riano-Pachon, W. Riekhof, L. Rymarquis, M. Schroda, D. Stern, J. Umen, R. Willows, N. Wilson, S.L. Zimmer, J. Allmer, J. Balk, K. Bisova, C.J. Chen, M. Elias, K. Gendler, C. Hauser, M.R. Lamb, H. Ledford, J.C. Long, J. Minagawa, M.D. Page, J. Pan, W. Pootakham, S. Roje, A. Rose, E. Stahlberg, A.M. Terauchi, P. Yang, S. Ball, C. Bowler, C.L. Dieckmann, V.N. Gladyshev, P. Green, R. Jorgensen, S. Mayfield, B. Mueller-Roeber, S. Rajamani, R.T. Sayre, P. Brokstein, et al. 2007. The Chlamydomonas genome reveals the evolution of key animal and plant functions. *Science*. 318:245-250.

Michaud, E.J., and B.K. Yoder. 2006. The primary cilium in cell signaling and cancer. *Cancer Res*. 66:6463-6467.

Mitchell, D.R., and W.S. Sale. 1999. Characterization of a Chlamydomonas insertional mutant that disrupts flagellar central pair microtubule-associated structures. *J Cell Biol*. 144:293-304.

Morita, Y., and C. Shingyoji. 2004. Effects of imposed bending on microtubule sliding in sperm flagella. *Curr Biol*. 14:2113-2118.

Moyer, J.H., M.J. Lee-Tischler, H.Y. Kwon, J.J. Schrick, E.D. Avner, W.E. Sweeney, V.L. Godfrey, N.L. Cacheiro, J.E. Wilkinson, and R.P. Woychik. 1994. Candidate gene associated with a mutation causing recessive polycystic kidney disease in mice. *Science*. 264:1329-1333.

Mumby, M. 2007. PP2A: Unveiling of reluctant tumor suppressor. *Cell* 130: 21-24.

Mumby, M.C., and G. Walter. 1993. Protein serine/threonine phosphatases: structure, regulation, and functions in cell growth. *Physiol Rev*. 73:673-699.

Myster, S.H., J.A. Knott, E. O'Toole, and M.E. Porter. 1997. The Chlamydomonas Dhc1 gene encodes a dynein heavy chain subunit required for assembly of the I1 inner arm complex. *Mol Biol Cell*. 8:607-620.

Myster, S.H., J.A. Knott, K.M. Wysocki, E. O'Toole, and M.E. Porter. 1999. Domains in the 1alpha dynein heavy chain required for inner arm assembly and flagellar motility in Chlamydomonas. *J Cell Biol*. 146:801-818.

Nachury, M.V., A.V. Loktev, Q. Zhang, C.J. Westlake, J. Peranen, A. Merdes, D.C. Slusarski, R.H. Scheller, J.F. Bazan, V.C. Sheffield, and P.K. Jackson. 2007. A core complex of BBS proteins cooperates with the GTPase Rab8 to promote ciliary membrane biogenesis. *Cell*. 129:1201-1213.

Nachury, M.V., E.S. Seeley, and H. Jin. 2010. Trafficking to the ciliary membrane: how to get across the periciliary diffusion barrier? *Annu Rev Cell Dev Biol*. 26:59-87.

Nakazawa, Y., M. Hiraki, R. Kamiya, and M. Hirono. 2007. SAS-6 is a cartwheel protein that establishes the 9-fold symmetry of the centriole. *Curr Biol*. 17:2169-2174.

Nelson, J.A., P.B. Savereide, and P.A. Lefebvre. 1994. The CRY1 gene in Chlamydomonas reinhardtii: structure and use as a dominant selectable marker for nuclear transformation. *Mol Cell Biol*. 14:4011-4019.

Nicastro, D. 2009. Cryo-electron microscope tomography to study axonemal organization. *Methods Cell Biol*. 91:1-39.

Nicastro, D., C. Schwartz, J. Pierson, R. Gaudette, M.E. Porter, and J.R. McIntosh. 2006. The molecular architecture of axonemes revealed by cryoelectron tomography. *Science*. 313:944-948.

Nigg, E.A. and J.W. Raff. 2009. Centrioles cilia in health and disease. *Cell* 139: 663-678.

Nonaka, S., Y. Tanaka, Y. Okada, S. Takeda, A. Harada, Y. Kanai, M. Kido, and N. Hirokawa. 1998. Randomization of left-right asymmetry due to loss of nodal cilia generating leftward flow of extraembryonic fluid in mice lacking KIF3B motor protein. *Cell*. 95:829-837.

Nunbhakdi-Craig, V., S. Schuechner, J.M. Sontag, L. Montgomery, D.C. Pallas, C. Juno, I. Mudrak, E. Ogris, and E. Sontag. 2007. Expression of protein phosphatase 2A mutants and silencing of the regulatory B alpha subunit induce a selective loss of acetylated and detyrosinated microtubules. *J Neurochem*. 101:959-971.

O'Toole, E.T., T.H. Giddings, J.R. McIntosh, and S.K. Dutcher. 2003. Three-dimensional organization of basal bodies from wild-type and delta-tubulin deletion strains of Chlamydomonas reinhardtii. *Mol Biol Cell*. 14:2999-3012.

Ogris, E., D.M. Gibson, and D.C. Pallas. 1997. Protein phosphatase 2A subunit assembly: the catalytic subunit carboxy terminus is important for binding cellular B subunit but not polyomavirus middle tumor antigen. *Oncogene*. 15:911-917.

Oiwa, K., and H. Sakakibara. 2005. Recent progress in dynein structure and mechanism. *Curr Opin Cell Biol*. 17:98-103.

Okada, Y., S. Takeda, Y. Tanaka, J.C. Belmonte, and N. Hirokawa. 2005. Mechanism of nodal flow: a conserved symmetry breaking event in left-right axis determination. *Cell*. 121:633-644.

Okagaki, T., and R. Kamiya. 1986. Microtubule sliding in mutant Chlamydomonas axonemes devoid of outer or inner dynein arms. *J Cell Biol*. 103:1895-1902.

Okita, N., N. Isogai, M. Hirono, R. Kamiya, and K. Yoshimura. 2005. Phototactic activity in Chlamydomonas 'non-phototactic' mutants deficient in Ca2+-dependent control of flagellar dominance or in inner-arm dynein. *J Cell Sci*. 118:529-537.

Ong, A.C., and D.N. Wheatley. 2003. Polycystic kidney disease--the ciliary connection. *Lancet*. 361:774-776.

Onuchic, L.F., J.J. Schrick, J. Ma, T. Hudson, L.M. Guay-Woodford, K. Zerres, R.P. Woychik, and S.T. Reeders. 1995. Sequence analysis of the human hTg737 gene and its polymorphic sites in patients with autosomal recessive polycystic kidney disease. *Mamm Genome*. 6:805-808.

Ostrowski, L.E., K. Blackburn, K.M. Radde, M.B. Moyer, D.M. Schlatzer, A. Moseley, and R.C. Boucher. 2002. A proteomic analysis of human cilia: identification of novel components. *Mol Cell Proteomics*. 1:451-465.

Patel-King, R.S., and S.M. King. 2009. An outer arm dynein light chain acts in a conformational switch for flagellar motility. *J Cell Biol*. 186:283-295.

Pazour, G.J. 2004. Intraflagellar transport and cilia-dependent renal disease: the ciliary hypothesis of polycystic kidney disease. *J Am Soc Nephrol*. 15:2528-2536.

Pazour, G.J., N. Agrin, J. Leszyk, and G.B. Witman. 2005. Proteomic analysis of a eukaryotic cilium. *J Cell Biol*. 170:103-113.

Pazour, G.J., B.L. Dickert, Y. Vucica, E.S. Seeley, J.L. Rosenbaum, G.B. Witman, and D.G. Cole. 2000. Chlamydomonas IFT88 and its mouse homologue, polycystic kidney disease gene tg737, are required for assembly of cilia and flagella. *J Cell Biol*. 151:709-718.

Pazour, G.J., and J.L. Rosenbaum. 2002. Intraflagellar transport and cilia-dependent diseases. *Trends Cell Biol*. 12:551-555.

Pazour, G.J., O.A. Sineshchekov, and G.B. Witman. 1995. Mutational analysis of the phototransduction pathway of Chlamydomonas reinhardtii. *J Cell Biol*. 131:427-440.

Pearson, C.G., D.P. Osborn, T.H. Giddings, Jr., P.L. Beales, and M. Winey. 2009. Basal body stability and ciliogenesis requires the conserved component Poc1. *J Cell Biol*. 187:905-920.

Pedersen, L.B., and J.L. Rosenbaum. 2008. Intraflagellar transport (IFT) role in ciliary assembly, resorption and signalling. *Curr Top Dev Biol*. 85:23-61.

Perrone, C.A., S.H. Myster, R. Bower, E.T. O'Toole, and M.E. Porter. 2000. Insights into the structural organization of the I1 inner arm dynein from a domain analysis of the 1beta dynein heavy chain. *Mol Biol Cell*. 11:2297-2313.

Perrone, C.A., P. Yang, E. O'Toole, W.S. Sale, and M.E. Porter. 1998. The Chlamydomonas IDA7 locus encodes a 140-kDa dynein intermediate chain required to assemble the I1 inner arm complex. *Mol Biol Cell*. 9:3351-3365.

Pfister, K.K., P.R. Shah, H. Hummerich, A. Russ, J. Cotton, A.A. Annuar, S.M. King, and E.M. Fisher. 2006. Genetic analysis of the cytoplasmic dynein subunit families. *PLoS Genet*. 2:e1.

Piperno, G., and Z. Ramanis. 1991. The proximal portion of Chlamydomonas flagella contains a distinct set of inner dynein arms. *J Cell Biol*. 112:701-709.

Piperno, G., Z. Ramanis, E.F. Smith, and W.S. Sale. 1990. Three distinct inner dynein arms in Chlamydomonas flagella: molecular composition and location in the axoneme. *J Cell Biol*. 110:379-389.

Porter, M.E., J. Power, and S.K. Dutcher. 1992. Extragenic suppressors of paralyzed flagellar mutations in Chlamydomonas reinhardtii identify loci that alter the inner dynein arms. *J Cell Biol*. 118:1163-1176.

Porter, M.E., and W.S. Sale. 2000. The 9 + 2 axoneme anchors multiple inner arm dyneins and a network of kinases and phosphatases that control motility. *J Cell Biol*. 151:F37-42.

Price, N.E., and M.C. Mumby. 1999. Brain protein serine/threonine phosphatases. *Curr Opin Neurobiol*. 9:336-342.

Price, N.E., B. Wadzinski, and M.C. Mumby. 1999. An anchoring factor targets protein phosphatase 2A to brain microtubules. *Brain Res Mol Brain Res*. 73:68-77.

Qin, H., D.R. Diener, S. Geimer, D.G. Cole, and J.L. Rosenbaum. 2004. Intraflagellar transport (IFT) cargo: IFT transports flagellar precursors to the tip and turnover products to the cell body. *J Cell Biol*. 164:255-266.

Quarmby, L.M., and J.D. Parker. 2005. Cilia and the cell cycle? *J Cell Biol*. 169:707-710.

Rohatgi, R., and W.J. Snell. 2010. The ciliary membrane. *Curr Opin Cell Biol*. 22:541-546.

Rosenbaum, J.L., J.E. Moulder, and D.L. Ringo. 1969. Flagellar elongation and shortening in Chlamydomonas. The use of cycloheximide and colchicine to study the synthesis and assembly of flagellar proteins. *J Cell Biol*. 41:600-619.

Rosenbaum, J.L., and G.B. Witman. 2002. Intraflagellar transport. *Nat Rev Mol Cell Biol*. 3:813-825.

Ruediger, R., M. Hentz, J. Fait, M. Mumby, and G. Walter. 1994. Molecular model of the A subunit of protein phosphatase 2A: interaction with other subunits and tumor antigens. *J Virol*. 68:123-129.

Ruediger, R., D. Roeckel, J. Fait, A. Bergqvist, G. Magnusson, and G. Walter. 1992. Identification of binding sites on the regulatory A subunit of protein phosphatase 2A for the catalytic C subunit and for tumor antigens of simian virus 40 and polyomavirus. *Mol Cell Biol*. 12:4872-4882.

Salathe, M. 2007. Regulation of mammalian ciliary beating. *Annu Rev Physiol*. 69:401-422.

Sale, W.S., and P. Satir. 1977. Direction of active sliding of microtubules in Tetrahymena cilia. *Proc Natl Acad Sci U S A*. 74:2045-2049.

Satir, P. 1968. Studies on cilia. 3. Further studies on the cilium tip and a "sliding filament" model of ciliary motility. *J Cell Biol*. 39:77-94.

Satir, P., and S.T. Christensen. 2007. Overview of structure and function of mammalian cilia. *Annu Rev Physiol*. 69:377-400.

Satir, P., L.B. Pedersen, and S.T. Christensen. 2010. The primary cilium at a glance. *J Cell Sci*. 123:499-503.

Schild, A., K. Schmidt, Y.A. Lim, Y. Ke, L.M. Ittner, B.A. Hemmings, and J. Gotz. 2006. Altered levels of PP2A regulatory B/PR55 isoforms indicate role in neuronal differentiation. *Int J Dev Neurosci*. 24:437-443.

Schmidt, K., S. Kins, A. Schild, R.M. Nitsch, B.A. Hemmings, and J. Gotz. 2002. Diversity, developmental regulation and distribution of murine PR55/B subunits of protein phosphatase 2A. *Eur J Neurosci*. 16:2039-2048.

Scholey, J.M., and K.V. Anderson. 2006. Intraflagellar transport and cilium-based signaling. *Cell*. 125:439-442.

Seeley, E.S., and M.V. Nachury. 2009. Constructing and deconstructing roles for the primary cilium in tissue architecture and cancer. *Methods Cell Biol*. 94:299-313.

Sharma, N., N. Berbari, B.K. Yoder. 2008. Ciliary dysfunction in develomental abnormaility. *Curr Top Dev Biol*. 85: 371-427.

Shi, Y. 2009b. Serine/threonine phosphatases: mechanism through structure. *Cell*. 139:468-484.

Shi, Y. 2009a. Assembly and strucutre of PP2A. *Sci China C. Life Sci.* 52: 135-146.

Shingyoji, C., A. Murakami, and K. Takahashi. 1977. Local reactivation of Triton-extracted flagella by iontophoretic application of ATP. *Nature*. 265:269-270.

Smith, E.F. 2007. Hydin seek: finding a function in ciliary motility. *J Cell Biol*. 176:403-404.

Smith, E.F., and W.S. Sale. 1991. Microtubule binding and translocation by inner dynein arm subtype I1. *Cell Motil Cytoskeleton*. 18:258-268.

Smith, E.F., and W.S. Sale. 1992. Regulation of dynein-driven microtubule sliding by the radial spokes in flagella. *Science*. 257:1557-1559.

Smith, E.F. and W.S.Sale. 1992. Structural and functional reconstitution of inner dynein arms in axonemes. *J. Cell Biol.* 117: 573-581.

Smith, E.F., and P. Yang. 2004. The radial spokes and central apparatus: mechano-chemical transducers that regulate flagellar motility. *Cell Motil Cytoskeleton*. 57:8-17.

Snell, W.J., J. Pan, and Q. Wang. 2004. Cilia and flagella revealed: from flagellar assembly in Chlamydomonas to human obesity disorders. *Cell*. 117:693-697.

Sontag, E., V. Nunbhakdi-Craig, G. Lee, R. Brandt, C. Kamibayashi, J. Kuret, C.L. White, 3rd, M.C. Mumby, and G.S. Bloom. 1999. Molecular interactions among protein phosphatase 2A, tau, and microtubules. Implications for the regulation of tau phosphorylation and the development of tauopathies. *J Biol Chem*. 274:25490-25498.

Stannard, W.A., M.A. Chilvers, A.R. Rutman, C.D. Williams, and C. O'Callaghan. 2010. Diagnostic testing of patients suspected of primary ciliary dyskinesia. *Am J Respir Crit Care Med*. 181:307-314.

Strack, S., J.A. Zaucha, F.F. Ebner, R.J. Colbran, and B.E. Wadzinski. 1998. Brain protein phosphatase 2A: developmental regulation and distinct cellular and subcellular localization by B subunits. *J Comp Neurol*. 392:515-527.

Summers, K.E., and I.R. Gibbons. 1971. Adenosine triphosphate-induced sliding of tubules in trypsin-treated flagella of sea-urchin sperm. *Proc Natl Acad Sci U S A*. 68:3092-3096.

Takada, S., and R. Kamiya. 1994. Functional reconstitution of Chlamydomonas outer dynein arms from alpha-beta and gamma subunits: requirement of a third factor. *J Cell Biol*. 126:737-745.

Takada, S., C.G. Wilkerson, K. Wakabayashi, R. Kamiya, and G.B. Witman. 2002. The outer dynein arm-docking complex: composition and characterization of a subunit (oda1) necessary for outer arm assembly. *Mol Biol Cell*. 13:1015-1029.

Tam, L.W., and P.A. Lefebvre. 1993. Cloning of flagellar genes in Chlamydomonas reinhardtii by DNA insertional mutagenesis. *Genetics*. 135:375-384.

Tar, K., A.A. Birukova, C. Csortos, E. Bako, J.G. Garcia, and A.D. Verin. 2004. Phosphatase 2A is involved in endothelial cell microtubule remodeling and barrier regulation. *J Cell Biochem*. 92:534-546.

Toba, S., L.A. Fox, H. Sakakibara, M.E. Porter, K. Oiwa, and W.S. Sale. 2011. Distinct roles of 1{alpha} and 1{beta} heavy chains of the inner arm dynein I1 of Chlamydomonas flagella. *Mol Biol Cell*. 22:342-353.

Tolstykh, T., J. Lee, S. Vafai, and J.B. Stock. 2000. Carboxyl methylation regulates phosphoprotein phosphatase 2A by controlling the association of regulatory B subunits. *EMBO J*. 19:5682-5691.

Turowski, P., and J.C. Lamb. 1998. Microinjection and immunological methods in the analysis of type 1 and 2A protein phosphatases from mammalian cells. *Methods Mol Biol*. 93:117-136.

Venter, J.C., M.D. Adams, E.W. Myers, P.W. Li, R.J. Mural, G.G. Sutton, H.O. Smith, M. Yandell, C.A. Evans, R.A. Holt, J.D. Gocayne, P. Amanatides, R.M. Ballew, D.H. Huson, J.R. Wortman, Q. Zhang, C.D. Kodira, X.H. Zheng, L. Chen, M.

Skupski, G. Subramanian, P.D. Thomas, J. Zhang, G.L. Gabor Miklos, C. Nelson, S. Broder, A.G. Clark, J. Nadeau, V.A. McKusick, N. Zinder, A.J. Levine, R.J. Roberts, M. Simon, C. Slayman, M. Hunkapiller, R. Bolanos, A. Delcher, I. Dew, D. Fasulo, M. Flanigan, L. Florea, A. Halpern, S. Hannenhalli, S. Kravitz, S. Levy, C. Mobarry, K. Reinert, K. Remington, J. Abu-Threideh, E. Beasley, K. Biddick, V. Bonazzi, R. Brandon, M. Cargill, I. Chandramouliswaran, R. Charlab, K. Chaturvedi, Z. Deng, V. Di Francesco, P. Dunn, K. Eilbeck, C. Evangelista, A.E. Gabrielian, W. Gan, W. Ge, F. Gong, Z. Gu, P. Guan, T.J. Heiman, M.E. Higgins, R.R. Ji, Z. Ke, K.A. Ketchum, Z. Lai, Y. Lei, Z. Li, J. Li, Y. Liang, X. Lin, F. Lu, G.V. Merkulov, N. Milshina, H.M. Moore, A.K. Naik, V.A. Narayan, B. Neelam, D. Nusskern, D.B. Rusch, S. Salzberg, W. Shao, B. Shue, J. Sun, Z. Wang, A. Wang, X. Wang, J. Wang, M. Wei, R. Wides, C. Xiao, C. Yan, et al. 2001. The sequence of the human genome. *Science*. 291:1304-1351.

Virshup, D.M., and S. Shenolikar. 2009. From promiscuity to precision: protein phosphatases get a makeover. *Mol Cell*. 33:537-545.

Wakabayashi, K., S. Takada, G.B. Witman, and R. Kamiya. 2001. Transport and arrangement of the outer-dynein-arm docking complex in the flagella of Chlamydomonas mutants that lack outer dynein arms. *Cell Motil Cytoskeleton*. 48:277-286.

Walczak, C.E., R.A. Anderson, and D.L. Nelson. 1993. Identification of a family of casein kinases in Paramecium: biochemical characterization and cellular localization. *Biochem J*. 296 (Pt 3):729-735.

Wallingford, J.B. 2010. Planar cell polarity signaling, cilia and polarized ciliary beating. *Curr Opin Cell Biol*. 22:597-604.

Wargo, M.J., E.E. Dymek, and E.F. Smith. 2005. Calmodulin and PF6 are components of a complex that localizes to the C1 microtubule of the flagellar central apparatus. *J Cell Sci*. 118:4655-4665.

Warner, F.D., and P. Satir. 1974. The structural basis of ciliary bend formation. Radial spoke positional changes accompanying microtubule sliding. *J Cell Biol*. 63:35-63.

Wei H, Ashby DG, Moreno CS, Ogris E, Yeong FM, Corbett AH, Pallas DC. 2001. Carboxymethylation of the PP2A catalytic subunit in Saccharomyces cerevisiae is required for efficient interaction with the B-type subunits Cdc55p and Rts1p. *J Biol Chem.* 276 (2):1570-7.

Welch, E.J., B.W. Jones, and J.D. Scott. 2010. Networking with AKAPs: context-dependent regulation of anchored enzymes. *Mol Interv*. 10:86-97.

Wirschell, M., T. Hendrickson, and W.S. Sale. 2007. Keeping an eye on I1: I1 dynein as a model for flagellar dynein assembly and regulation. *Cell Motil Cytoskeleton*. 64:569-579.

Wirschell, M., D. Nicastro, M.E. Porter, and W.S. Sale. 2009a. Structural basis for regulation of flagellar motility: organization of the dynein regulatory complex, inter-dynein linkers and a network of axonemal kinases and phosphatases. . *In* The Chlamydomonas Sourcebook. . Vol. 3. G.B. Witman, editor. Academic Press, Kidlington, Oxford. 253-282.

Wirschell, M., C. Yang, P. Yang, L. Fox, H.A. Yanagisawa, R. Kamiya, G.B. Witman, M.E. Porter, and W.S. Sale. 2009b. IC97 is a novel intermediate chain of I1 dynein that interacts with tubulin and regulates interdoublet sliding. *Mol Biol Cell*. 20:3044-3054.

Witman, G.B. 1986. Isolation of Chlamydomonas flagella and flagellar axonemes. *Methods Enzymol*. 134:280-290.

Witman, G.B. 1993. Chlamydomonas phototaxis. *Trends Cell Biol*. 3:403-408.

Wong, S.Y., and J.F. Reiter. 2008. The primary cilium at the crossroads of mammalian hedgehog signaling. *Curr Top Dev Biol*. 85:225-260.

Wong, W., and J.D. Scott. 2004. AKAP signalling complexes: focal points in space and time. *Nat Rev Mol Cell Biol*. 5:959-970.

Woolley, D.M. 1997. Studies on the eel sperm flagellum. I. The structure of the inner dynein arm complex. *J Cell Sci*. 110 (Pt 1):85-94.

Wu, J., T. Tolstykh, J. Lee, K. Boyd, J.B. Stock, and J.R. Broach. 2000. Carboxyl methylation of the phosphoprotein phosphatase 2A catalytic subunit promotes its functional association with regulatory subunits in vivo. *EMBO J*. 19:5672-5681.

Xie, H., and S. Clarke. 1993. Methyl esterification of C-terminal leucine residues in cytosolic 36-kDa polypeptides of bovine brain. A novel eucaryotic protein carboxyl methylation reaction. *J Biol Chem*. 268:13364-13371.

Xie, H., and S. Clarke. 1994a. An enzymatic activity in bovine brain that catalyzes the reversal of the C-terminal methyl esterification of protein phosphatase 2A. *Biochem Biophys Res Commun*. 203:1710-1715.

Xie, H., and S. Clarke. 1994b. Protein phosphatase 2A is reversibly modified by methyl esterification at its C-terminal leucine residue in bovine brain. *J Biol Chem*. 269:1981-1984.

Xing, Y., Y. Xu, Y. Chen, P.D. Jeffrey, Y. Chao, Z. Lin, Z. Li, S. Strack, J.B. Stock, and Y. Shi. 2006. Structure of protein phosphatase 2A core enzyme bound to tumor-inducing toxins. *Cell*. 127:341-353.

Xu, Y., Y. Chen, P. Zhang, P.D. Jeffrey, and Y. Shi. 2008. Structure of a protein phosphatase 2A holoenzyme: insights into B55-mediated Tau dephosphorylation. *Mol Cell*. 31:873-885.

Xu, Y., Y. Xing, Y. Chen, Y. Chao, Z. Lin, E. Fan, J.W. Yu, S. Strack, P.D. Jeffrey, and Y. Shi. 2006. Structure of the protein phosphatase 2A holoenzyme. *Cell*. 127:1239-1251.

Yagi, T., K. Uematsu, Z. Liu, and R. Kamiya. 2009. Identification of dyneins that localize exclusively to the proximal portion of Chlamydomonas flagella. *J Cell Sci*. 122:1306-1314.

Yang, C., and P. Yang. 2006a. The flagellar motility of Chlamydomonas pf25 mutant lacking an AKAP-binding protein is overtly sensitive to medium conditions. *Mol Biol Cell*. 17:227-238.

Yang, P., D.R. Diener, J.L. Rosenbaum, and W.S. Sale. 2001. Localization of calmodulin and dynein light chain LC8 in flagellar radial spokes. *J Cell Biol*. 153:1315-1326.

Yang, P., D.R. Diener, C. Yang, T. Kohno, G.J. Pazour, J.M. Dienes, N.S. Agrin, S.M. King, W.S. Sale, R. Kamiya, J.L. Rosenbaum, and G.B. Witman. 2006b. Radial spoke proteins of Chlamydomonas flagella. *J Cell Sci*. 119:1165-1174.

Yang, P., L. Fox, R.J. Colbran, and W.S. Sale. 2000b. Protein phosphatases PP1 and PP2A are located in distinct positions in the Chlamydomonas flagellar axoneme. *J Cell Sci*. 113 (Pt 1):91-102.

Yang, P., and W.S. Sale. 1998. The Mr 140,000 intermediate chain of Chlamydomonas flagellar inner arm dynein is a WD-repeat protein implicated in dynein arm anchoring. *Mol Biol Cell*. 9:3335-3349.

Yang, P., and W.S. Sale. 2000a. Casein kinase I is anchored on axonemal doublet microtubules and regulates flagellar dynein phosphorylation and activity. *J Biol Chem*. 275:18905-18912.

Yu, X.X., X. Du, C.S. Moreno, R.E. Green, E. Ogris, Q. Feng, L. Chou, M.J. McQuoid, and D.C. Pallas. 2001. Methylation of the protein phosphatase 2A catalytic subunit is essential for association of Balpha regulatory subunit but not SG2NA, striatin, or polyomavirus middle tumor antigen. *Mol Biol Cell*. 12:185-199.

Zariwala, M.A., M.R. Knowles, and H. Omran. 2007. Genetic defects in ciliary structure and function. *Annu Rev Physiol*. 69:423-450.

Zhao, W.Q., C. Feng, and D.L. Alkon. 2003. Impairment of phosphatase 2A contributes to the prolonged MAP kinase phosphorylation in Alzheimer's disease fibroblasts. *Neurobiol Dis*. 14:458-469.